

สภาพย่อยสลายได้ทางชีวภาพของวัสดุเชิงประกอบไมโครคริสตัลไลน์เซลลูโลส/พอลิแล็กติก  
แอซิดกราฟต์มาเลอิกแอนไฮไดรด์/พอลิแล็กติกแอซิด

นางสาวธัญญา มาสำราญ

วิทยานิพนธ์นี้เป็นส่วนหนึ่งของการศึกษาตามหลักสูตรปริญญาวิทยาศาสตรมหาบัณฑิต  
สาขาวิชาวิทยาศาสตร์พอลิเมอร์ประยุกต์และเทคโนโลยีสิ่งทอ ภาควิชาวัสดุศาสตร์  
คณะวิทยาศาสตร์ จุฬาลงกรณ์มหาวิทยาลัย  
ปีการศึกษา 2554  
ลิขสิทธิ์ของจุฬาลงกรณ์มหาวิทยาลัย

บทคัดย่อและแฟ้มข้อมูลฉบับเต็มของวิทยานิพนธ์ตั้งแต่ปีการศึกษา 2554 ที่ให้บริการในคลังปัญญาจุฬาฯ (CUIR)  
เป็นแฟ้มข้อมูลของนิสิตเจ้าของวิทยานิพนธ์ที่ส่งผ่านทางบัณฑิตวิทยาลัย

The abstract and full text of theses from the academic year 2011 in Chulalongkorn University Intellectual Repository (CUIR)  
are the thesis authors' files submitted through the Graduate School.

BIODEGRADABILITY OF MICROCRYSTALLINE CELLULOSE/POLY(LACTIC ACID)-GRAFTED-  
MALEIC ANHYDRIDE/POLY(LACTIC ACID) COMPOSITES

Miss Dhananya Masamran

A Thesis Submitted in Partial Fulfillment of the Requirements  
for the Degree of Master of Science Program in Applied Polymer Science and Textile Technology

Department of Materials Science

Faculty of Science

Chulalongkorn University

Academic Year 2011

Copyright of Chulalongkorn University



รณัญญา มาสำราญ : สภาพย่อยสลายได้ทางชีวภาพของวัสดุเชิงประกอบไมโครคริสตัล  
 ลีนเซลลูโลส/พอลิแล็กติกแอซิดกราฟต์มาเลอิกแอนไฮไดรด์/พอลิแล็กติกแอซิด.  
 (BIODEGRADABILITY OF MICROCRYSTALLINE CELLULOSE/POLY(LACTIC  
 ACID)-GRAFTED-MALEIC ANHYDRIDE/POLY(LACTIC ACID) COMPOSITES)  
 อ. ที่ปรึกษาวิทยานิพนธ์ : รศ. ดร. ดวงดาว อัจจงค์, 151 หน้า.

งานวิจัยนี้ทำการเตรียมฟิล์มวัสดุเชิงประกอบที่สามารถย่อยสลายได้ทางชีวภาพของพอลิแล็กติกแอซิดเสริมแรง  
 ด้วยไมโครคริสตัลลีนเซลลูโลสจากผ้าฝ้าย โดยได้ทำการเตรียมไมโครคริสตัลลีนเซลลูโลสจากเศษผ้าฝ้ายโดยวิธีการไฮโดร  
 ลิซิสด้วยกรดไฮโดรคลอริกเจือจาง และสังเคราะห์พอลิแล็กติกแอซิดกราฟต์มาเลอิกแอนไฮไดรด์เป็นสารช่วยผสมด้วย  
 กระบวนการแบบสารละลาย โดยทำการศึกษาเวลาและอุณหภูมิในการทำปฏิกิริยา พบว่าสภาวะที่เหมาะสมในการ  
 สังเคราะห์พอลิแล็กติกแอซิดกราฟต์มาเลอิกแอนไฮไดรด์ คือการใช้เตตระไฮโดรฟิวเรนเป็นตัวทำละลาย และเบนโซอิล  
 เปอร์ออกไซด์เป็นสารเริ่มปฏิกิริยา ภายใต้บรรยากาศไนโตรเจน ที่อุณหภูมิ 85 องศาเซลเซียส เป็นเวลา 3 ชั่วโมง แล้วทำ  
 การวิเคราะห์ลักษณะโครงสร้างทางเคมีและทางกายภาพของสารช่วยผสม จากนั้นจึงเตรียมวัสดุเชิงประกอบโดย  
 ทำการศึกษาค่าผลของปริมาณของไมโครคริสตัลลีนเซลลูโลสจากผ้าฝ้าย ซึ่งใช้อัตราส่วนโดยน้ำหนักที่ร้อยละ 0 10 20 30  
 และ 40 และใช้ปริมาณพอลิแล็กติกแอซิดกราฟต์มาเลอิกแอนไฮไดรด์ที่ร้อยละ 5 โดยน้ำหนักโดยการผสมด้วยเครื่องผสม  
 แบบเกลียวหนอนคู่และขึ้นรูปเป็นชิ้นงานด้วยเครื่องอัดแบบ จากนั้นนำไปทดสอบสมบัติเชิงกล วิเคราะห์ลักษณะพื้นผิวที่  
 แตกหัก ความสามารถในการดูดซึมน้ำ สมบัติทางความร้อนและความสามารถในการย่อยสลายทางชีวภาพ จากผล  
 การศึกษาพบว่า สมบัติเชิงกลของวัสดุเชิงประกอบได้แก่ ร้อยละการยืดตัว ณ จุดขาด มีค่าเพิ่มขึ้นตามการเพิ่มปริมาณ  
 ของไมโครคริสตัลลีนเซลลูโลสจากผ้าฝ้าย และที่สำคัญพบว่าการปรับปรุงแรงยึดเหนี่ยวระหว่างพอลิแล็กติกแอซิดและไม  
 โครคริสตัลลีนเซลลูโลสจากผ้าฝ้ายด้วยพอลิแล็กติกแอซิดกราฟต์มาเลอิกแอนไฮไดรด์ ทำให้วัสดุเชิงประกอบมีสมบัติ  
 เชิงกลที่ดีกว่าการไม่ใช้พอลิแล็กติกแอซิดกราฟต์มาเลอิกแอนไฮไดรด์ วัสดุเชิงประกอบที่มีปริมาณไมโครคริสตัลลีน  
 เซลลูโลสจากผ้าฝ้ายร้อยละ 10 โดยน้ำหนักและใช้พอลิแล็กติกแอซิด กราฟต์มาเลอิกแอนไฮไดรด์เป็นสารช่วยผสมมีค่า  
 ความทนแรงดึงสูงสุด โดยสามารถยืนยันได้จากการวิเคราะห์ลักษณะพื้นผิวที่แตกหักด้วยกล้องจุลทรรศน์อิเล็กตรอนแบบ  
 ส่องกราด พบว่า พอลิแล็กติกแอซิดกราฟต์มาเลอิกแอนไฮไดรด์ ช่วยเพิ่มแรงยึดเหนี่ยวระหว่างไมโครคริสตัลลีนเซลลูโลส  
 จากผ้าฝ้ายกับพอลิแล็กติกแอซิด นอกจากนี้ยังพบว่าวัสดุเชิงประกอบที่ไม่มีไมโครคริสตัลลีนเซลลูโลสจากผ้าฝ้ายมีแนวโน้ม  
 ในการดูดซึมน้ำสูงขึ้น ขณะที่เมื่อใส่พอลิแล็กติกแอซิดกราฟต์มาเลอิกแอนไฮไดรด์ลงไปแล้วจะทำให้ความสามารถในการ  
 ดูดซึมน้ำมีแนวโน้มที่ต่ำลง เนื่องจากการสร้างพันธะระหว่างหมู่ฟังก์ชันของมาเลอิกแอนไฮไดรด์และหมู่ไฮดรอกซิลของไม  
 โครคริสตัลลีนเซลลูโลสจากผ้าฝ้าย นอกจากนี้ งานวิจัยนี้ได้ทดสอบความสามารถในการย่อยสลายทางชีวภาพโดย  
 วิธีการใช้เอนไซม์และวิธีการจุ่มในบ่อบำบัดน้ำเสียแบบตะกอนเร่ง พบว่า ฟิล์มที่ย่อยสลายโดยใช้วิธีเอนไซม์สามารถย่อย  
 สลายทางชีวภาพได้เมื่อจุ่มอยู่ในสารละลายเอนไซม์เป็นเวลา 4 วันขึ้นไป ในขณะที่ฟิล์มที่ย่อยสลายโดยใช้วิธีการจุ่มใน  
 บ่อบำบัดน้ำเสียแบบตะกอนเร่งสามารถย่อยสลายทางชีวภาพได้เมื่อจุ่มในบ่อบำบัดน้ำเสียเป็นเวลา 4 สัปดาห์ขึ้นไป  
 หลังจากการย่อยสลายไปเป็นเวลา 7 วัน ฟิล์มวัสดุเชิงประกอบของพอลิแล็กติกแอซิดที่ไม่มีไมโครคริสตัลลีนเซลลูโลสจาก  
 ผ้าฝ้ายร้อยละ 40 ภายใต้เอนไซม์ไลเปส เอนไซม์เซลลูเลสและระบบบำบัดน้ำเสียแบบตะกอนเร่ง พบว่ามีค่าร้อยละโดย  
 น้ำหนักของฟิล์มที่ลดลงคือ 4.3 และ 1.74 ตามลำดับ

ภาควิชา.....วัสดุศาสตร์..... ลายมือชื่อ.....

สาขาวิชาวิศวกรรมพอลิเมอร์ประยุกต์และเทคโนโลยีสิ่งทอ ลายมือชื่อ อ.ที่ปรึกษาวิทยานิพนธ์.....

ปีการศึกษา.....2554.....

# #5272332823 : MAJOR APPLIED POLYMER SCIENCE AND TEXTILE TECHNOLOGY

KEYWORDS : PLA / PLA-g-MA / MICROCRYSTALLINE CELLULOSE / BIODEGRADABLE PLASTIC / COMPOSITE FILM

DHANANYA MASAMRAN : BIODEGRADABILITY OF MICROCRYSTALLINE CELLULOSE/POLY(LACTIC ACID)-GRAFTED-MALEIC ANHYDRIDE/POLY(LACTIC ACID) COMPOSITES. ADVISOR : ASSOC. PROF. DUANGDAO AHT-ONG, Ph.D., 151 pp.

This research aimed to prepare microcrystalline cellulose (MCC)/PLA composite films in which MCC was obtained from acid hydrolysis of cotton fabric (CT-MCC) by hydrochloric acid. In addition, maleic anhydride – grafted-poly(lactic acid) (PLA-g-MA) was synthesized and used as a compatibilizer. The optimum conditions for PLA-g-MA synthesis were investigated in terms of reaction time and temperature. The results showed that the optimum conditions for synthesis PLA-g-MA was that PLA was dissolved in THF and using BPO as an initiator under nitrogen atmosphere at 85 °C until 3 h. NMR, FT-IR, TGA, DSC, and SEM were used to characterize chemical structure and properties of PLA-g-MA. After that, the CT-MCC/PLA composites were prepared at various ratios (0, 10, 20, 30, and 40 wt%) while the amount of PLA-g-MA was fixed at 5 wt% based on MCC content by using a twin screw extruder and a compression molding, respectively. The mechanical properties, fractured surface, water absorption, thermal properties, and biodegradability of the composites were investigated. The results showed that the elongation at break of all composites increased with increasing CT-MCC loading. The composite films consisted of PLA-g-MA showed better mechanical properties than the uncompatibilized films. In particular, the 10%wt CT-MCC/5%PLA-g-MA/PLA composite films exhibited the highest tensile strength. These results were confirmed and in good agreement with the results from SEM analysis. Better adhesion and dispersion of the CT-MCC/PLA-g-MA/PLA composite films was observed. Moreover, uncompatibilized composite films exhibited higher water absorption than neat PLA, while the compatibilized composites showed lower water absorption than the uncompatibilized composite films. This is due to the hydrophobic surface of the formation of covalent bonds between the functional groups of maleic anhydride and the hydroxyl groups at the surfaces of CT-MCC. Finally, the biodegradability of the films was evaluated under (1) enzymatic degradation using lipase and cellulase and (2) controlled composting condition according to the waste water treatment system condition. The composite films can be degraded under both conditions, especially the biodegradation rate was increased after 4 days in enzymatic condition, and 4 weeks in the waste water treatment system condition. After degradation for 7 days, the %weight loss of 40%CT-MCC/PLA composite films under cellulase solution, lipase solution, and activated sludge system was 4%, 3%, and 1.74%, respectively.

Department : Materials Science .....

Student's Signature.....

Field of Study : Applied Polymer Science and Textile Technology ..

Advisor's Signature.....

Academic Year : 2011 .....

## ACKNOWLEDGEMENTS

I feel much delighted to being offered a completed thesis and sincerely appreciate the contributions of the many people who have helped shaping it.

Firstly, I would like to thank my advisor, Associate Professor Dr. Duangdao Aht-Ong who has tirelessly guided and supported me every steps of the way in my research, and who was never short on valuable advice and direction when it was needed most.

On particular aspects of the thesis committee, I have had the advantage of insight from experts whose specialist advice was much appreciated: Assistant Professor Dr. Sirithan Jiemsirilers, Associate Professor Paiparn Santisuk, Associate Professor Dr. Kawee Srikulkit and Associate Professor Dr. Pranut Potiyaraj.

I am also thankful to Dr. Duangduen Atong for supporting in NMR experiments. Also, I would like to express my sincere thanks to the Department of Materials Science, Faculty of Science, Chulalongkorn University for providing me with a good environment and facilities to complete my research. My special thanks go to National Center for Petroleum, Petrochemicals, and Advanced Materials for scholarship and financial support and National Innovation Agency for financial support through research grant no. D4-52.

Gratefulness is also expressed to the waste water treatment plant at the Si Phraya Water Environment Control Plant (SPWECP) in Bangkok composting facility for the use of their place in biodegradation experiment, Brenntag Ingredients (Thailand) Public Co., Ltd. for supplying lipase and cellulase enzymes.

I would also like to thank the other bioplastics and composites research group members for their constant encouragement and valuable suggestions. I also thank to all my friends at the Department of Materials Science who have been encouraging and helping me while I was studying at Chulalongkorn University.

The most important part of my life is my family. I would never have been able to accomplish any of my goals without the support of my parents and my sister.

Without helps of these particular persons that mentioned above, I would face many difficulties while doing this thesis.

# CONTENTS

	Page
Abstract (Thai).....	iv
Abstract (English).....	v
Acknowledgements.....	vi
Contents.....	viii
List of Tables .....	xii
List of Figures.....	xiv
<b>Chapter</b>	
1. Introduction.....	1
2. Literature Survey.....	4
2.1 Composite.....	4
2.1.1 Definition of Composites.....	4
2.1.2 Classify Composites.....	5
2.1.2.1 Classification of Composite based on the Geometry of the Reinforcement.....	5
2.1.2.2 Classification of Composite based on the Type of Matrix	6
2.1.3 Interfacial Bonding.....	7
2.2 Polymer Degradation.....	7
2.3 Biodegradable Polymer.....	8
2.3.1 Polylactic Acid.....	10
2.4 Natural Fibers.....	14
2.5 Cellulose: Structure Features and Properties.....	15
2.5.1 Source of Cellulose.....	15
2.5.2 Structure of Cellulose.....	15
2.5.3 Crystalline Structure.....	16
2.6 Cotton( <i>Gossypium</i> spp., Malvaceae).....	17
2.7 Crystalline Cellulose Preparation.....	18
2.7.1 Hydrolysis.....	18
2.8 Fiber-Reinforced PLA Composites .....	20



Chapter	Page
2.9 Biodegradation.....	23
2.9.1 Defining Biodegradability.....	23
2.10 Method of Biodegradation .....	26
2.10.1 Environmental Chamber Method.....	26
2.10.2 Soil Burial tests.....	27
2.10.3 Specific Microorganism or Enzyme Degradation.....	27
2.10.4 Activative sludge Waste water treatment.....	28
3. Experimental.....	31
3.1 Materials and Chemicals.....	31
3.2 Equipments and Instruments.....	33
3.3 Experimental Procedure.....	35
3.3.1 Preparation of Microcrystalline Cellulose.....	36
3.3.2 Preparation of Polylactic Grafted Maleic Anhydride (PLA-g-MA).....	36
3.3.3 Film Formation.....	37
3.4 Characterization of Microcrystalline Cellulose (MCC).....	38
3.4.1 Particle Size Analysis.....	38
3.4.2 Morphology.....	38
3.4.3 Fourier Transform Infrared Spectroscopy.....	39
3.4.4 Thermogravimetric analysis (TGA).....	39
3.5 Characterization of Polylactic Acid-Grafted Maleic Anhydride (PLA-g-MA).....	40
3.5.1 Titration.....	40
3.5.2 Fourier Transform Infrared Spectroscopy.....	41
3.5.3 Nuclear Magnetic Resonance Spectroscopy (NMR).....	41
3.5.3.1 <sup>1</sup> H-NMR Spectroscopy.....	41
3.5.3.2 <sup>13</sup> C- NMR Spectroscopy.....	42
3.5.4 Thermal properties.....	42
3.5.4.1 Thermogravimetric Analysis (TGA).....	42
3.5.4.2 Differential Scanning Calorimetry (DSC).....	43

Chapter	Page
3.5.5 Morphology.....	43
3.6 Characterization of PLA Biocomposite Films.....	44
3.6.1 Physical Properties.....	44
3.6.1.1 Water Absorption.....	44
3.6.1.2 Morphology.....	45
3.6.2 Mechanical properties.....	45
3.6.2.1 Tensile testing.....	45
3.6.3 Thermal properties.....	46
3.6.3.1 Thermalgravimetric Analysis (TGA).....	46
3.6.3.2 Differential Scanning Calorimeter (DSC).....	46
3.6.4 Biodegradability.....	46
3.6.4.1 Enzymatic Degradation.....	46
3.6.4.2 Activated Sludge Degradation.....	47
3.7 Evaluation of the Degradation.....	48
3.7.1 Weight Loss.....	48
3.7.2 Gel Permeation Chromatography (GPC).....	48
3.7.3 Morphology.....	49
4 Results and Discussion.....	50
4.1 Characterization of Microcrystalline Cellulose Prepared from Acid Hydrolysis of Cotton Fabric.....	50
4.1.1 Particle Size and Morphology.....	50
4.1.2 FT-IR spectroscopy.....	51
4.1.3 Thermogravimetric analysis (TGA).....	53
4.2 The Grafting Reaction of Polylactic Acid with Maleic Anhydride.....	54
4.2.1 The Optimum Conditions for Preparation of PLA-g-MA.....	55
4.2.1.1 The Influence of Time for Adding Maleic Anhydride and Benzoyl Peroxide.....	56
4.2.1.2 The Effect of reaction temperature.....	62
4.2.2 Characterization of Polylactic Acid Grafted Maleic Anhydride (PLA-g-MA).....	66

Chapter	Page
4.2.2.1 Titration.....	66
4.2.2.2 Fourier Transform Infrared Spectroscopy.....	68
4.2.2.3 Carbon Nuclear Magnetic Resonance Spectroscopy ( <sup>13</sup> C-NMR).....	70
4.2.2.4 Differential scanning calorimetry (DSC) .....	72
4.2.2.5 Thermogravimetric analysis(TGA).....	74
4.2.2.6 Scanning electron microscopy (SEM).....	75
4.3 Characterization of PLA Composite Film.....	76
4.3.1 Physical Properties.....	76
4.3.1.1 Water absorption.....	76
4.3.1.2 Morphology.....	77
4.3.2 Mechanical Properties.....	82
4.3.3 Thermal properties.....	86
4.3.3.1 Thermalgravimetric Analysis (TGA).....	86
4.3.3.2 Differential Scanning Calorimetry (DSC).....	89
4.4 Biodegradability of PLA composite films.....	92
4.4.1 Enzymatic Degradation .....	93
4.4.1.1 Lipase .....	93
4.4.1.2 Cellulase .....	99
4.4.2 Activated Sludge Degradation.....	106
5 Conclusions.....	113
References.....	117
Appendices.....	123
Appendix A.....	124
Appendix B.....	125
Biography.....	150

## List of Tables

Table		Page
2.1	Chemical composition of some cellulose source.....	16
3.1	Experimental instruments.....	33
3.2	The various ratios of PLA biocomposites.....	37
4.1	SEM micrographs and particle size of cotton MCC and Avicel PH101...	51
4.2	FT-IR assignments for CT-MCC.....	52
4.3	Thermal decomposition temperature and char yield of cotton and commercial MCC.....	54
4.4	The reaction time profiles to add the maleic anhydride at 50 °C.....	56
4.5	<sup>1</sup> H-NMR chemical shift of PLA and PLA-g-MA.....	59
4.6	The PLA-g-MA synthesis reaction temperature profiles.....	63
4.7	The concentration constant of potassium hydroxide.....	66
4.8	The acid number and %grafting of PLA-g-MA .....	67
4.9	The acid number and %grafting of PLA.....	67
4.10	FT-IR assignments for PLA and PLA-g-MA.....	69
4.11	<sup>13</sup> C-NMR chemical shift of PLA and PLA-g-MA.....	72
4.12	The glass transition temperature, the melting point, and the decomposition temperature of PLA and PLA-g-MA.....	73
4.13	Tensile properties of CT-MCC/PLA films.....	83
4.14	The decomposition temperature at onset and char yield of uncompatibilized MCC/PLA composites .....	87
4.15	The decomposition temperature at onset and char yield of compatibilized MCC/PLA composites .....	89
4.16	Second-order transition temperature of MCC/PLA composites.....	92
4.17	Photographs of PLA and PLA biocomposites showing dependence on degradation time in lipase enzymatic degradation at 4 days .....	95

Table	Page
4.18	Photographs of PLA and 40%MCC/PLA biocomposites showing dependence on degradation time in lipase enzymatic degradation ... 95
4.19	SEM micrographs of uncompatibilized and compatibilized biocomposite films before and after biodegradation testing under lipase enzymatic degradation for 4 days..... 98
4.20	Photographs of PLA and PLA biocomposites showing dependence on degradation time in cellulase enzymatic degradation at 4 days ..... 101
4.21	Photographs of PLA and 40%MCC/PLA biocomposites showing dependence on degradation time in cellulase enzymatic degradation 101
4.22	SEM micrographs of uncompatibilized and compatibilized biocomposite films before and after biodegradation testing under cellulase enzymatic degradation for 4 days..... 104
4.23	Photographs of PLA and PLA biocomposites showing dependence on degradation time in activated sludge system at 8 weeks ..... 109
4.24	Photographs of PLA and 40%MCC/PLA biocomposites showing dependence on degradation time in activated sludge system ..... 109
4.25	SEM micrographs of uncompatibilized and compatibilized biocomposite films before and after biodegradation testing under activated sludge system at 6 weeks..... 112

## List of Figures

Figure		Page
2.1	Types of composites based on reinforcement shape.....	5
2.2	Classification of biodegradable polymer.....	10
2.3	Two common approaches used to synthesize PLA.....	12
2.4	Nonsolvent process to prepare polylactic acid.....	13
2.5	Molecular structure of cellulose.....	15
3.1	Chemical structure of polylactic acid.....	31
3.2	Flow chart of the experimental process.....	35
3.3	Experimental set up for PLA-g-MA solution polymerization.....	36
3.4	The laser particle size analyzer, Malvern Instruments Mastersizer 2000..	38
3.5	Fourier Transform Infrared Spectrometer, Thermo Scientific, Nicolet 6700.....	39
3.6	Thermogravimetric instrument, Mettler Toledo TGA/SDTA 851 <sup>e</sup> .....	40
3.7	Proton Nuclear Magnetic Resonance Spectroscopy, Bruker ACF-200 NMR Spectrometer.....	41
3.8	Carbon Nuclear Magnetic Resonance Spectroscopy, Bruker DPX-300 MHz NMR Spectrometer .....	42
3.9	Differential scanning calorimeter, PerkinElmer Pyris Diamond DSC.....	43
3.10	Scanning electron microscope, SEM JSM-6480LV JEOL.....	44
3.11	Universal Testing Machine, LLOYD LR 100K.....	45
3.12	Gel Permeation Chromatography, Shimadzu .....	49
4.1	Physical appearance of acid hydrolyzed CT-MCC.....	51
4.2	FT-IR spectra of CT-MCC and commercial MCC (Avicel PH101).....	52
4.3	TGA thermogram of CT-MCC and Avicel PH101.....	53
4.4	The schematic of maleic anhydride grafting on the PLA by solution polymerization .....	55
4.5	The schematic of side effect of maleic anhydride grafting on the PLA....	58
4.6	<sup>1</sup> H-NMR spectra of PLA in CDCl <sub>3</sub> .....	60

Figure	Page	
4.7	<sup>1</sup> H-NMR spectra of PLA-g-MA in CDCl <sub>3</sub> ; a) 1A b) 2A c) 3A, and d) 4A formula.....	62
4.8	<sup>1</sup> H-NMR spectra of PLA-g-MA in CDCl <sub>3</sub> ; a) 1B b) 2B c) 3B, and d) 4B formula.....	65
4.9	Infrared spectra of PLA and PLA-g-MA.....	69
4.10	<sup>13</sup> C-NMR spectrum of PLA .....	70
4.11	<sup>13</sup> C-NMR spectrum of PLA-g-MA prepared from the optimum condition	71
4.12	DSC thermograms (second heating scan) of a) PLA and b) PLA-g-MA	73
4.13	TGA thermograms of PLA, PLA-g-MA, and Maleic anhydride.....	74
4.14	Physical appearance of PLA-g-MA.....	75
4.15	SEM micrographs of PLA-g-MA a) 500X magnification b) 1000X magnification.....	76
4.16	The water absorption of composites with compatibilizer and uncompatibilizer.....	77
4.17	SEM micrographs of the uncompatibilized MCC/PLA composite; (a) Neat PLA; (b) 10%MCC/PLA; (c) 20%MCC/PLA; (d) 30%MCC/PLA; (e) 40%MCC/PLA(500X magnification).....	79
4.18	SEM micrographs of the compatibilized MCC/PLA composite; (a) Neat PLA; (b) 10%MCC/PLA; (c) 20%MCC/PLA; (d) 30%MCC/PLA; (e) 40%MCC/PLA(500X magnification).....	80
4.19	SEM micrographs of 20% MCC/PLA composite (a) without compatibilizer, (b) with compatibilizer (1000X magnification).....	82
4.20	Mechanical properties of uncompatibilized and compatibilized MCC/PLA composites (a) tensile strength; (b) Young's modulus; and (c) elongation at break.....	85
4.21	TGA curves of uncompatibilized MCC/PLA composites .....	87
4.22	TGA curves of compatibilized MCC/PLA composites.....	88
4.23	DSC thermograms of uncompatibilized CT-MCC/PLA composites.....	90

Figure	Page
4.24 DSC thermograms of 10%CT-MCC/PLA and 10%CT-MCC/5%PLA-g-MA/PLA composite films).....	91
4.25 Effect of MCC content and exposure time on % weight loss of uncompatibilized CT-MCC/PLA composite films under lipase enzymatic degradation.....	96
4.26 Effect of PLA-g-MA and exposure time on % weight loss of 10%CT-MCC/PLA composite films under lipase enzymatic degradation	96
4.27 Effect of MCC content and exposure time on molecular weight of uncompatibilized CT-MCC/PLA composite films under lipase enzymatic degradation.....	97
4.28 Effect of PLA-g-MA and exposure time on molecular weight of 10%MCC /PLA composite films under lipase enzymatic degradation....	97
4.29 Effect of MCC content and exposure time on %weight loss of uncompatibilized CT-MCC/PLA composite films under cellulase enzymatic degradation.....	102
4.30 Effect of PLA-g-MA and exposure time on %weight loss of 10%CT-MCC /PLA composite films under cellulase enzymatic degradation.....	102
4.31 Effect of MCC content and exposure time on molecular weight of uncompatibilized CT-MCC/PLA composite films under cellulase enzymatic degradation.....	103
4.32 Effect of PLA-g-MA and exposure time on molecular weight of 10%CT-MCC/PLA composite films under cellulase enzymatic degradation...	103
4.33 Effect of MCC content and exposure time on %weight loss of uncompatibilized CT-MCC/PLA composite films under activated sludge system .....	110
4.34 Effect of MCC content and exposure time on the %weight loss of 10%CT-MCC/PLA composite films under activated sludge system .....	110



Figure		Page
4.35	Effect of MCC content and exposure time on molecular weight of uncompatibilized CT-MCC/PLA composite films under activated sludge system.....	111
4.36	Effect of PLA-g-MA and exposure time on molecular weight of 10%CT-MCC/PLA composite films under activated sludge degradation .....	111

# CHAPTER 1

## INTRODUCTION

Plastics are widely used in everyday life since they have many benefits and they are used in many fields such as packaging, plastic bag, and automotive applications. This is because of their advantages such as light, strong, and inexpensive. Nevertheless, the tenacity of plastics in the environment is gradually considered as the source of the problem in ecosystem.

In the recent years, the use of renewable resources for the preparation of a polymeric material has been increased greatly because of the increasing demand for environmentally friendly materials. [1,2] Furthermore, efforts in development of biodegradable polymers is one of the ways to solve the problems of plastic waste management. In fact, biodegradable polymers are expected to replace conventional plastics for time-limited applications such as packaging materials in agriculture, which should contribute to reduce environmental pollution. [3]

Polymers from renewable resources can be classified into four groups based on source: (1) agro-polymers obtained from biomass by fraction such as starch, cellulose, protein, and lipid; (2) polyester obtained by fermentation of biomass or from genetically modified plants such as polyhydroxyalkanoate (PHA), poly(hydroxybutyrate) (PHB); (3) polyester totally synthesized by the petrochemical process such as polycaprolactone (PCL), polyesteramide (PEA) and aliphatic or aromatic copolyesters; and (4) polyester synthesized from monomer obtained from biomass such as polylactide and polylactic acid (PLA). [4] Among biodegradable plastics, poly (lactic acid) (PLA) is a very interesting material. It is a degradable thermoplastic polymer with good mechanical properties and can be processed with a large number of techniques. PLA is a commercial biodegradable plastic and can be manufactured on a large scale from the fermentation of corn starch to lactic acid. Moreover, PLA can also reduce emissions of

carbon dioxide, water, and methane in the environment over the last several months to 2 years compared with other petroleum plastics that need to be a very long period. [5] Although PLA has many advantages and can be used in different fields from pharmaceutical to packaging, brittleness and high cost limit its applications.

On the other hand, it is well known that the natural fiber reinforcement is a way to improve the mechanical properties as Young's modulus of biodegradable plastics and to reduce the overall costs of the prepared materials. In addition, it also enhances the ability to degrade them. However, the use of natural fibers in microcrystalline form is expected to be able to add them in higher amount than in any other forms and might be possible to get it well dispersed in the matrix. Thus, in this research, microcrystalline cellulose (MCC) was prepared from cotton fabric and used as reinforcement to PLA matrix. The selection of cotton fiber as a cellulose source for preparing MCC is based on the fact that cotton fiber is a plant fiber that composed the highest cellulose content up to 95%.

From previous work [6], the problem of composite reinforced with natural fibers is the lack of interfacial adhesion between fiber and matrix, which results in poor properties of the final material. Therefore, to develop such composites with good properties, it is necessary to reduce the hydrophilicity of the fibers by chemical modification or by the use of the compatibilizer. Chemical modification is usually obtained with reagents that contain functional groups that are capable of bonding to the hydroxyl groups of the fiber. Another effective way to improve the interface between fiber and matrix is the use of compatibilizers, which are usually graft copolymers of a polymeric matrix and anhydride, such as maleic anhydride (MA). These reagents are compatible with the polymer matrix and can react with the hydroxyl groups of the fiber to form covalent bonds.

However, the biodegradation is a critical factor in determining the biodegradability of biodegradable plastic. Biodegradation is a degradation catalyzed by biological activity, ultimately leading to mineralization and/or biomass. There are wide varieties of methods currently available for measuring the biodegradability of polymeric materials such as soil burial method, pure culture method, compost method, enzymatic degradation, and an aerobic degradation in the presence of sewage sludge.

Thus, the main goal of this research is to prepare new kind of material from microcrystalline cellulose (MCC)/PLA composite in which MCC was obtained from acid hydrolysis of cotton fabric. However, due to poor chemical bonding between the two components, maleic anhydride – grafted polylactic acid (PLA-g-MA) was synthesized and used as a compatibilizer. The MCC/PLA composites were prepared at various ratios by using a twin screw extruder and a compression molding, respectively. The MCC content was varied as 0, 10, 20, 30, and 40 wt%, while the amount of PLA-g-MA was fixed at 5 wt% based on MCC content. The obtained MCC was characterized by fourier transform infrared spectrometer (FT-IR), particle size analyzer, scanning electron microscope (SEM), and thermogravimetric analyzer (TGA). While, the PLA-g-MA was characterized by FT-IR, nuclear magnetic resonance spectroscopy (NMR), TGA, differential scanning calorimetry (DSC), titration, and SEM. Mechanical properties of the composites were assessed in terms of tensile properties as a function of compatibilizer and MCC content. Furthermore, the effects of MCC content and PLA-g-MA on physical properties, thermal properties, and morphology were investigated. Finally, the biodegradability of the films was evaluated under (1) controlled composting condition according to the waste water treatment system condition and (2) enzymatic degradation using lipase and cellulase by observing the changes in physical appearance, weight change, morphology, and molecular weight.

## CHAPTER 2

### LITERATURE SURVEY

#### 2.1 Composite [7]

In the past, Israelites using bricks made of clay and reinforced with straw are an early example of application of composites. The individual constituents, clay and straw, could not serve the function by themselves but did when put together. Some believe that the straw was used to keep the clay from cracking, but others suggest that it blunted the sharp cracks in the dry clay.

Historical examples of composites are abundant in the literature. Significant examples include the use of reinforcing mud walls in houses with bamboo shoots, glued laminated wood by Egyptians (1500 B.C.), and laminated metals in forging swords (A.D.1800). In the 20<sup>th</sup> century, modern composites were used in the 1930s when glass fibers reinforced resins. Boats and aircraft were built out of these glass composites, commonly called fiberglass. Since the 1970s, application of composites has widely increased due to development of new fibers such as carbon, boron, and aramids, and new composite systems with matrices made of metals and ceramics.

##### 2.1.1 Definition of composites [8]

A composite is a structural material that consists of two or more components are combined constituents that are combined at a macroscopic level and not soluble in each other. One constituent is called the reinforcing phase and the one in which it is embedded is called the matrix. The reinforcing phase material may be in the form of fibers, particles, or flakes. The matrix phase materials are generally continuous. Examples of composite systems include concrete reinforced with steel and epoxy reinforced with graphite fiber, etc.

### 2.1.2 Classify composites

Composites are classified by the geometry of the reinforcement – particulate, flake, and fiber. (Figure 2.1)

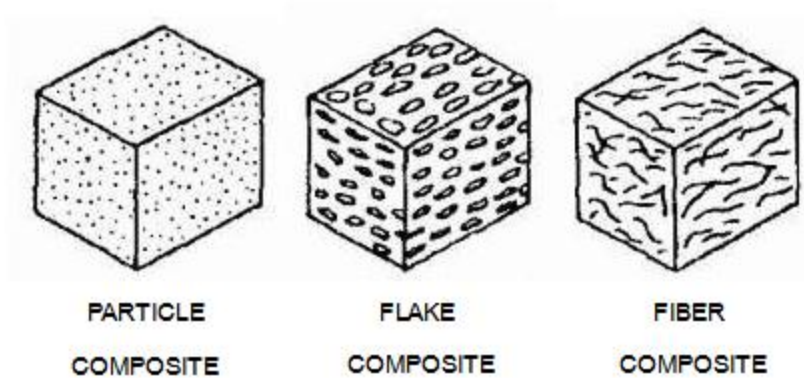


Figure 2.1 Types of composites based on reinforcement shape.

#### 2.1.2.1 Classification of composite based on the geometry of the reinforcement.

[7.9]

- *Particulate composites* consist of a matrix reinforced with a dispersed phase in form of particles. They are usually isotropic because the particles are added randomly. Particulate composites have advantages such as improved strength, increased operating temperature, oxidation resistance, etc. Typical examples include use of aluminum particles in rubber; silicon carbide particles in aluminum; and gravel, sand, and cement to make concrete.

- *Flake composites* consist of flat reinforcements of matrices. Typical flake materials are glass, mica, aluminum, and silver. Flake composites provide advantages such as high out-of- plane flexural modulus, higher strength, and low cost. However, flakes cannot be oriented easily and only a limited number of materials are available for use.

- *Fiber composites* consist of matrices reinforced by short (discontinuous) or long (continuous) fibers. Fibers are generally anisotropic and examples include carbon and aramids. Examples of matrices are resins such as epoxy, metals such as aluminum, and ceramics such as calcium-alumino silicate.

#### 2.1.2.2 Classification of composite based on the type of matrix [10]

- *Polymer Matrix Composites (PMCs)* consist of a polymer (e.g., epoxy, polyester, urethane) reinforced by thin diameter fibers (e.g., graphite, aramids, boron), such as graphite/epoxy composites, glass fiber/polyester. The PMCs is the most common advanced composites due to its can be fabricated into large, complex shapes, and have been accepted in a variety of aerospace and commercial applications.

- *Metal Matrix Composites (MMCs)*, as the name implies, have a metal matrix. Examples of matrices in such composites include aluminum, magnesium, and titanium. Typical fibers include carbon and silicon carbide. Because of their use of metals as matrix materials, they have a higher temperature resistance than PMCs but in general are heavier.

- *Ceramic Matrix Composites (CMCs)* have a ceramic matrix such as alumina calcium alumino silica reinforced by fibers such as carbon or silicon carbide. They have the potential for high-temperature resistance but also have fundamental limitations in structural applications owing to their propensity for brittle fracture.

### 2.1.3 Interfacial bonding [11]

Good bonding (adhesion) between the matrix phase and dispersed phase to transfer the load of applied to the material the dispersed phase via the interface. Adhesion is necessary for achieving high level of mechanical properties of the composite.

There are three forms of interface between the two phases:

1. Direct bonding with no intermediate layer. In this case adhesion ("wetting") is provided by either covalent bonding or van der Waals force.
2. Intermediate layer in form of solid solution of the matrix and dispersed phases constituents.
3. Intermediate layer (interphase) in form of a third bonding phase (adhesive).

### 2.2 Polymer degradation [12]

The American Society for Testing of Materials (ASTM) and the International Standard Organization (ISO) define degradable polymer or degradable plastic as those which undergo a significant change in chemical structure under specific environmental conditions. These changes result in a loss of physical and mechanical properties, as measured by standard methods. So the degradable plastic was grouped by ASTM D20.96 as

1. Photodegradable or light-induced degradation plastic is a degradable plastic in which the degradation results from the action of natural daylight.



2. Oxidatively degradable plastic is a degradable plastic in which the degradation results from the oxidation.

3. Hydrolytically degradable plastic is a degradable plastic in which degradation result from hydrolysis.

4. Biodegradable plastics are plastics in which the degradation results from the action of naturally occurring are two classes of microorganism such as bacteria, fungi and algae.

However, according to the definition of degradable plastic in categories, 1 to 3. Additional input such as light (UV) or oxygen is required for degradation, the biodegradation plastic in number 4 offers only products which are naturally degradable.

### 2.3 Biodegradable polymer

When considering biodegradable plastic, there biodegradable plastic has been popular in many applications for decades, which leads the scientists focused on research and development in the current situation. Moreover, these polymer materials are usually referred to in the general class of plastics by consumers and industry. [13]

1. The first class of biodegradable plastic under consideration is partially degradable. The products of this class usually have a matrix (petroleum base) and biodegradable materials were used as filler in matrix. It is designed with the goal of more rapid degradation than the conventional plastic. When it is disposed, microorganisms are able to consume the biodegradable material within the conventional plastic matrix. This leaven causes a weakened material, with rough, open edges. Further degradation is occurred. This group of materials usually has an impenetrable petroleum based matrix such as starch filled polyethylene film.

2. The second class of biodegradable plastic is compostable polymer. This is a completely biodegradable plastic that is attracting a lot of attention from researchers and industry. The product in this class includes only the biodegradable polymer material such as biocomposite that matrix is derived from natural sources, i.e. starch or microbially grown polymers, and the fiber reinforcements are produced from common crops such as flax or hemp. Microorganisms are able to consume these materials in their entirety eventually leaving carbon dioxide and water as by-products.

In recent years, there has been increased interest in biodegradable material for packaging application. The belief is that biodegradable polymer will reduce the need for synthetic polymer production and reduce pollution. Moreover, it is producing a positive effect on both environmentally and economically. The innovations in the development of materials from biopolymers, complete biological degradability, the reduction in the volume of waste and compostability, reduction of atmospheric carbon dioxide released are some of the reasons for the increased public interest. Furthermore, biodegradable polymers are growing into mainstream use and the polymers that are biopolymer or based on renewable feedstock may soon be competing with commodity plastics.

Biodegradable polymer was categorized into four families based on source as shown in **Figure 2.2** [4].

1. Agro-polymers obtained from biomass by fraction such as starch, cellulose, protein and lipid.

2, Polyester obtained by fermentation of biomass or from genetically modified plants such as polyhydroxyalkanoate: PHA, poly(hydroxybutyrate): PHB.

3. Polyester synthesis from monomer obtained from biomass such as polylactide and polylactic acid: PLA.

4, Polyester totally synthesized by the petrochemical process such as polycaprolactone: PCL, polyesteramide: PEA and aliphatic or aromatic copolyesters.

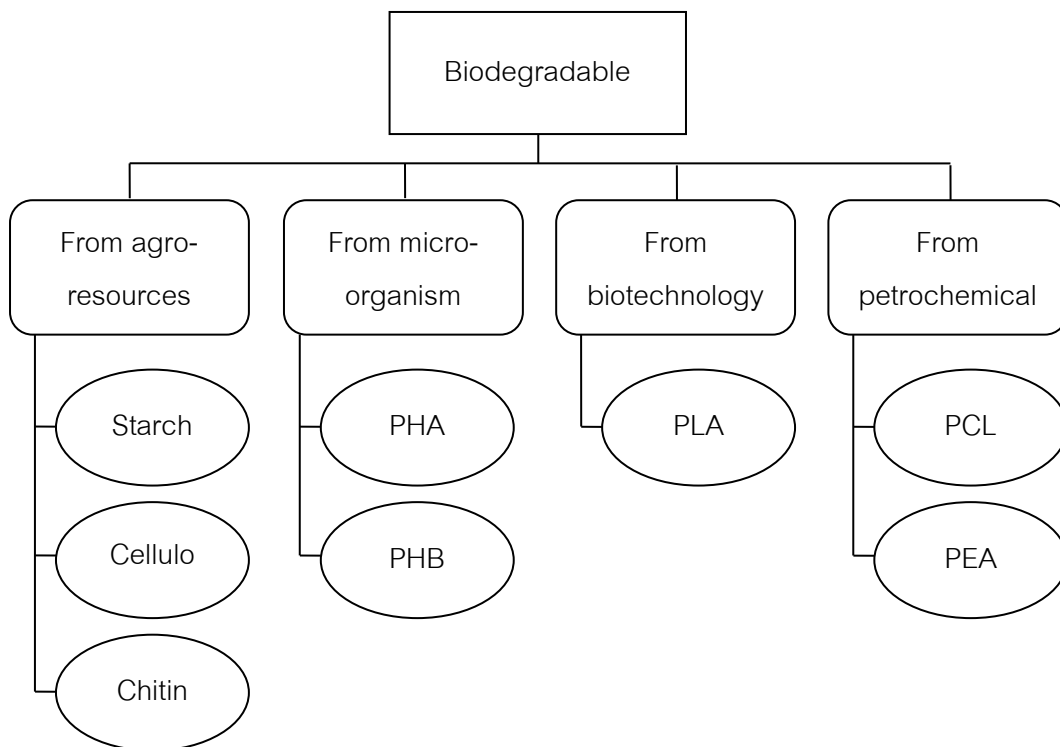


Figure 2.2 Classification of biodegradable polymer [4]

Among biodegradable polymer, PLA is at present one of the most promising biopolymers and can be processed with a large number of techniques and is commercially available (large-scale production) in a wide range of grades.

### 2.3.1 Polylactic acid [14, 15]

Polylactic acid (PLA) is a rigid thermoplastic polymer that can be semicrystalline or totally amorphous, depending on the stereo purity of the polymer backbone. L(-)-lactic acid (2-hydroxy propionic acid) is the natural and most common form of the acid, but D(+)-lactic acid can also be produced by microorganisms or through racemization and this “impurity” acts much like comonomers in other polymers such as polyethylene terephthalate (PET) or polyethylene (PE). In PET, diethylene glycol or isophthalic acid is

copolymerized into the backbone at low levels (1-10%) to control the rate of crystallization. In the same way, D-lactic acid units are incorporated into L-PLA to optimize the crystallization kinetics for specific fabrication processes and applications.

PLA is a unique polymer that in many ways behaves like PET, but also performs a lot like polypropylene (PP), a polyolefin. Ultimately it may be the polymer with the broadest range of applications because of its ability to be stress crystallized, thermally crystallized, impact modified, filled, copolymerized, and processed in most polymer processing equipment. It can be formed into transparent films, fibers, or injection molded into blow moldable preforms for bottles, like PET. PLA also has excellent organoleptic characteristics and is excellent for food contact and related packaging applications.

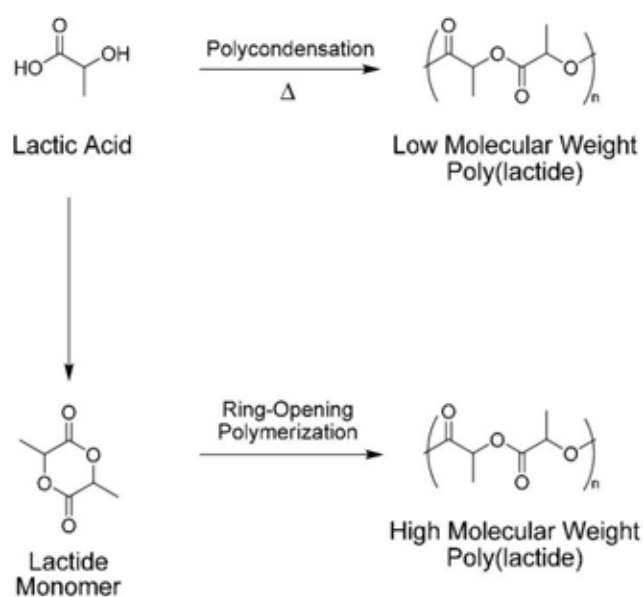
In spite of this unique combination of characteristics, the commercial viability has historically been limited by high production costs (greater than \$2/lb). Until now PLA has enjoyed little success in replacing petroleum-based plastics in commodity applications, with most initial uses limited to biomedical applications such as sutures.

PLA is not new to the world of polymers. Carothers investigated the production of PLA from the cyclic dimer (lactide) of lactic acid as early as 1932. Even before that, low molecular weight dimers and oligomers were detected when water was removed from an aqueous solution of lactic acid. The announcement of the formation of a new company, Cargill Dow LLC, in 1997 brought two large companies together to focus on the production and marketing of PLA with the intention of significantly reducing the cost of production and making PLA a large-volume plastic.

In today's world of green chemistry and concern for the environment, PLA has additional drivers that make it unique in the marketplace. The starting material for the final polymer, lactic acid, is made by a fermentation process using 100% annually

renewable resources. The polymer will also rapidly degrade in the environment and the by-products are of very low toxicity, eventually being converted to carbon dioxide and water.

PLA can be prepared by both direct condensation of lactic acid and by the ring-opening polymerization of the cyclic lactide dimer, as shown in **Figure 2.3**. Due to the direct condensation route is an equilibrium reaction, difficulties of removing trace amounts of water in the last stages of polymerization generally limit the ultimate molecular weight achievable by this approach. Most work has focused on the ring-opening polymerization of lactide, although other approaches, such as azeotropic distillation to drive the removal of water in the direct esterification process, have been evaluated.



**Figure 2.3** Two common approaches used to synthesize PLA [16]

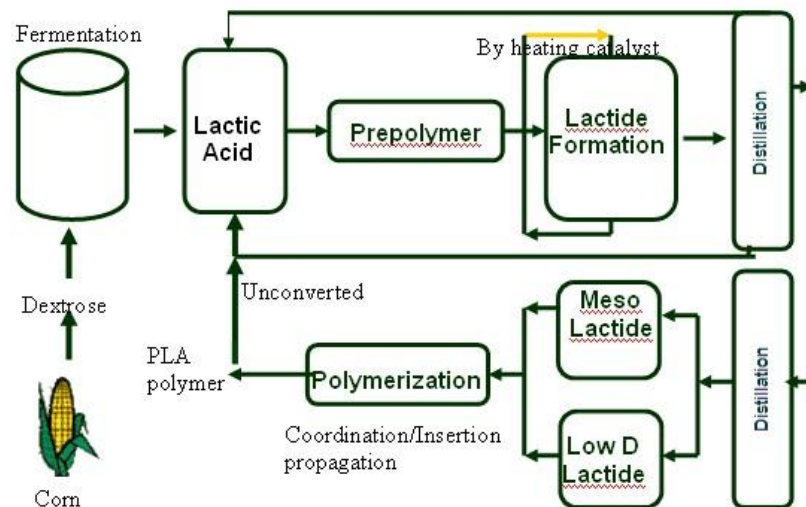


Figure 2.4 Nonsolvent process to prepare polylactic acid [17]

Cargill Dow LLC has developed a patented, low-cost continuous process for the production of lactic acid-based polymers. The process combines the substantial environmental and economic benefits of synthesizing both lactide and PLA in the melt rather than in solution and, for the first time, provides a commercially viable biodegradable commodity polymer made from renewable resources. The process starts with lactic acid produced by fermentation of dextrose, followed by a continuous condensation reaction of aqueous lactic acid to produce low molecular weight PLA polymer (Figure 2.3). Next, the low molecular weight oligomers are converted into a mixture of lactide stereoisomers using a catalyst to enhance the rate and selectivity of the intramolecular cyclization reaction. The molten lactide mixture is then purified by vacuum distillation. Finally, PLA high polymer is produced using an organo tin-catalyzed, ring-opening lactide polymerization in the melt, completely eliminating the use of costly and environmentally unfriendly solvents. After the polymerization is complete, any remaining monomer is removed under vacuum and recycled to the beginning of the process. (Figure 2.4)

PLA has been extensively studied by many researchers and reviewed in detail in several recent publications. For example, Jacobsen et al. (2000) developed, based on a new catalytic system, a reactive extrusion polymerization process, which can be used to produce PLA continuously in larger quantities and at lower costs than before. This extrusion polymerization process has been developed and tested with laboratory scale machines and the possibilities to extend this polymerization process to lactide based block copolymers have been investigated. [18] Recently, Lim et al. (2008) discussed the specific process technologies such as extrusion, injection molding, injection stretch blow molding, casting, blown film, thermoforming, foaming, blending, fiber spinning, and compounding related to PLA. [19]

#### **2.4 Natural Fibers [14]**

Depending on their origin, natural fibers can be grouped into bast (jute, flax, hemp, kenaf), leaf (pineapple, sisal, screw pine), and seed or fruit fibers (coir, cotton, oil palm). Cellulose is the main component of natural fibers and can be found in plant cell wall. Unlike conventional fibers like glass, aramid, and carbon that can be produced with a definite range of properties, natural fibers will vary considerably. The cellulose of natural fibers contains different natural substances such as lignin and waxes. The fibers are made up of cellulose microfibrils bonded together by lignin. The physical properties of natural fibers are basically influenced by the chemical structure such as cellulose content, degree of polymerization, orientation, and crystallinity, which are affected by conditions during growth of plants as well as extraction methods used. The fiber properties vary considerably depending on where they are taken from a plant, the plant quality, and location. Different fibers have different lengths and cross-sectional areas and also different defects such as microcompression or pits or cracks.





### 2.5.3 Crystalline structure

Solid cellulose shows a highly ordered microcrystalline structure alternating with regions of distinctly lower (amorphous regions). The crystalline nature of cellulose originates from intermolecular forces between neighbouring cellulose chains over long lengths. All native cellulose shows the same crystal lattice structure, called cellulose I. However, various modification of native cellulose can alter the lattice structure to yield other types of crystals [20, 22]. The intermolecular forces in the crystalline domains are mainly hydrogen bonds between adjacent cellulose chains in the same lattice plane, which results in a sheet-like structure of packed cellulose chains. In addition, the sheets are probably connected to one another by hydrogen bonds and/or van der Waal's forces. The organization of cellulose molecules into parallel arrangements is responsible for the formation of crystallites. The length of an elementary crystallite range from 12 to 20 nm and the width from 2.5 to 4 nm.

**Table 2.1** Chemical composition of some cellulose source (according to Horn [23])

Source	Composition (%)			
	Cellulose	Hemicellulose	Lignin	Extract
Wheat straw	30	50	15	5
Flax	71.5	20.6	2.2	60
Jute	71.2	13.6	13.1	1.8
Soft wood	40-44	25-29	25-31	1-5
Hard wood	43-47	25-35	16-24	2-8
Ramie	76.2	16.7	0.7	6.4

Cotton

95

2

0.9

0.4

---

## 2.6 Cotton (*Gossypium* spp., Malvaceae) [14]

The variety *Gossypium hirsutum* accounts for most of the world's production of cotton (87% of the overall production), *G. barbadense* for 8%, the species *G. herbaceum* and *G. arboretum* for only 5%. Cotton fibers consist of the unicellular seed hairs of the bolls of the cotton plant. The cotton fruit burst when mature, revealing a fist-sized tuft of fibers with a length from 25 to 60 mm and diameters varying between 12 and 45  $\mu\text{m}$ . Cotton is of tropical origin but is most successfully cultivated in temperate climates with well-distributed rainfall. Cotton fibers have been used by early societies to produce textiles. The oldest archeological evidence of cultivated cotton is some cottonseed fragments discovered in a cage in Mexican Tehuacan Valley, dated to 5800 B.C. Cotton was used to fabricate textiles as early as 3000 B.C. in Indus Valley in Pakistan and around 2500 B.C. in Peru. Increased use of cotton fibers in Europe was boosted by the development of the first ring-spinning wheel ("Spinning Jenny"), invented by James Hargreaves in 1764, and by the rippling machine (the "cotton gin" invented by Eli Whitney in 1794).

Cotton fibers have a pronounced three-walled structure. An outer wax layer protects the primary wall. The secondary cell wall consists mainly of cellulose. The tertiary wall surrounds the lumen. Mature cotton fibers have kidney-ben shaped cross sections. The surface contour of the fibers is flat and twisted, ribbon-like. The color of cotton ranges from creamy white to dirty gray depending upon the conditions under which it is produced. Cotton is hydrophilic and the fibers swell considerably in water. Cotton release a considerable amount of heat when absorbing moisture. It dries slowly. Cotton has high soil and oil absorption but also high release. It is stable in water and its wet tenacity is higher than its dry tenacity. The toughness and initial modulus of cotton are lower compared to hemp fibers, whereas its elongation at break, its flexibility, and its elastic recovery are higher. The fibers are resistant to alkalis but degraded by acids.

The microbial resistance of cotton is low but the fibers are highly resistant to moths and beetles. Cotton burns readily and quickly, can be boiled and sterilized, and does not cause skin irritation or other allergies.

Innumerable products are made from cotton, primary textile and yarn goods, cordage, and automobile tire cords. Cotton fibers are the backbone of the textile trade of the world.

## 2.7 Crystalline Cellulose Preparation [21]

Crystalline cellulose has been widely used especially in food, cosmetic, medical and biocomposite film as a water-retainer, a suspension stabilizer, a flow characteristics controller in the systems used for final products and as a reinforcing agent for biocomposite films. The basic step for preparing crystalline cellulose from native plant has generally three steps that is delignification, bleaching and hydrolysis. The step of delignification and bleaching is remove lignin and other composition in microfibrils to produce cellulose microfibrils. Moreover, lignin and other composition effects on hydrolysis reaction in cellulose microfils because they are obstructive to the hydrolysis reaction, that to dissolve the amorphous regions of the polysaccharide. So they are must be remove as much possible. This research focuses on the preparation of microcrystalline cellulose (MCC) from acid hydrolysis.

### 2.7.1 Hydrolysis

Crystalline cellulose is prepared from removing of amorphous regions in cellulose microfibrils. Under controlled conditions, this transformation consists of the disruption of amorphous regions surrounding and embedded within cellulose microfibrils that is occurred on  $\beta$ -1,4- glycosidic linkage, while leaving the micro or nanocrystalline segments intact. However, size and shape of crystalline depend on type and nature of plant.

- Enzyme hydrolysis process is the mild condition. This process is depolymerization of cellulose via chemical reaction catalyzed by enzymes which are synthesized by microorganisms such as cellulase which is isolated from bacteria and fungi. The reaction of enzyme hydrolysis depends on the reaction condition such as temperature, pH and pressure. The advantage of enzyme hydrolysis is the mild condition and has very specific action. Furthermore, the product from this process is high purification. However, this process is not well-known for industries owing to the enzyme hydrolysis is a slow reaction and high cost.

- The acid hydrolysis of cellulose is strong condition. The reaction of acid hydrolysis depends on type of acid, temperature and time. The great advantage of this process is simple and economical. Furthermore, acid hydrolysis is quite rapid reaction and low cost. On the other hand, the advantage of acid hydrolysis is not specific reaction and the product is not purification. However, the acid hydrolysis is well-known process for industry because it is viable commercially and simple. In fact, concentrated acids give quantitative yields of hydrolysis of micro-crystalline cellulose powder (MCP). However, in native cellulose it is difficult to hydrolyse because it is presented as a highly ordered crystalline structure and lignin accompanying the cellulose fiber inhibits hydrolysis. In addition, treatment with alkali could remove lignin as well as some hemicelluloses from the native cellulose and thus make cellulose more accessible to hydrolytic attack. Alkali treatment also makes the cellulose structure amorphous and may render it more prone to hydrolysis [23].

From the several advantages of acid hydrolysis, many researches have been studied crystalline cellulose prepared from acid hydrolysis process. Their researches have been focused on physical and chemical properties and size of crystalline cellulose.

In 1953, Nelson and Tripp [24] prepared microcrystalline cellulose from cotton and rayon. The cotton and rayon were hydrolyzed by hydrochloric acid (HCl) at 100, 80°C. By various concentration of HCl were 0.01N, 0.1N, 1.0N, and 2.5N, respectively. The result showed that conditions in the reaction at higher concentrations and temperature were effect on the reaction faster than at lower concentrations and temperature.

## 2.8 Fiber-reinforced PLA composites

Natural fiber-reinforced polymers has recently grown because of increasing environmental concerns. Natural fiber reinforcements could considerably lower the price of bio-based composites that is still the higher barrier for their wider application. Further advantages of natural over synthetic fibers are good specific mechanical properties, reduced tool wear, enhanced energy recovery, biodegradability, etc. Besides this, the natural fibers can also affect the mechanical properties of bio-matrices. In the last years different natural fibers have been employed in order to modify the properties of PLA. Up to now, the most studied natural fiber reinforcements for PLA were kenaf [5,25,26], flax [27,28], hemp [29], bamboo [30], and wood fibers [31].

For example, in 2003, Plackett, Andersen, Pedersen, and Nielsen[32] used PLA and then used in combination with jute fiber mats to generate biodegradable composites by a film stacking technique. The tensile properties of composites produced at temperatures in the 180–220 °C range were significantly higher than those of PLA alone. Examination of composite fracture surfaces using electron microscopy showed voids occurring between the jute fiber bundles and the polylactide matrix.

Later in 2008, Bax and Mussig [27] studied the mechanical properties of PLA composites reinforced with Cordenka® rayon fibers and flax fibers which are examples for completely biodegradable composites were tested and compared. The samples were produced using injection moulding. The highest impact strength of 72 kJ·m<sup>-2</sup> and

tensile strength of 58 MPa were found for Cordenka® reinforced PLA at 30 wt% fiber-mass content. The highest Young's modulus of 6.31 GPa was found for the composite made of PLA and flax. A poor adhesion between the matrix and the fibers was shown for both composites using SEM. The promising impact properties of the presented PLA/Cordenka® composites show their potential as an alternative to traditional composites.

Within the same year, Buzarovska et al [33] investigated the effects of rice straw content on thermal and mechanical properties of poly (hydroxybutyrate-co-hydroxyvalerate) (PHBV) composites. It was shown that the value of tensile modulus value almost doubled with the increase of rice straw content, while the tensile strength slightly decreased, compared to pure PHBV resin. The decreasing of tensile strength related to very poor adhesion between the polymer matrix and the filler, are confirmed by SEM photomicrographs of the fractured samples.

Natural fibers are hydrophilic in nature and poor resistance to moisture and incompatible to hydrophobic polymer matrix. This incompatibility of natural fibers results in poor fiber/matrix interface which in turn leads to reduce mechanical properties of the composites (John & Anandjiwala, 2008) [34]. The researchers have been used many methods to improve interfacial between matrix and fiber such as the treatment of the fibers may be alkali, acetylation, bleaching, grafting of monomer, and so on. However, plasma surface treatment and plasma polymerization as an alternative coating technique have been mainly used for surface modification of fibers. The details are as follows

In 2007, the effects of the alkali treated natural fibers on the mechanical properties of PLA/hemp fibers were studied by Hu and Lim [29]. They fabricated completely biodegradable composites of PLA reinforced with short hemp fibers by using the hot-press method. The results show that the composite with 40% volume fraction of alkali treated fiber possessed the best mechanical properties. The tensile strength,

elastic modulus, and flexural strength of the composite with 40% treated fiber were 54.6 MPa, 8.5 GPa, and 112.7 MPa respectively, which are much higher than those of neat PLA. The composites have lower densities, which were measured to be from  $1.19 \text{ g}\cdot\text{cm}^{-3}$  to  $1.25 \text{ g}\cdot\text{cm}^{-3}$ . Surface treatment of the natural fibers was used also to improve the impact resistance of the PLA-based composites.

A more efficient way to improve the adhesion between fibers and biodegradable resin could be provided by the utilization of coupling agents. In PLA/kenaf fiber composites a suitable reactive coupling agent was obtained by grafting maleic anhydride onto PLA [25,26]. PLA-based composites were prepared by a proper *in situ* reactive compatibilization. Namely, low amount of PLA grafted with maleic anhydride (PLA-g-MA) was added to the composite components. Maleic anhydride groups grafted onto PLA chain are reactive with respect to hydroxyl groups present on the fiber surface. In this way, interactions between hydroxyl and maleic anhydride groups are responsible for *in situ* formed grafted species that are able to effectively compatibilize PLA/fiber composites. In fact, morphological analysis carried out on these systems revealed that a significant enhancement of the adhesion level between the fibers and the matrix is observed for PLA/kenaf composites compatibilized by using 5 wt% PLA-g-MA. Significant improvements of the flexural modulus, up to 55%, were recorded as a function of kenaf fiber content. Higher modulus values were obtained in presence of the reactive coupling agent. The same behavior has been observed for the flexural strength, the highest values being obtained for compatibilized composites reinforced with 30 wt% of kenaf fibers. Also the resilience of neat PLA was improved, up to about 190%, for compatibilized composites.

Later on 2011, Nyambo et al [35] investigated the use of PLA-g-MA as a potential method for improving interfacial adhesion between agricultural residues and PLA. The result showed that addition of 3 and 5 phr PLA-g-MA to the composites resulted in significant improvements in tensile strength (20%) and flexural strength (14%) of the composites, matching that of the neat polymer. The observed improvement in strength was attributed to the good interfacial adhesion between the fiber and matrix.



## 2.9 Biodegradation [12,13]

### 2.9.1 Defining Biodegradability

In 1992, an international workshop on biodegradability was organized to bring together experts from around the world to achieve areas of agreement on definitions, standards and testing methodologies. Participants came from manufacturers, legislative authorities, testing laboratories, environmentalists and standardization organizations in Europe, USA and Japan. Since this fruitful meeting, there is a general agreement concerning the following key points.

- For all practical purposes of applying a definition, material manufactured to be biodegradable must relate to specific disposal pathway such as composting, sewage treatment, denitrification and anaerobic sludge treatment.
- The rate of degradation of a material manufactured to be biodegradable has to be consistent with the disposal method and other components of the pathway into which it is introduced, such that accumulation is controlled.
- The ultimate end products of aerobic biodegradation of a material manufactured to be biodegradable are CO<sub>2</sub>, water and minerals and that the intermediate products include biomass and humic materials. (Anaerobic biodegradation was discussed in less detail by the participants).
- Materials must biodegrade safely and not negatively impact the disposal process or the use of the end product of the disposal.

As a result, specified periods of time, specific disposal pathway, and standard test methodologies were incorporated into definitions. Standardization organizations such as CEN, ISO and ASTM were consequently encouraged to rapidly develop standard biodegradation tests so these could be determined. Society further demanded

undebatable criteria for the evaluation of the suitability of polymeric materials for disposal in specific waste streams such as composting or anaerobic digestion. Biodegradability is usually just one of the essential criteria, besides ecotoxicity, effects on waste treatment processes, etc.

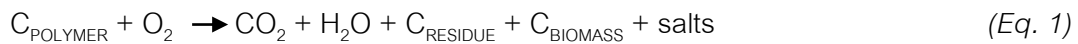
The used definitions for biodegradation remain rather broad since they have to be acceptable to all parties involved. In this paper, however, biodegradation is addressed from a more scientific point of view. The following definitions are therefore applied as a basis.

- **Degradation** is the irreversible process in which a material undergoes physical, chemical and/or biochemical changes leading to an increase in entropy.
- **Biodegradation** is degradation catalysed by biological activity, ultimately leading to mineralization and/or biomass.
- **Mineralization** is the conversion of (organic) material to naturally occurring gasses and/or inorganic elements.
- **Biodegradability** is the potential of a material to be biodegraded. Biodegradability of a material shall be specified and measured by standard test methods in order to determine its classification with respect to specific environmental conditions.
- **Biodegradable** A material is called biodegradable with respect to specific environmental conditions if it undergoes biodegradation to a specified extent, within a given time, measured by standard test methods.

The chemistry of the key degradation process is represented below by equation (1) and (2) where  $C_{\text{POLYMER}}$  represents either a polymer or a fragment from any of the degradation processes defined earlier. For simplicity here, the polymer or fragment is

considered to be composed only of carbon, hydrogen and oxygen; other elements may, of course, be incorporated in the polymer, and these would appear in an oxidized or reduced form after biodegradation depending on whether the conditions are aerobic or anaerobic, respectively.

*Aerobic biodegradation:*



*Anaerobic biodegradation:*



Complete biodegradation occurs when no residue remains, and complete mineralization is established when the original substrate,  $C_{\text{POLYMER}}$  in this example, is completely converted into gaseous product and salts. However, mineralization is a very slow process under natural conditions because some of the polymer undergoing biodegradation will initially be turned into biomass. Therefore, complete biodegradation and not mineralization is the measurable goal when assessing removal from the environment.

## 2.10 Method of Biodegradation

Biodegradation is the natural process. The biodegradable process is organic substances are attacked by living organisms. The organic material can be degraded aerobically, with oxygen, or anaerobically, without oxygen, and it is converted into small molecule such as  $H_2O$  and  $CO_2$ . The change in the chemical structure of biodegradable plastics under specific environmental conditions results in a loss of some properties including physical and mechanical properties. The biodegradation processes are usually followed by monitoring the changes in these properties using standard test methods appropriate to the plastic. Today's plastics are designed with little

consideration for their ultimate disposability. This has resulted in mounting worldwide concerns over the environmental consequences of such materials because they were entered to the waste stream after their uses especially in single use and disposal plastic applications. Polymer waste management requires sound complementary practices of conservation, recycling, incineration and biodegradation. Since biodegradation is potentially the most environmentally friendly of all these practices, there is activity in the area of biodegradable polymers as packaging materials. Generally, starch removal does occur when the starch-based films are exposed to microbial. The first mechanism of degradation is the production of enzyme amylase by microbial [17].

Generally, there are several ways to test the biodegradability of plastics. The methods for testing biodegradability are highlighted as following:

#### **2.10.1 Environmental Chamber Method**

Environmental chambers employ high humidity (>90%) situation to encourage microbial growth. Test material are hung in the chamber, sprayed with a standard mixed in columns of known fungi in the absence of additional nutrients and incubated for 28 to 56 day at constant temperature. A visual assessment is subsequently made and a rating given based on the amount of growth on the material. This test is particularly stringent and was designed to simulate the effects of high humidity condition on electronic components and electrical equipment. Growth of fungi across a printed circuit board can result in gross systems failure in a computer system or military equipment.

#### **2.10.2 Soil Burial tests**

The material is buried in soil beds prepared in the laboratory. The soil beds containing the samples are incubated at a constant temperature for between 28 days and 12 months. The soil beds are normally conditioned for up to 4 weeks prior to use and may be supplemented with organic fertilizer to encourage an active microbial. The

microbial activity is tested using a cotton textile strip, which should lose 90% of its tensile strength within 10 days of exposure to the soil. The moisture content is normally set at 20-30%. Samples are removed for assessment of changes in their properties such as weight loss, mechanical properties or morphology that is surface damage. However, the soil burial tests are that a 3 to 6 month tests is sufficient to demonstrate the environmental resistance of polymer materials [46].

### **2.10.3 Specific Microorganism or Enzyme Degradation**

Biodegradation is an event which takes place through the action of enzymes associated with living organisms (bacteria, fungi, etc.). Generally, microorganism produced enzyme involving in the chemical mode of degradation and attack natural polymer. The attack is specific with specific with respect to both the enzyme and biopolymer couple. All enzymes are protein, even small changes in temperature or pH can result in changes in the enzyme activity. The accessibility of a polymer to be degradatively attacked by living organisms has no direct reaction to its origin and not all biopolymer are truly biodegradable. This test method is also appropriate for the evaluation of degradable plastic that have undergo specific chemical, thermal or photo degradation or combination.

### **2.10.4 Activative sludge Waste water treatment**

This method is the simulation studies range from laboratory designed equipment, which replicates aerobic sewage treatment anaerobic sludge digestion, through the exposure trials and where material is submerged in activated sludge environment. Exposure trials require that the samples be securely held on some form of racking for aqueous environments. The racks, normally made of stainless steel, are submerged in the test situation and samples periodically removed. This test method is

designed to be applicable to all plastic materials that are not inhibitory to the bacterial present in the activated sludge.

Biodegradation is nature's way of recycling wastes, or breaking down organic matter into nutrients that can be used by other organisms. "Degradation" means decay, and the "bio-" prefix means that the decay is carried out by a huge assortment of bacteria, fungi, insects, worms, and other organisms that eat dead material and recycle it into new forms.

In nature, there is no waste because everything gets recycled. The waste products from one organism become the food for others, providing nutrients and energy while breaking down the waste organic matter. Some organic materials will break down much faster than others, but all will eventually decay.

By harnessing these natural forces of biodegradation, people can reduce wastes and clean up some types of environmental contaminants. Through composting, we accelerate natural biodegradation and convert organic wastes to a valuable resource. Wastewater treatment also accelerates natural forces of biodegradation. In this case the purpose is to break down organic matter so that it will not cause pollution problems when the water is released into the environment. Through bioremediation, microorganisms are used to clean up oil spills and other types of organic pollution. Composting and bioremediation provide many possibilities for student research.

Currently, there are standard test methods that are designed for determining biodegradation of plastic materials in order to properly select for studying rate of biodegradation of various plastics both degradable and nondegradable plastics. Many researchers have been studied on biodegradation of plastics by comparing the standard test methods and type of plastics.

For instance, in 2010, Moura et al [36] studied the biodegradability of blends containing aliphatic polyesters using standard methods. Biodegradable polymers used

were poly(lactic acid) (PLA), poly( $\epsilon$ -caprolactone) (PCL), and Mater-Bi (thermoplastic starch with PLA or PCL). Biodegradation tests were carried out using two standard methods: (i) ISO 14851 (1999), biochemical oxygen demand in a closed respirometer and (ii) ASTM G 22-76, microbial growth of test microorganisms. Both biodegradability tests suggested that the blend containing PCL is more biodegradable than the one containing PLA. Addition of starch increased the biodegradability of the PLA blend. The biodegradability of the blends evaluated in this study by the biochemical oxygen demand method ranged from 22% (PLA 60) to 52% for corn starch/PCL 30/70 (% wt) (SPCL 70). Therefore, the blends may not be considered “readily biodegradable” according to the OECD standard.

In the same year, Chin-San Wu [37] investigated biodegradability of composite materials composed of polylactide (PLA) and sisal fibers (SFs) were buried in soil. Both the PLA and the PLA-g-AA/SF composite films were eventually completely degraded, and severe disruption of film structure was observed after 6–10 weeks of incubation. Although the degree of weight loss after burial indicated that both materials were biodegradable even with high levels of SF, the higher water resistance of PLA-g-AA/SF films indicates that they were more biodegradable than those made of PLA.

As far as biodegradability is concerned, it has been confirmed that PLA is naturally degraded in soil or compost even if it is known that PLA is less susceptible to degradation than other aliphatic biodegradable polymers such as poly( $\epsilon$ -caprolactone) (PCL) in natural environment (Ghorpade et al., 2001). It was reported that the products of the PLA hydrolytic degradation can be totally assimilated by microorganisms such as fungi or bacteria (Tsuji et al., 1998; Li et al., 2000; Hoshino et al., 2003). Biodegradation of PLA and its copolymers are usually done by esterases, proteases and lipases secreted from microorganisms.

In 2009, Sebastien Lenglet, Suming Li, Michel Vert [3] reported on the enzymatic biodegradation of copolymers of 3-caprolactone and DL-lactide in the presence of

Pseudomonas lipase with the aim of identifying the effect of composition on the degradation characteristics of PCL/PLA copolymers. The copolymers were processed to films by compression moulding, and allowed to degrade at 37 °C in a 0.05 M pH 7.6 phosphate buffer containing Pseudomonas lipase. Degradation in the presence of Pseudomonas lipase shows that copolymers with caprolactone (CL) contents lower than 25% are not degradable. The degradation rate increases with CL content for CL rich copolymers.



## CHAPTER 3

### EXPERIMENTAL

#### 3.1 Materials and Chemicals

3.1.1 Polylactic acid (PLA 2002D) purchased from Naturework<sup>®</sup> LLC (Cargill-Dow, Minneapolis, MN) was used as a matrix of composites. The MFI for the PLA is between 5 and 7 g/10 min. It has a specific gravity of 1.24. The glass transition and melting temperatures of PLA are 60 °C and 210°C, respectively. Its chemical structure is shown in Figure 3.1

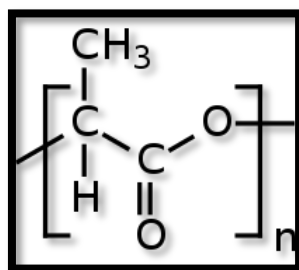


Figure 3.1 Chemical structure of polylactic acid

3.1.2 Bleached knitted cotton fabric obtained from a local company in Thailand was used as a raw material for microcrystalline cellulose preparation.

3.1.3 Hydrochloric acid (HCl, analytical reagent) purchased from Labscan Asia Co., Ltd., Bangkok, Thailand was used to hydrolyze cotton fabric.

3.1.4 Tetrahydrofuran (THF, analytical reagent) purchased from Labscan Asia Co., Ltd., Bangkok, Thailand was used as a solvent for PLA.

3.1.5 Benzoyl peroxide (BPO, analytical reagent) obtained from Merck Ltd., Bangkok, Thailand was used as an initiator.

3.1.6 Maleic anhydride (MA, analytical reagent) obtained from Siam Chemical Industry Co., Ltd., Bangkok, Thailand was used as a grafting material for maleic anhydride – grafted polylactic acid (PLA-g-MA) preparation.

3.1.7 Diethyl ether purchased from Labscan Asia Co., Ltd., Bangkok, Thailand, was used as a precipitate reagent.

3.1.8 Sodium acetate ( $\text{NaC}_2\text{H}_3\text{O}_2$ , analytical reagent) obtained from Merck Ltd., Bangkok, Thailand was used as a buffer for preparing acetate buffer solution.

3.1.9 Acetic acid ( $\text{CH}_3\text{COOH}$ , analytical reagent) obtained from Labscan Asia Co., Ltd., Bangkok, Thailand was used as a buffer for preparing acetate buffer solution.

3.1.10 Potassium dihydrogen orthophosphate ( $\text{KH}_2\text{PO}_4$ , analytical reagent) obtained from Ajax Finechem Nuplex Industries Pty., Ltd., New South Wales, Australia was used as a buffer for preparing phosphate buffer solution.

3.1.11 di-potassiumhydrogen orthophosphate  $\text{K}_2\text{HPO}_4$ , analytical reagent) obtained from Ajax Finechem Nuplex Industries Pty., Ltd., New South Wales, Australia was used as a buffer for preparing phosphate buffer solution.

### 3.2 Equipments and Instruments

Table 3.1 lists the instruments used in this research.

**Table 3.1** Experimental instruments

Instruments	Model	Manufacturer
1. Hot plate	MR Hei-standard	Heidolph, Germany
2. Scanning electron microscope (SEM)	JSM-6480LV	JEOL, Japan
3. Fourier Transform Infrared Spectrometer (FT-IR)	Nicolet 6700	Thermo Scientific, USA
4. Laser particle size analyzer	Mastersizer 2000	Malvern Instruments, UK
5. Thermogravimetric analyzer (TGA)	TGA/SDTA 851 <sup>e</sup>	Mettler Toledo, Switzerland
6. Differential scanning calorimeter (DSC)	Pyris Diamond DSC	PerkinElmer, USA
7. Proton nuclear magnetic resonance spectroscopy ( <sup>1</sup> H-NMR)	Bruker ACF-200 spectrometer	Bruker, USA
8. Carbon nuclear magnetic resonance spectroscopy ( <sup>13</sup> C-NMR)	Bruker DPX-300 spectrometer	Bruker, USA
9. Gel permeation chromatography (GPC)	Column oven : CTO-10Acvp Injector : SIL-10Acvp Liquid chromatograph : LC-	Shimadzu, Japan

	10ACvp System controller : SCL- 10ACvp UV-vis detector : SPD-10AVvp Refractive index detector : RID-10A	
10. Twin screw extruder	PRISM TSE 16 TC	Thermo Electron Corporation, USA
11. Micrometer	Model G	Peacock, Japan
12. Universal testing machine	LR 100K	LLOYD, UK

### 3.3 Experimental Procedure

Flow chart of the experimental process is shown in Figure 3.2 and the details for each step are described as follows.

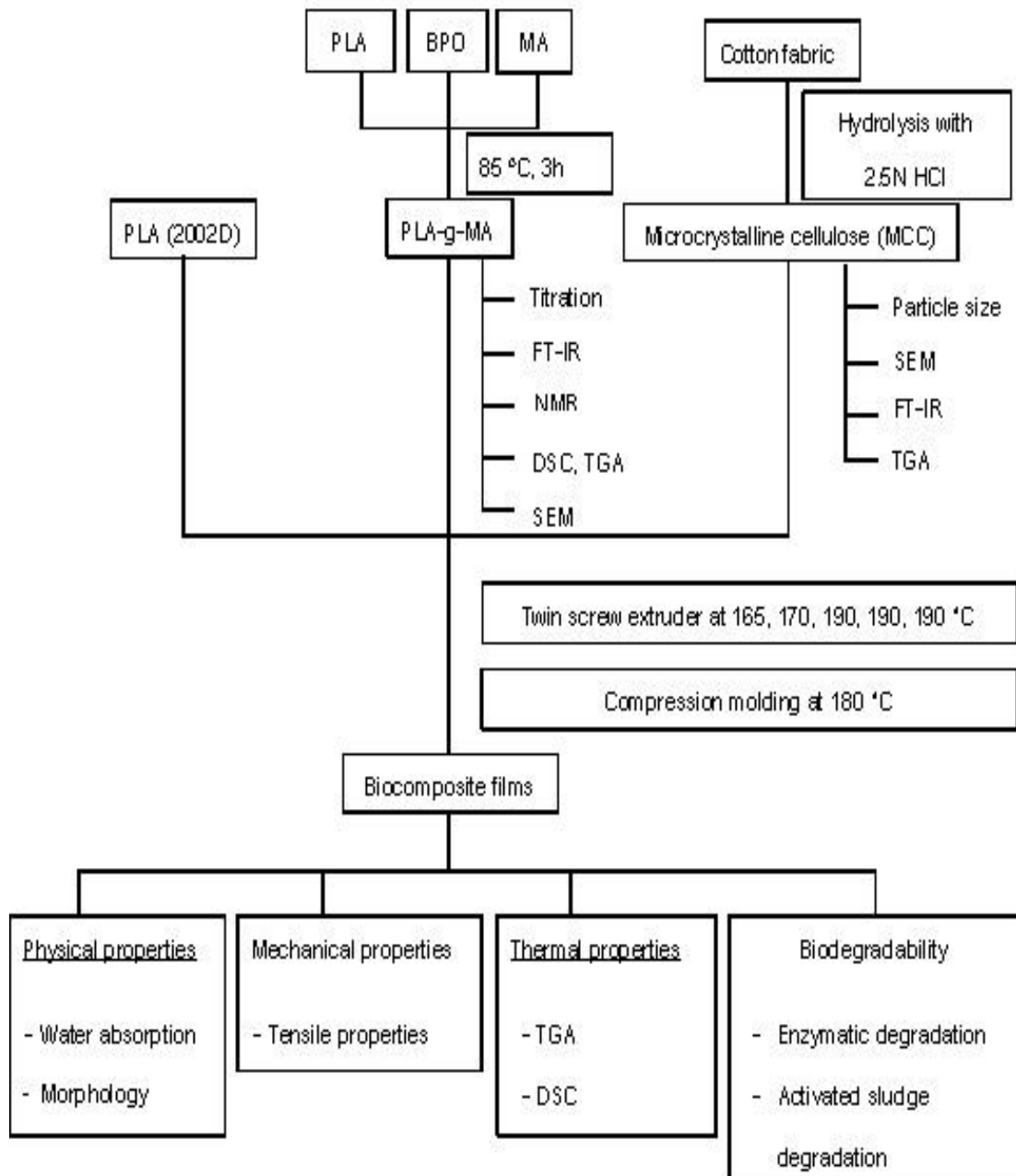


Figure 3.2 Flow chart of the experimental process

### 3.3.1 Preparation of Microcrystalline Cellulose

Small pieces of cotton fabric were hydrolyzed with 2.5 N hydrochloric acid (HCl) solution at 80 °C for 2 h. After that, the cellulose solution was filtered and washed with distilled water several times until the pH value of CT-MCC was neutral. Then, the MCC was dried in an oven at 60 °C for 24 h.

### 3.3.2 Preparation of Polylactic Acid Grafted Maleic Anhydride (PLA-g-MA)

Firstly, 15 g of PLA was dissolved in 150 ml of tetrahydrofuran (THF) and then added into the four-neck round bottom flask. Then, 0.5 g of the initiator (BPO) was added and stirred at 80 rpm for 3 h under a nitrogen atmosphere at 85 °C. Thirty minute later, 2 g of maleic anhydride (MA) was added into the reactor and stirred at 80 rpm for another 150 min at 85 °C. The grafted product was washed with acetone to remove the unreacted MA, and subsequently precipitating with excess diethyl ether. The resulting solid was filtered and dried in a vacuum oven at 60 °C for 24 h. The grafting percentage was determined using a titration method.



Figure 3.3 Experimental set up for PLA-g-MA solution polymerization.

### 3.3.3 Film Formation

Dried MCC powder, PLA, and PLA-g-MA were pre-mixed in a zip-lock bag at various ratios as shown in Table 3.2. Then, the mixtures were fed into a twin screw extruder (PRISM TSE 16 TC, Thermo Electron Corporation, Staffordshire, UK), which had a twin screw diameter of 17.8 and L/D ratio of 40. The temperature profiles for compounding MCC/PLA composites were set at 165, 170, 190, 190, 190 °C, respectively; while the rotational speed was maintained at 45 rpm. After that, the compound was fabricated into film by a compression molding with a pressure of 10 MPa at 180 °C. The average thickness of the films was  $2.83 \pm 0.09$  mm.

**Table 3.2** The various ratios of PLA biocomposites

Materials	PLA (g)	CT-MCC* (g)	PLA-g-MA (5%wt of CT-MCC) (g)
Neat PLA	100	-	-
10%CT-MCC/PLA	90	10	-
20%CT-MCC/PLA	80	20	-
30%CT-MCC/PLA	70	30	-
40%CT-MCC/PLA	60	40	-
10%CT-MCC/5%PLA-g- MA/PLA	90	10	0.5
20%CT-MCC/5%PLA-g- MA/PLA	80	20	1
30%CT-MCC/5%PLA-g- MA/PLA	70	30	1.5
40%CT-MCC/5%PLA-g- MA/PLA	60	40	2

\* Cotton Microcrystalline Cellulose (CT-MCC)

### 3.4 Characterization of Microcrystalline Cellulose (MCC)

#### 3.4.1 Particle Size Analysis

Average particle size of MCC was determined by the laser particle size analyzer (Mastersizer 2000, Malvern instruments, Worcestershire, UK) at room temperature, operated between the size ranges of 0.02 to 2000  $\mu\text{m}$ . To avoid possible agglomeration, prior to measurements powders were suspended in distilled water and ultrasonically stirred for about 4 min. The intensity of scattered light from the laser which was scattered at different angles from the different particle sizes, was measured with a series of detectors. A refractive index of 1.53 was used as a model parameter.



Figure 3.4 Laser Particle Size Analyzer, Malvern Instruments Mastersizer 2000

#### 3.4.2 Morphology

Morphology of MCC was examined by Scanning electron microscope (SEM; JSM-6480LV, JEOL, Tokyo, Japan). The MCC was coated with a thin layer of gold before being scanned in order to prevent charging on the MCC surface. SEM was operated at an accelerating voltage of 10 kV.







Figure 3.6 Thermogravimetric Analyzer, Mettler Toledo TGA/SDTA 851<sup>e</sup>

### 3.5 Characterization of Polylactic Acid-Grafted Maleic Anhydride (PLA-g-MA)

#### 3.5.1 Titration

The grafting percentage of PLA-g-MA was calculated from the acid number and was determined as follows. First, about 2 g of PLA-g-MA sample was dissolved in 200 ml of chloroform. The solution was then titrated immediately with a 0.03N ethanolic KOH solution, which was standardized against a solution of potassium hydrogen phthalate, by using phenolphthalein as an indicator. The acid number was calculated using eq. (3.1) below, and the grafting percentage was calculated using eq. (3.2). [2]

$$\text{Acid number (mgKOH/g)} = \frac{V_{\text{KOH}} (\text{ml}) \times C_{\text{KOH}} (\text{N}) \times 56.1}{\text{Polymer (g)}} \quad (\text{E.q. 3.1})$$

$$\text{Grafting percentage (\%)} = \frac{\text{Acid number} \times 98.1}{2 \times 561} \quad (\text{E.q. 3.2})$$

Where :

$V_{\text{KOH}}$  is the volume of the KOH (mL)

$C_{\text{KOH}}$  is the concentration of the KOH (N)

### 3.5.2 Fourier Transform Infrared Spectroscopy

Fourier Transform Infrared (FT-IR) spectrum was acquired with a Thermo Scientific Spectrum Nicolet 6700 FTIR spectrometer to characterize the functional group of PLA-g-MA. Powdered sample was evaluated with KBr pellet technique in transmission mode. For PLA-g-MA sample spectrum was recorded with 64 consecutive scans at a frequency range of 400-4000  $\text{cm}^{-1}$ .

### 3.5.3 Nuclear Magnetic Resonance Spectroscopy (NMR)

#### 3.5.3.1 $^1\text{H}$ -NMR Spectroscopy

Proton ( $^1\text{H}$ ) nuclear magnetic resonance analysis was used to characterize PLA and PLA-g-MA structures. The sample was dissolved in Deuterated chloroform ( $\text{CDCl}_3$ ). The NMR experiment was carried out by using Bruker ACF-200 NMR spectrometer.  $^1\text{H}$ -NMR was operated at 400 MHz by using tetramethylsilane as an internal standard. Chemical shifts ( $\delta$ ) were reported in parts per million (ppm) relative to the residual protonated solvent signal as a reference between 0-13 ppm.



**Figure 3.7** Proton Nuclear Magnetic Resonance Spectroscopy, Bruker ACF-200 NMR Spectrometer

### 3.5.3.2 $^{13}\text{C}$ - NMR Spectroscopy

Carbon ( $^{13}\text{C}$ ) Nuclear Magnetic Resonance Analysis was used to characterize PLA and PLA-g-MA structures. Solid-state  $^{13}\text{C}$ -NMR spectrum performed with a Bruker DPX-300 MHz spectrometer, was obtained at 75 MHz. Chemical shifts ( $\delta$ ) were reported in parts per million (ppm) between 0-200 ppm. All samples were characterized at room temperature ( $20\pm 1^\circ\text{C}$ ). The spectral parameters used were as follows: 4,000 numbers of scan (NS), relaxation delay of 4 s., and spin rate of 5 kHz.



**Figure 3.8** Carbon Nuclear Magnetic Resonance Spectroscopy, Bruker DPX-300 MHz NMR Spectrometer

### 3.5.4 Thermal properties

#### 3.5.4.1 Thermogravimetric analysis (TGA)

Thermogravimetric analysis (TGA) was carried out with a TGA/SDTA 851<sup>o</sup>. PLA-g-MA sample (7 mg) was run from 30 °C to 500 °C at a heating rate of 10°C/min under a nitrogen atmosphere. Prior to do the experiment, the sample was dried in an oven at 60 °C for 24 h. The decomposition temperature (Td) was reported as the onset of weight loss of heated sample.

### 3.5.4.2 Differential scanning calorimetry (DSC)

The differential scanning calorimeter (DSC; Pyris Diamond DSC, PerkinElmer, Connecticut) was used to determine glass transition temperature ( $T_g$ ), melting temperature ( $T_m$ ), and crystallization temperature ( $T_c$ ). Sample of about 7 mg was placed in a sealed aluminum pan. During the cycle, the sample was heated from 50°C to 200°C and maintained at that temperature for 1 min, thereafter it was cooled down to 50°C and heated to 200°C, respectively. The heat-cool-heat experiment was carried out by using heating and cooling rates at 10 °C/min under nitrogen atmosphere.



Figure 3.9 Differential Scanning Calorimeter, PerkinElmer Pyris Diamond DSC

### 3.5.5 Morphology

Morphology of PLA-g-MA was examined by Scanning electron microscope (SEM; JSM-6480LV, JEOL, Tokyo, Japan). Prior to the examination, PLA-g-MA was dried overnight in air oven at 60 °C and mounted on stub with sticky tape. Then, it was coated with a thin evaporated layer of gold in order to improve conductivity and prevent electron charging on the surface. The SEM was operated at 10 kV to image the sample.



Figure 3.10 Scanning electron microscope, JEOL JSM-6480LV

### 3.6 Characterization of PLA Biocomposite Films

#### 3.6.1 Physical Properties

##### 3.6.1.1 Water Absorption

Water absorption of the PLA biocomposite films was measured using a specimen size of 20 mm × 30 mm following the ASTM D570 standard method. The samples were dried in a vacuum oven at 50±2 °C for 24 h, cooled in a desiccator, and then immediately weighed (this weight was designated as  $W_i$ ). After that, the samples were immersed in distilled water and maintained at room temperature for 24 h. During this time, the films were removed from the beaker, gently blotted with tissue paper to remove excess water from their surfaces, immediately weighed (this weight was designated as  $W_A$ ). The water absorption capacity (WAC) was determined from the following equation.

$$\text{WAC \%} = \frac{W_A - W_i}{W_i} \times 100 \quad (\text{E.q. 3.3})$$

Where :

$W_A$  is weight of sample at absorbing equilibrium (g)

$W_i$  is initial dry weight of sample (g)

### 3.6.1.2 Morphology

A Scanning electron microscope (SEM; JSM-6480LV, JEOL, Tokyo, Japan) operated at an accelerating voltage of 10 kV was used to study the interfacial adhesion and the dispersion of MCC in the PLA composite. The composite film was coated with a thin layer of gold before being scanned in order to prevent charging on the film surface.

### 3.6.2 Mechanical properties

#### 3.6.2.1 Tensile testing

Mechanical properties such as tensile strength, tensile modulus, and percent elongation at break of film samples were determined according to ASTM D882 standard method. The film samples were carried out by Universal Testing Machine (LR 100K ,LLOYD,UK), using a crosshead speed of 10 mm/min, a gauge length of 100 mm, and load cell of 1000 N. All the film samples with the dimensions of 10 mm wide and 150 mm long were conditioned for 24 h at 25 °C before testing. At least five specimens were tested and the results were averaged to obtain a mean value.



Figure 3.11 Universal Testing Machine, LLOYD LR 100K

### 3.6.3 Thermal properties

#### 3.6.3.1 Thermalgravimetric analysis (TGA)

A thermogravimetric analyzer (TGA; TGA/SDTA 851<sup>e</sup>, Mettler Toledo, Greifensee, Switzerland) was performed at a heating rate of 10°C/min from 30 °C to 500 °C under nitrogen atmosphere. Approximately 7-8 mg of each sample was used. Prior to do the experiment, the samples were dried in an oven at 60 °C for 24 h. The change in weight due to thermal decomposition and the onset of degradation temperature ( $T_d$ ) of the sample were investigated.

#### 3.6.3.2 Differential scanning calorimeter (DSC)

The differential scanning calorimeter (DSC; Pyris Diamond DSC, PerkinElmer, Connecticut) was used to investigate the thermal properties. The Sample of about 7 mg was placed in a sealed aluminum pan. The same temperature profile was applied to all the sample : the first heating from 50°C up to 200°C, followed by cooling the sample to 50 °C, and finally heating again to 200 °C. The heat-cool-heat experiment was carried out by using heating and cooling rates at 10 °C/min under nitrogen atmosphere. The glass transition temperature ( $T_g$ ) values were reported in the glass transition region during the second heating scan while the melting temperature ( $T_m$ ) values were reported as the peak temperature of melting endotherms reported on the second heating scan and the crystallization temperatures ( $T_c$ ) values were reported on the second heating scan.

### 3.6.4 Biodegradability

#### 3.6.4.1 Enzymatic degradation

Biodegradability of the film sample was investigated by enzymatic degradation method using cellulase and lipase. The specimens were cut into 2 cm × 2 cm squares



and subjected into 40 ml vial. Then, cellulase enzyme solution consisting of 0.2 M acetate buffer pH 5.5 (5.5 ml) and cellulase solution (4.5 ml) was prepared. After that, the enzyme solution was added into the vial containing film samples. The vial was then put into water bath, with continuously shaking and heating at 55 °C. The film specimens were removed from the vial every 24 h for evaluation of their biodegradability. [38]

In addition, lipase enzyme solution consisting of 0.025 M phosphate buffer pH7 (5 ml) and lipase solution (5 ml) was prepared. Each sample was incubated at 37 °C with gentle shaking in water bath. Specimens were withdrawn from the degradation media every 24 h. [3]

After removing from the media, specimens were washed with distilled water and dried under vacuum oven at 60 °C for 24 h to get rid of moisture before testing. Film samples were then weighted to determine their percentage of weight loss and measured their molecular weight before and after degradation. The evidence of enzymatic degradation was also confirmed by the SEM analysis.

#### **3.6.4.2 Activated sludge degradation**

Biodegradation by activated sludge was carried out at the waste water treatment plant at the Si Phraya Water Environment Control Plant (SPWECP) in Bangkok for 2 months. The biocomposite in the form of thin films were prepared in square shape with the size of 2 cm× 2 cm, and placed into the bag which made from nylon net. After that, the bag was floated into the waste water at a depth of 1m from the surface. The films were removed from the waste water treatment system, washed with distilled water, and dried in vacuum oven at 60 °C for 24 h. As will be described in the next section, the rate of biodegradation was followed by measuring the percentage of weight loss and molecular weight of the film samples before and after being exposed to activated sludge

at every 7 days. The change in physical appearance of the film surfaces was also observed by SEM analysis.

### 3.7 Evaluation of the Degradation

#### 3.7.1 Weight Loss

Weight loss of the film specimens was measured by weighing the sample before and after biodegradation. The percentage of weight loss for the film samples was calculated using the following equation :

$$\text{Weight loss (\%)} = \frac{W_i - W_f}{W_i} \times 100\% \quad (\text{E.q. 3.4})$$

Where :

$W_i$  is initial weight of sample before degradation (g)

$W_f$  is final weight of sample after degradation (g)

#### 3.7.2 Gel Permeation Chromatography (GPC)

Gel Permeation Chromatography (GPC, Shimadzu, Kyoto, Japan) was used to evaluate the molecular weight of biocomposite films. The sample (15 mg) was dissolved in tetrahydrofuran (THF) (3ml) and filtered by syringe filter (diameter 13 mm. nylon). GPC chromatogram of sample was obtained from Shimadzu chromatography equipped with Shodex GPC KF-805L columns at 40 °C. THF was used as an eluent with the flow rate of 2.0 ml/min. Degassed THF mobile phase was passed through the column for 20 min before injecting the samples. The sample (20  $\mu$ l) was injected and run through the column for 15 min. Polystyrenes (PSS Inc, USA) were used as standards for calibration. The molecular weight was determined by a reflection index detector.



Figure 3.12 Gel Permeation Chromatography, Shimadzu

### 3.7.3 Morphology

Scanning electron microscope (SEM; JSM-6480LV, JEOL, Tokyo, Japan) was employed to investigate the film surface of the samples collected before and after biodegradation testing in enzymatic and activated sludge degradation. Each sample was cleaned and dried in vacuum oven at 60 °C for 24 h. The composite film was coated with a thin layer of gold before being scanned in order to prevent charging on the film surface. SEM was operated at an accelerating voltage of 10 kV.

## CHAPTER 4

### RESULTS AND DISCUSSION

This work aimed to investigate the preparation of PLA biocomposite films reinforced with various amounts of cotton microcrystalline cellulose (CT-MCC). The synthesis of PLA-g-MA for improving interfacial adhesion between CT-MCC and PLA was also focused, with the goal of enhancing mechanical properties and biodegradability. The results were divided mainly into 4 parts as follows:

1. Characterization of microcrystalline cellulose prepared from acid hydrolysis of cotton fabric
2. Characterization of PLA-g-MA
3. Characterization and testing of PLA biocomposite films
4. Biodegradability of PLA composite films

#### 4.1 Characterization of Microcrystalline Cellulose Prepared from Acid Hydrolysis of Cotton Fabric


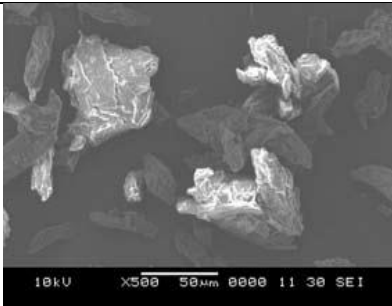
##### 4.1.1 Particle Size and Morphology

The physical appearance of CT-MCC prepared from hydrolysis of cotton fabric was exhibited in **Figure 4.1**. CT-MCC appeared as white fine powder as same as calcium carbonate powder. Comparing with commercial MCC (Avicel PH101), the results from laser particle size analyzer summarized in **Table 4.1**. showed that the average particle size of the CT-MCC was smaller than that of the Avicel PH101. Similar results were also observed in previous researches [39]. In addition, SEM micrographs displayed in **Table 4.1** showed that CT-MCC presented as short fiber shape with smooth surface having aspect ratio of approximately 5-20  $\mu\text{m}$ ; whereas Avicel PH101 showed flake shape with rough surface.



Figure 4.1 Physical appearance of acid hydrolyzed CT-MCC

Table 4.1 SEM micrographs and particle size of cotton MCC and Avicel PH101

	CT-MCC	Avicel PH101
SEM		
particle size	26.11 $\mu\text{m}$	64.22 $\mu\text{m}$

#### 4.1.2 FT-IR spectroscopy

FT-IR spectra of CT-MCC and Avicel PH101 were compared and showed in Figure 4.2. Two types of MCC showed similar spectrum, which was observed by a strong broad band at  $3346\text{ cm}^{-1}$  originating from the O-H stretching of hydroxyl groups. The band at  $2900\text{ cm}^{-1}$  was corresponding to the C-H stretching in cellulose unit. The peak at  $1638\text{ cm}^{-1}$  was attributed to the absorbed water of O-H bending. The peaks at  $1370\text{ cm}^{-1}$  and  $1281\text{ cm}^{-1}$  were assigned to the C-H bending. The absorption band at

1165  $\text{cm}^{-1}$  was contributed to the C-O stretching; while a strong band at 1059  $\text{cm}^{-1}$  was originated from the C-O-C pyranose ring skeletal vibration. Table 4.2 summarizes all the FT-IR assignments for cellulose structure. Abeer and co-worker (2011) have also reported the same results of FT-IR spectra for rice hulls MCC and Avicel PH101. [40]

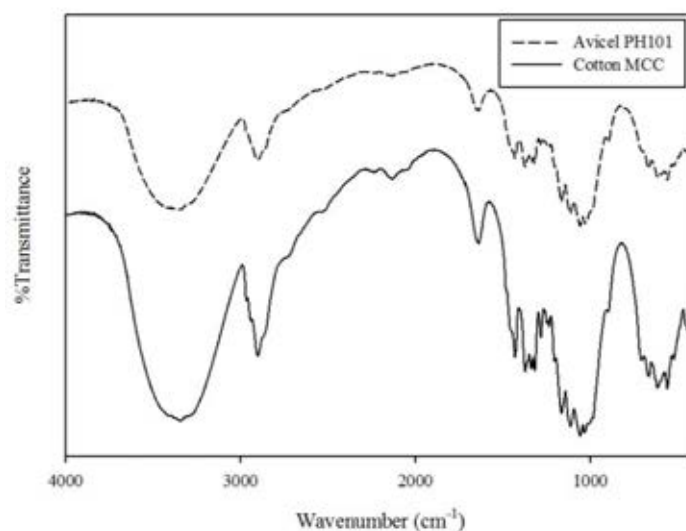


Figure 4.2 FT-IR spectra of CT-MCC and commercial MCC (Avicel PH101)

Table 4.2 FT-IR assignments for CT-MCC

Wavenumber ( $\text{cm}^{-1}$ )	FT-IR assignments
3346	O-H stretching
2900	C-H stretching
1638	absorbed water of O-H bending
1370, 1281	C-H bending
1165	C-O stretching
1059	C-O-C pyranose ring skeletal vibration

### 4.1.3 Thermogravimetric Analysis (TGA)

The decomposition temperatures ( $T_d$ ) is an important parameter for the processing and is the most widely used technique to observe the structural dependence of polymer on the thermal degradation. Figure 4.3 shows TGA curves of CT-MCC and Avicel PH101. Obviously, both CT-MCC and Avicel PH101 illustrated two steps of weight loss. The first step around 80-110 °C was attributed to the moisture decomposition from CT-MCC and Avicel PH101. The second step of CT-MCC and Avicel PH101 started to decompose at 285.48 °C and 280.25 °C, respectively, was contributed to the degradation of cellulose.

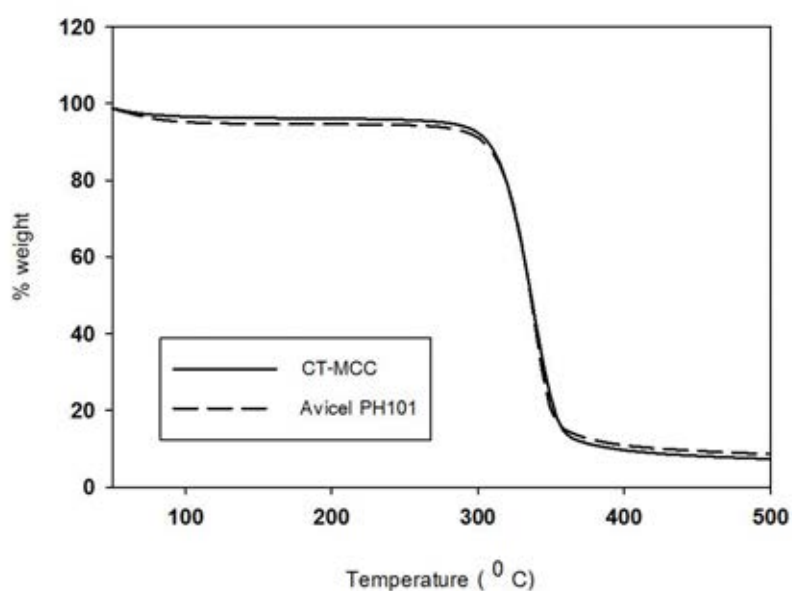


Figure 4.3 TGA thermograms of CT-MCC and Avicel PH101

From Figure 4.3, it can be observed that the thermal stability of CT-MCC was similar to that of Avicel PH101. The onset of thermal decomposition temperature and the decomposition temperature at 50% weight loss, as well as char yield of CT-MCC and Avicel PH101 were summarized in Table 4.3.

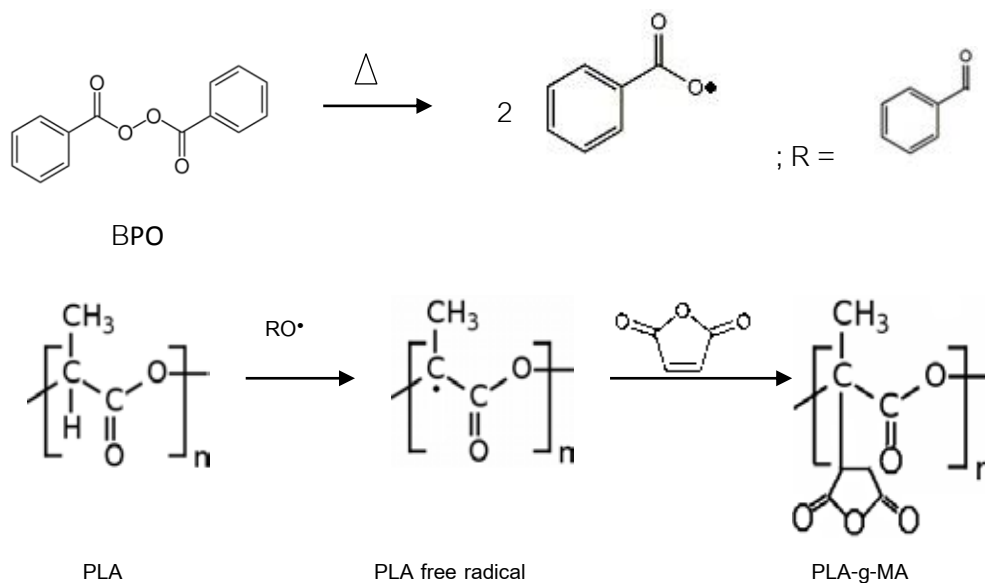
**Table 4.3** Thermal decomposition temperature and char yield of cotton and commercial MCC.

Sample	$T_d^{\text{onset}}$ ( $^{\circ}\text{C}$ )	$T_d^{50\%}$ ( $^{\circ}\text{C}$ )	Char yield at 500 $^{\circ}\text{C}$ (%)
CT-MCC	285.48	315.04	5.64
Avicel PH101	280.25	313.89	6.37

#### 4.2 The Grafting Reaction of Polylactic Acid with Maleic Anhydride

The grafting reaction of polylactic acid with maleic anhydride was achieved in this work via free radical polymerization using benzoyl peroxide (BPO) as an initiator, the PLA-g-MA was synthesized by solution polymerization in THF under nitrogen atmosphere as reported by Chin-San Wu [2]. The formation of an initiator radical is the first step in reaction. Once the radical is formed, hydrogen abstraction, that occurs on the PLA backbone. After that, the addition of maleic anhydride to radical on the PLA backbone was result shown that polymer radical may combine with maleic anhydride. The common reaction scheme of polylactic acid with maleic anhydride to produce polylactic acid grafted maleic anhydride (PLA-g-MA) is shown in **Figure 4.4**





**Figure 4.4** The schematic of maleic anhydride grafting on the PLA by solution polymerization.

In this research, the optimum conditions for preparation of PLA-g-MA were investigated. The investigating parameters included reaction time and reaction temperature (50, 70, 85, and 100 °C). The influences of these variables on the chemical structure of PLA-g-MA were characterized.

#### 4.2.1 The Optimum Conditions for Preparation of PLA-g-MA

To find the optimum conditions for grafting reaction of PLA with MA, the reactions were conducted and assessed by varying in (1) time of adding maleic anhydride and benzoyl peroxide and (2) reaction temperature. The grafting reaction of PLA-g-MA or grafting product was mainly determined by investigating the chemical structure obtained from  $^1\text{H-NMR}$  spectroscopy.

#### 4.2.1.1 The Influence of Time for Adding Maleic Anhydride and Benzoyl Peroxide

From schematic shown in **Figure 4.4**, after adding BPO for a certain period of time (0,15,30, and 45 min) as shown in **Table 4.4**, MA was added into the reaction and the total reaction time was kept constant at 50 °C for 6 h, according to Chin-San Wu [2, 37]. The first formula (1A) means that, BPO and MA was added at the same time since reaction started; while the other formula(2A, 3A, and 4A) represent the various reaction times for adding MA. After that <sup>1</sup>H-NMR was carried out to study the effect of reaction time on chemical structure of PLA and PLA-g-MA.

**Table 4.4** The reaction time profiles to add the maleic anhydride at 50 °C

Formula	Time to add the MA (min)
1A	0
2A	15
3A	30
4A	45

The chemical structure of PLA and PLA-g-MA was investigated by <sup>1</sup>H-NMR spectroscopy in liquid system using tetramethylsilane as internal standard. The NMR spectroscopy has advantages over FTIR and most other spectroscopic methods since the chemical shifts are very sensitive to the chemical environment. Thus, ideally it should be possible to establish not only the nature of the group but also how and where it is attached to the polymer backbone.

The <sup>1</sup>H-NMR spectra and chemical structure of PLA and PLA-g-MA were shown in **Figure 4.6** and **4.7**, respectively; whereas their chemical shifts were given in **Table 4.5**. From **Figure 4.6**, these are three peaks corresponding to proton atoms in the unmodified PLA. The first peak between 1.5 and 1.7 ppm (peak a) is corresponding to

the proton of  $\text{CH}_3$ , while peak of the CH of PLA backbone (peak c) is presented between 5.0 and 5.3 ppm, and finally, the peak at 7.29 ppm (peak d) is attributed to the proton joined to the oxygen atom. Meanwhile, the spectra of PLA-g-MA showed new peak at 2.1 ppm (peak b) which was a characteristic of the proton of  $\text{CH}_3$  atom connected with carbon atom and the peak between 4.2 and 4.5 ppm (peak e), corresponding to the proton of  $\text{CH}_2$  atom joined to the carbonyl of acid anhydride bond.

$^1\text{H-NMR}$  was useful for investigating the position of PLA-g-MA. Comparing among four  $^1\text{H-NMR}$  spectra presented in **Figure 4.7**, obviously, formula 1A exhibited an extra peak between 6.5 and 6.8 ppm, referring to the proton of either (1) CH of MA residue or (2) CH of MA reacted with BPO, as shown in **Figure 4.5**. The latter case could be possible due to the greater reactivity of MA monomer comparing to PLA towards the free radical reaction with BPO. In other words, by adding BPO and MA at the same time, once the BPO radical was formed, it may tentatively react with MA monomer instead of PLA (step 2), owing to the difference in the reactivity of those two reagents. After that, the unstable radical from the second step can react with PLA radical to form the PLA-g-MA which has the alkoxy group (RO) in its structure. It is postulated that the extra peak between 6.5 and 6.8 ppm would belong to the proton of CH atom joined to the alkoxy group and carbonyl of acid anhydride bond.

Besides, the intensity of peaks b and e which were designated as maleic anhydride grafting on the PLA are too low to confirm the efficiency of grafting.

In order to solve this problem, three other formula (formula 2A-4A) were designed, by adding MA at various reaction times after BPO was added. The purpose of this step was to assume that the BPO radicals will react with PLA first and resulted in the free radical on the PLA backbone which should be ready to be grafted with MA in the next step to form PLA-g-MA. By adding MA 15 min after adding BPO, the peak at 6.7 ppm was still existed although with the very small intensity, as shown in **Figure 4.7 b**.

However, upon increasing this reaction time to 30 and 45 min, the  $^1\text{H-NMR}$  spectra showed that the peak around 6.7 ppm was dissappear. There was no significant difference between these two spectra (Figure 4.7 c and d); thus we decided to choose formula 3A as the optimum condition for preparing PLA-g-MA at this stage. However, the intensity of the interested peaks was still low, it is expected that the intensity may be improved when reaction temperature is increased. Therefore, different reaction temperatures was investigested, as discussed in the next section.

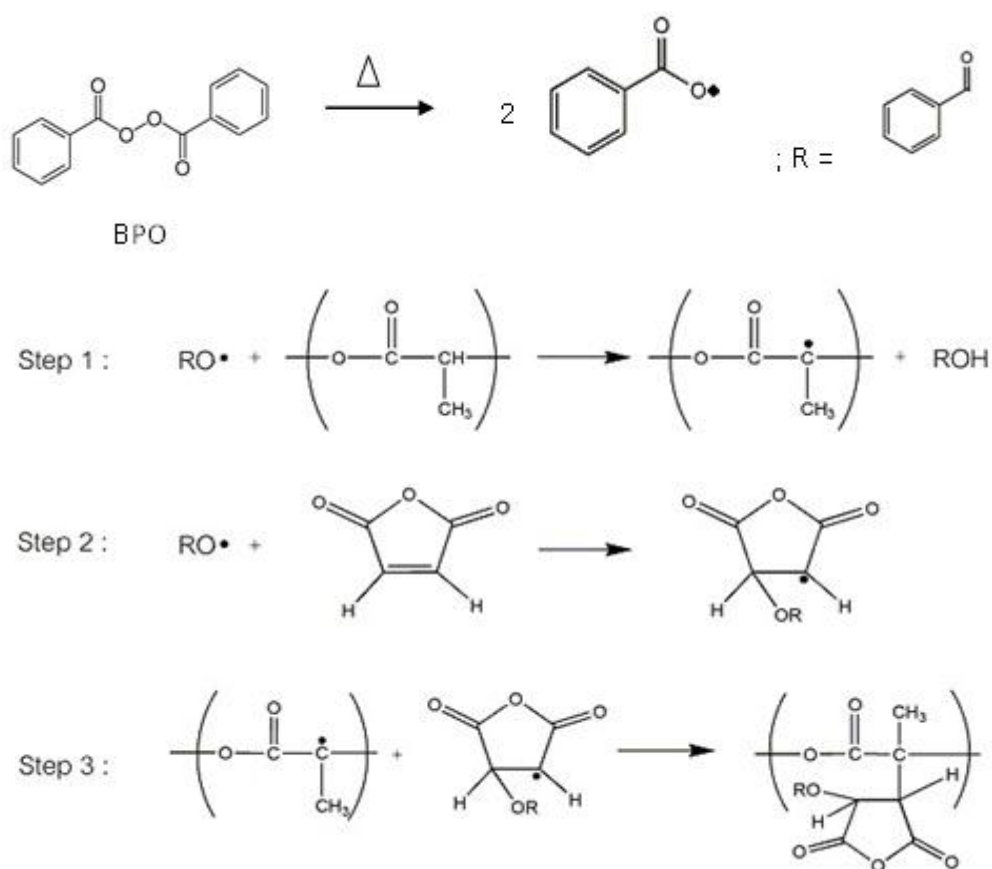


Figure 4.5 The schematic of side effect of maleic anhydride grafting on the PLA

Table 4.5  $^1\text{H-NMR}$  chemical shift of PLA and PLA-g-MA

Proton in PLA backbone	
Position	$\delta$ (ppm)
PLA	
a	1.61
c	5.16
d	7.29
PLA-g-MA	
a	1.60
b	2.10
c	5.29
d	7.16
e	4.38

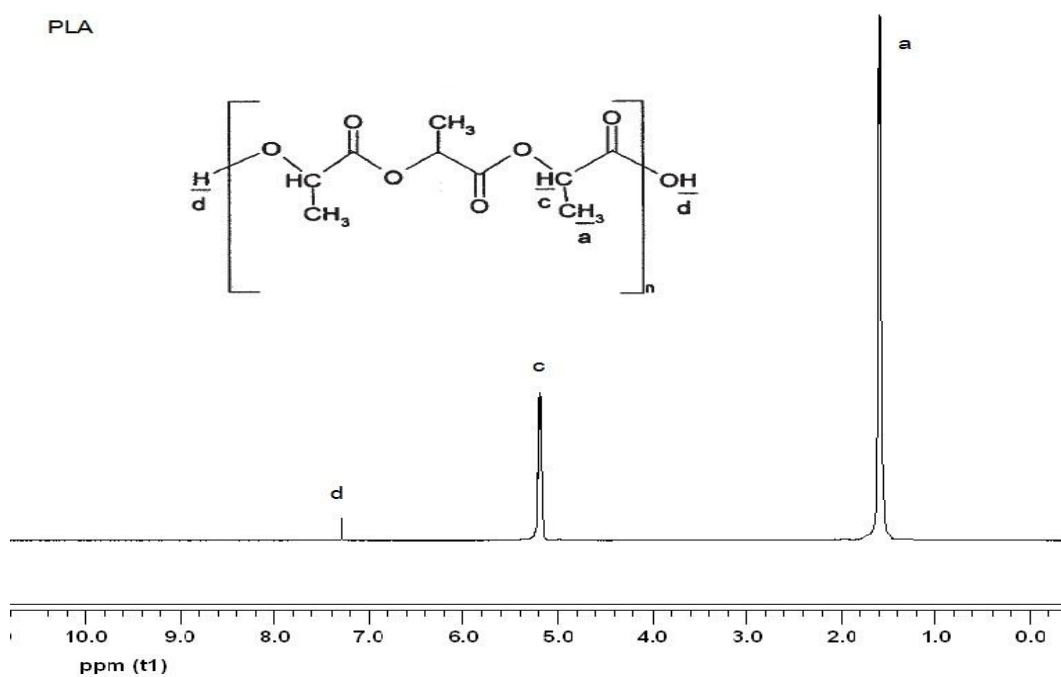
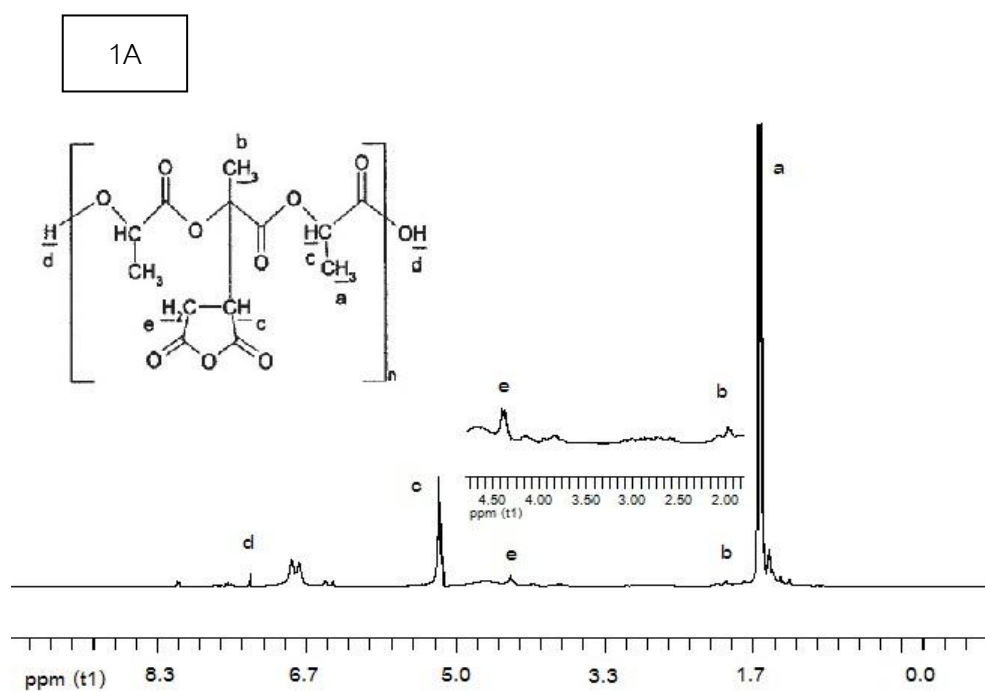
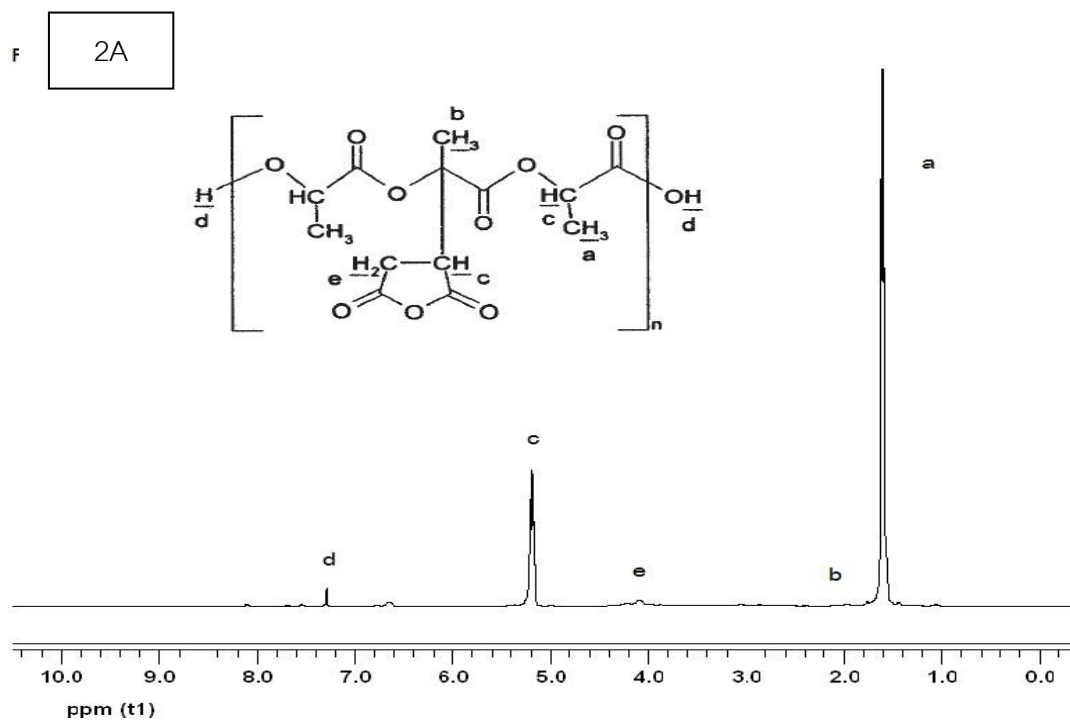


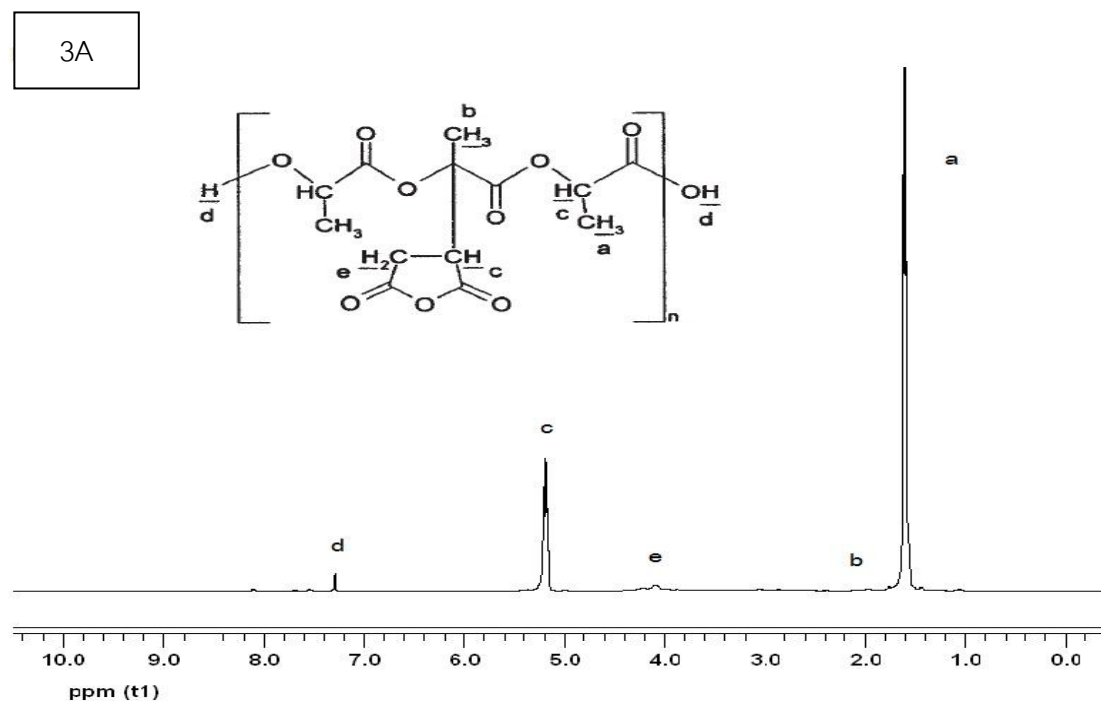
Figure 4.6  $^1\text{H-NMR}$  spectrum of PLA in  $\text{CDCl}_3$ .



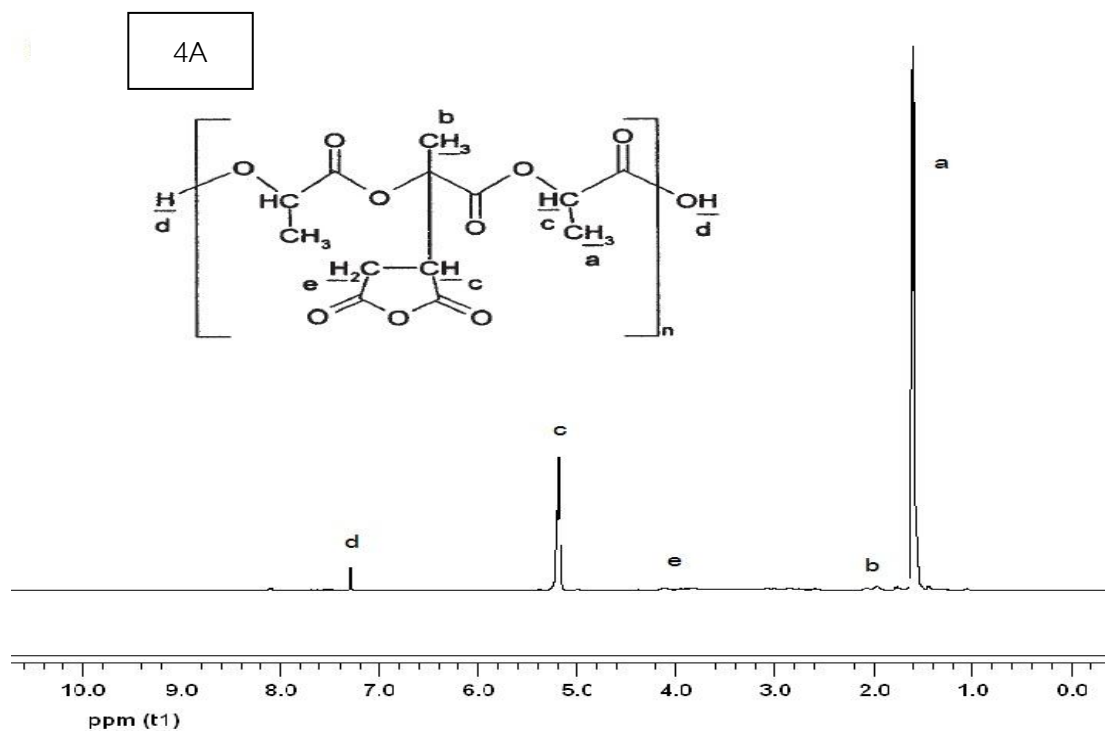
a) Formula 1A



b) Formula 2A



c) Formula 3A



d) Formula 4A

Figure 4.7 <sup>1</sup>H-NMR spectra of PLA-g-MA in CDCl<sub>3</sub>; a) 1A b) 2A c) 3A, and d) 4A formula

#### 4.2.1.2 The Effect of Reaction Temperature

Four reaction temperatures as well as reaction time based on the cleavage of initiator was selected, as shown in Table 4.6. According to the results presented in previous section, BPO was used as an initiator and MA was added into the reaction 30 min after adding BPO. Total reaction time was dependent on the reaction temperature, which directly related to the half-life of BPO initiator. To identify the MA grafted PLA was analyzed by <sup>1</sup>H NMR spectra. Figure 4.8 shows the <sup>1</sup>H NMR spectra of PLA-g-MA synthesized at each reaction temperature.

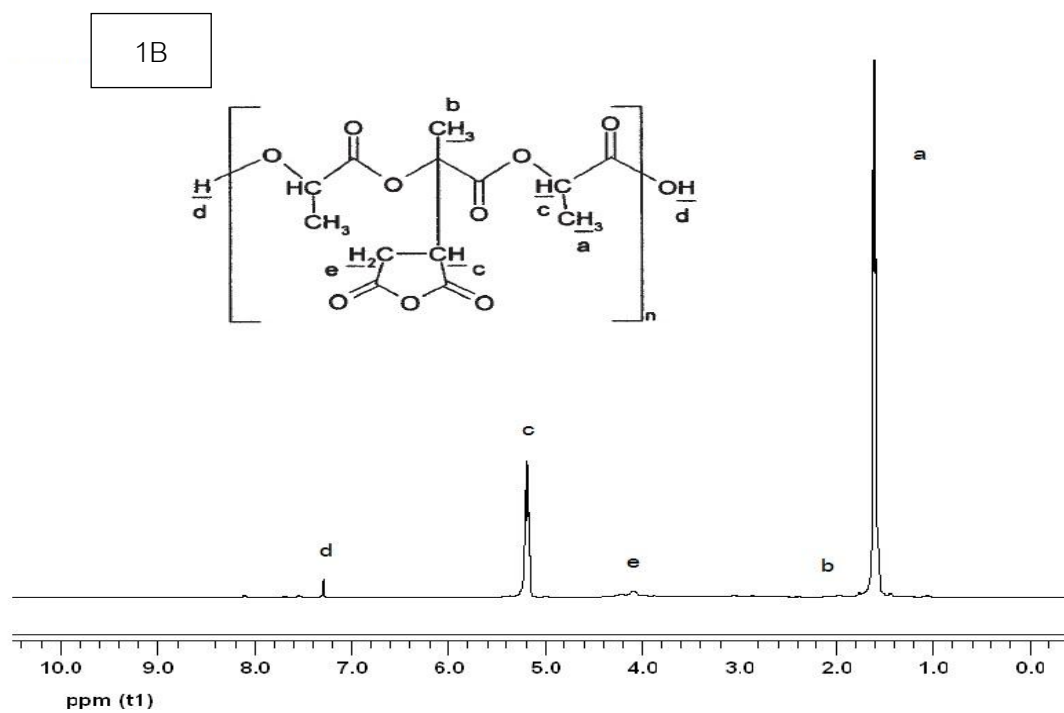


**Table 4.6** The PLA-g-MA synthesis reaction temperature profiles adopt from [41]

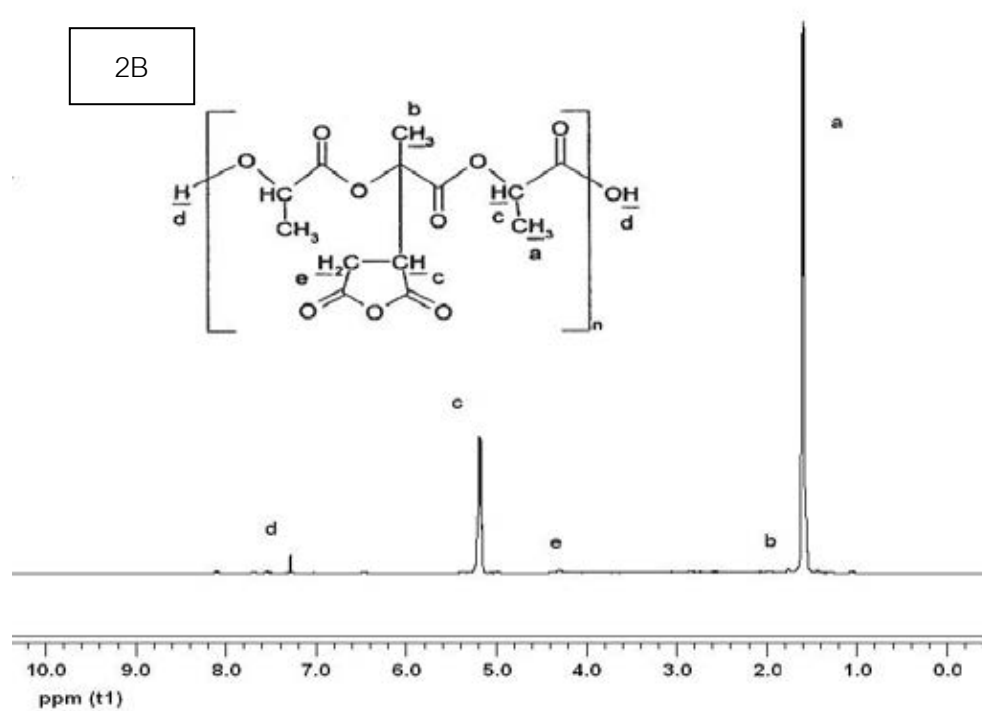
Formula	Temperature (°C)	Reaction time (h)
1B	50	6
2B	70	14
3B	85	3
4B	100	2

As previously discussed, the intensity of peak e of PLA-g-MA formula 1B (or formula 3A), which was synthesized at low temperature (50°C), was low. Similarly, the grafting product synthesized at 70 °C (formula 2B) also showed low intensity of the interested peak. These results may be assumed that the temperature is not suitable for this reaction possibly because (1) the kinetic of this reaction is too slow or (2) the energy is not enough to generate adequate radicals. Nevertheless, the intensity of peak b and peak e increased, when the reaction temperature was increased up to 85 °C. At the same trend, peak b and peak e still had high intensity at 100 °C. However, at 100 °C, this temperature is not proper for PLA-g-MA synthesis because it is closed to the boiling point of THF which is the solvent in this reaction. [42] From these results, it can be concluded that the optimum temperature for PLA-g-MA synthesis is 85 °C.

Conclusively, from the above results, the suitable condition for PLA-g-MA synthesis was that PLA was dissolved in tetrahydrofuran (THF) and using benzoyl peroxide (BPO) as an initiator under a nitrogen atmosphere at 85 °C. Thirty minute later, maleic anhydride (MA) was added into the reactor and stirred at 80 rpm until 3 h. The grafted product was washed with acetone to remove the unreacted MA, and subsequently precipitating with excessive diethyl ether. The resulting solid was filtered and dried in a vacuum oven at 60 °C for 24 h.



a) Formula 1B



b) Formula 2B



#### 4.2.2 Characterization of Polylactic Acid Grafted Maleic Anhydride (PLA-g-MA)

The obtained PLA-g-MA was characterized quantitatively by titration technique and qualitatively by FT-IR,  $^{13}\text{C}$ -NMR, DSC, TGA, and SEM to confirm that MA was successfully grafted on PLA backbone.

##### 4.2.2.1 Titration

Quantitative Analysis of maleic anhydride grafted on the PLA backbone by titration gave the result as the grafting percentage. While, the grafting percentage of PLA-g-MA was calculated from the acid number and was determined as follows. First, PLA-g-MA sample was dissolved in chloroform, the solution was then titrated immediately with a KOH in ethanol solution, which was standardized against a solution of potassium hydrogen phthalate (KHP), using phenolphthalein as an indicator.

KHP solution (standard solution) is used to react with KOH solution to observe the concentration of KOH as showed in **Table 4.7**. The average volume and concentration of KOH are, then used to calculate the acid number as shown in equation 3.1

$$\text{Acid number (mg KOH/g)} = \frac{V_{\text{KOH}} \text{ (ml)} \times C_{\text{KOH}} \text{ (N)} \times 56.1}{\text{Polymer (g)}} \quad (\text{E.q. 3.1})$$

**Table 4.7** The concentration of potassium hydroxide.

Sample	Weight of KHP (g)	Volume of KOH (ml)	Concentration of KOH (N)
1.	0.62	95.58	$3.14 \times 10^{-2}$
2.	0.61	96.76	$3.10 \times 10^{-2}$
3.	0.61	97.64	$3.07 \times 10^{-2}$
Average			$3.10 \times 10^{-2}$
S.D.			$0.03 \times 10^{-2}$

After that, the acid number was used to calculate, the grafting percentage of PLA-g-MA according to equation 3.2. The results are presented in **Table 4.8**.

$$\text{Grafting percentage (\%)} = \frac{\text{Acid number} \times 98.1}{2 \times 561} \quad (\text{E.q. 3.2})$$

**Table 4.8** The acid number and %grafting of PLA-g-MA.

Sample	Weight of PLA-g-MA (g)	Volume of KOH (ml)	Acid number (mg KOH/g)	% Grafting
1.	2.01	40.48	35.02	3.06
2.	2.02	45.66	35.99	3.15
3.	2.02	39.17	33.70	2.95
			Average	3.05
			S.D.	0.10

**Table 4.9** The acid number and %grafting of PLA.

Sample	Weight of PLA (g)	Volume of KOH (ml)	Acid number (mg KOH/g)	% Grafting
1.	2.01	5.31	4.59	0.40
2.	2.01	5.28	4.57	0.40
3.	2.02	5.46	4.70	0.41
			Average	0.40
			S.D.	0.01

It should be noted that the acid number of PLA-g-MA was calculated based on volume of KOH which reacted with anhydride functional group grafted on PLA backbone. However, it is possible that KOH can also react with carboxylic end group of PLA backbone. Thus, the same procedure for calculating acid number and grafting percentage of PLA-g-MA was applied to ungrafted PLA and those values were shown in **Table 4.9**. As a result, the real amount of maleic anhydride in PLA-g-MA was calculated

from subtraction between % grafting of PLA-g-MA and PLA. Therefore, it can be concluded that the real grafting percentage of PLA-g-MA in this work is  $2.65 \pm 0.09\%$ .

#### 4.2.2.2 Fourier Transform Infrared Spectroscopy

Infrared spectroscopy is currently the most widely used method for identifying in modified polylactic acid. **Figure 4.9** shows IR-spectra of PLA and PLA-g-MA. The PLA spectrum shows  $\text{CH}_3$  stretching at  $3000\text{-}2916\text{ cm}^{-1}$  and the  $\text{C}=\text{O}$  stretching at  $1749\text{ cm}^{-1}$ . The absorption band at  $1500\text{-}1361\text{ cm}^{-1}$  contributes to the  $\text{CH}_3$  bending and the peak at  $1195\text{-}1034\text{ cm}^{-1}$  corresponds to the  $\text{O}-\text{C}=\text{O}$  stretching characteristic of ester bond. Meanwhile, the PLA-g-MA spectrum shows a band at  $3008\text{-}2838\text{ cm}^{-1}$  originating from the  $\text{CH}_3$  stretching and the  $\text{CH}_3$  bending at  $1448\text{-}1341\text{ cm}^{-1}$ . The peak at  $1181\text{-}1034\text{ cm}^{-1}$  attributes to the  $\text{O}-\text{C}=\text{O}$  stretching characteristic of ester bond. The double characteristic adsorption bands of acid anhydride appeared at  $1744\text{ cm}^{-1}$  and  $1769\text{ cm}^{-1}$ . These double peaks were the evidence of grafting of maleic anhydride onto the PLA main chain. Since the amount of maleic anhydride presented in the blends is small, the  $\text{C}=\text{O}$  stretching of maleic acid or anhydride peak is very weak and might be overlapping with the carbonyl peak of PLA. This result suggests that if the level of grafting is too low, the IR spectroscopy is probably not a suitable technique or not sensitive enough to identify these changes. Similar observations have been reported in several studies. [2,43]. The FT-IR band assignments for PLA and PLA-g-MA were summarized in **Table 4.10**.

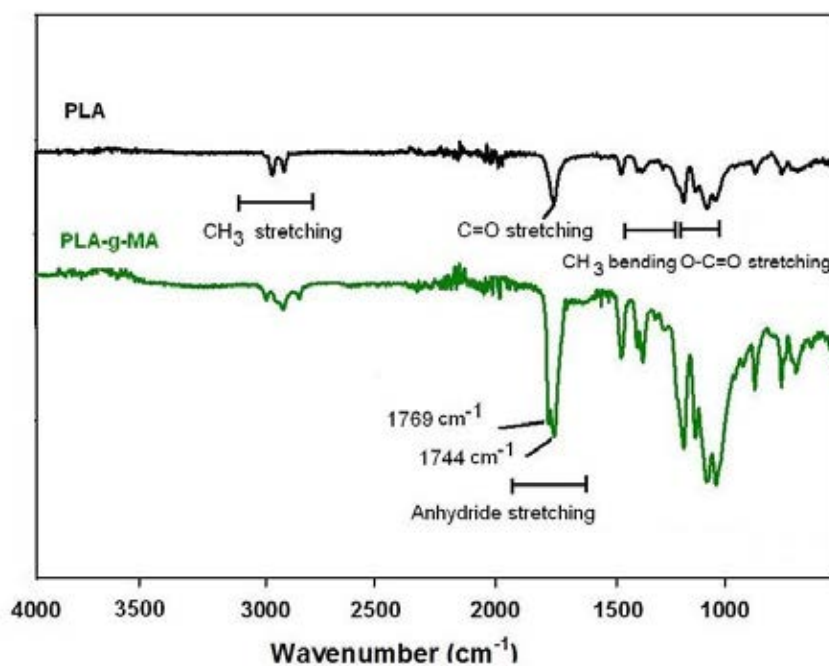


Figure 4.9 Infrared spectra of PLA and PLA-g-MA.

Table 4.10 FT-IR assignments for PLA and PLA-g-MA

Wavenumber (cm <sup>-1</sup> )	FT-IR assignments
<b>Polylactic acid</b>	
3000-2916	CH <sub>3</sub> stretching
1749	C=O stretching
1500-1361	CH <sub>3</sub> bending
1195-1034	O-C=O stretching
<b>PLA-g-MA</b>	
3008-2838	CH <sub>3</sub> stretching
1749	C=O stretching
1744, 1769	adsorption bands of acid anhydride
1448-1341	CH <sub>3</sub> bending
1181-1034	O-C=O stretching







**Table 4.11**  $^{13}\text{C}$ -NMR chemical shift of PLA and PLA-g-MA

Carbon in PLA backbone	
Position	$\delta$ (ppm)
PLA	
a	170.08
b	70.15
c	17.53
PLA-g-MA	
a	170.23
b	70.28
c	17.65
d	176.08
e	84.30
f	54.97
g	37.50

#### 4.2.2.4 Differential scanning calorimetry (DSC)

Figure 4.12 illustrates the second heating scan of the DSC thermograms of PLA and PLA-g-MA. It can be seen that the thermograms consisted of glass transition temperature ( $T_g$ ) and melting temperature ( $T_m$ ). The  $T_g$  of PLA and PLA-g-MA were 60 °C and 40.6 °C, whereas the melting temperature of PLA and PLA-g-MA were 153, and 141 °C, respectively. The  $T_g$  (40.6°C) and  $T_m$  (141°C) of PLA-g-MA were lower than PLA due to the grafted branches that increased the spacing between the PLA chains and disrupted the regularity of the chain structure might explain the lower  $T_g$  and  $T_m$  of PLA-g-MA.[44] From Table 4.12, it can be seen that the glass transition temperature

results indicated that the flexibility of PLA-g-MA molecular structure was greater than that of PLA and the melting temperature decreased after PLA was modified by MA. This may be due to the increased difficulty in arranging the polymer chain as the PLA prohibited the movements of the polymer segments and by the steric effect. [2,44]

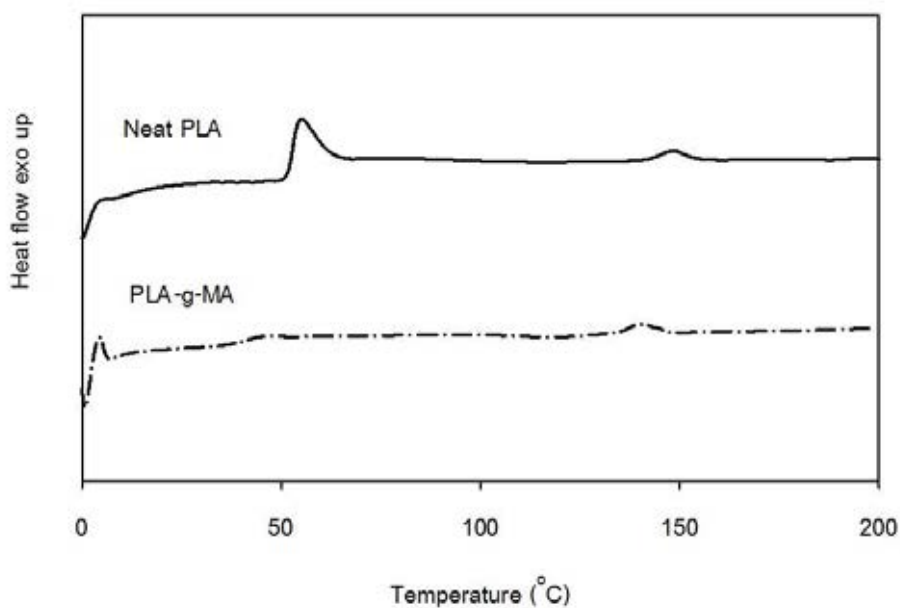


Figure 4.12 DSC thermograms (second heating scan) of a) PLA and b) PLA-g-MA

Table 4.12 The glass transition temperature, the melting temperature, and the decomposition temperature of PLA and PLA-g-MA.

Sample	T <sub>g</sub> (°C)	T <sub>m</sub> (°C)	T <sub>d</sub> (°C)	
			1 <sup>st</sup>	2 <sup>nd</sup>
PLA	61.82	149.53	302.45	-
PLA-g-MA	40.6	141	120.85	300

#### 4.2.2.5 Thermogravimetric analysis (TGA)

The thermogravimetric analysis of the PLA-g-MA sample shows that the decomposition temperature was lower than that of the pure PLA, implying a less thermally stable product (Figure 4.13). In other words, the PLA-g-MA sample obtained exhibited lower thermal stability as compared to the original PLA. The decomposition peak of PLA was  $302.45^{\circ}\text{C}$ , whereas the decomposition peak of PLA-g-MA showed two steps of weight-loss: the first one is due to loss of maleic anhydride, while the second step is attributed to the thermal decomposition of PLA. This is because the degradation temperature of maleic anhydride starts at  $\sim 120.85^{\circ}\text{C}$ , whereas the degradation temperature of PLA is  $\sim 300^{\circ}\text{C}$ . In addition, both PLA and PLA-g-MA were completely degraded at  $400^{\circ}\text{C}$ . The decomposition temperatures of PLA and PLA-g-MA were summarized in Table 4.13.

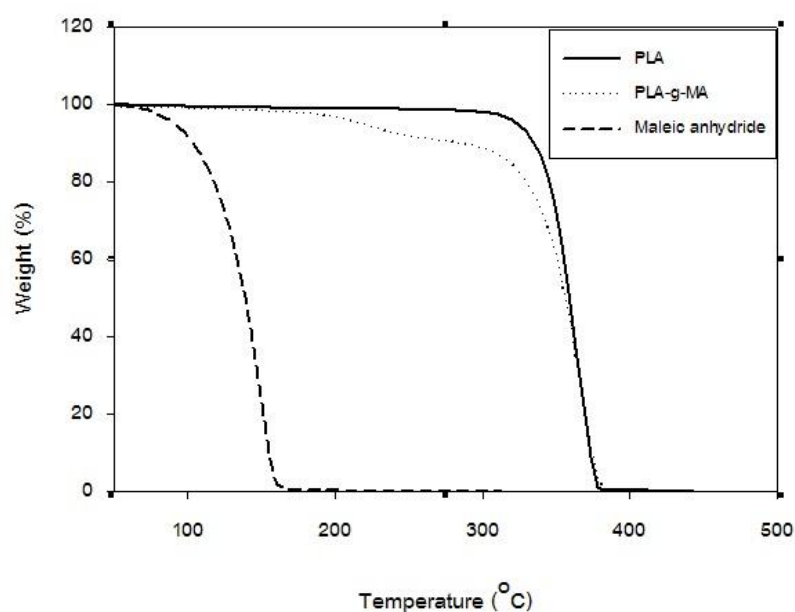


Figure 4.13 TGA thermograms of PLA, PLA-g-MA, and Maleic anhydride.

#### 4.2.2.6 Scanning electron microscopy (SEM)

The morphological study of PLA-g-MA was observed by scanning electron microscopy. After modification reaction similar to CT-MCC, PLA-g-MA can be seen by naked eyes as white powder, as illustrated in **Figure 4.14**. The SEM micrographs of PLA-g-MA are exhibited in **Figure 4.15** a) and b). As seen, the PLA-g-MA showed a rough surface particle. Its particle size seemed to be approximately 50-80  $\mu\text{m}$ , which is



larger than that of the CT-MCC.

**Figure 4.14** Physical appearance of PLA-g-MA

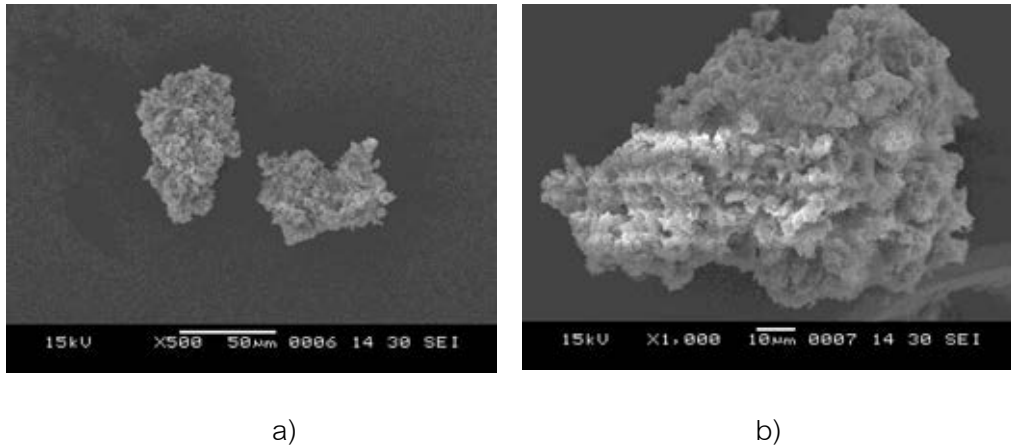


Figure 4.15 SEM micrographs of PLA-g-MA a) 500X magnification b) 1000X magnification.

### 4.3. Characterization of PLA Composite Films

#### 4.3.1 Physical Properties

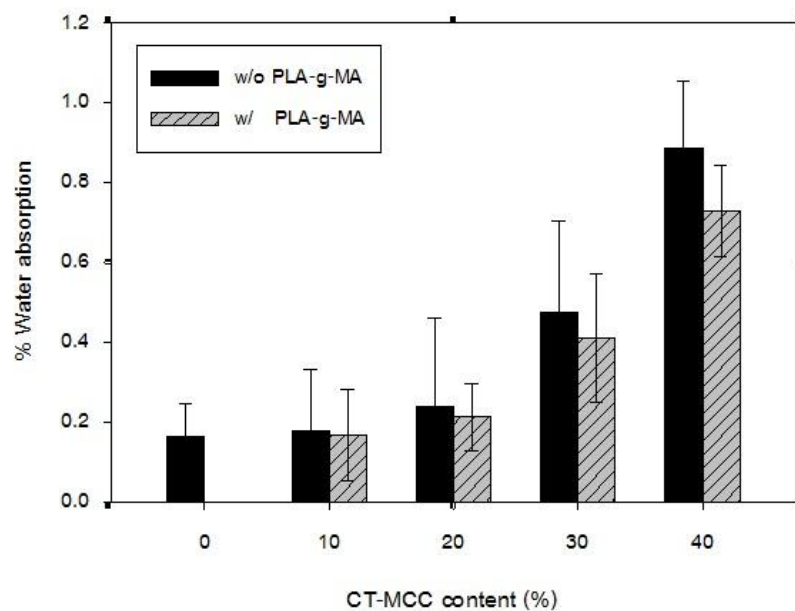
##### 4.3.1.1 Water absorption

##### - Effect of MCC content on water absorption

Figure. 4.16 illustrates water absorption of neat PLA and PLA composites at various CT-MCC content. All the composite films were uncompatibilized. As seen in Figure 4.16 the water absorption increased with the addition of CT-MCC content. The PLA film with 40% CT-MCC showed higher water absorption than neat PLA approximately 0.7%. This evidence supported that the natural fiber is more hydrophilic than PLA. This is a main drawback of using natural fiber in composites because poor water resistance of fiber can cause severe decrease in mechanical properties of the composites. In addition, the adhesion between matrix and fiber gets weak when the composite is wet. So, moisture may reduce the strength of adhesion between the fiber-matrix interface by breaking the bonds and the water absorption may cause rapid debonding. [25,26,29,45]

### - Effect of compatibilizer on water absorption

The addition of compatibilizer reduced the water absorption of the composites when compared with the uncompatibilized ones as seen in **Figure.4.16**. The reduction in % water absorption has been attributed to the formation of covalent bonds between the functional groups of maleic anhydride and the hydroxyl groups at the surfaces of CT-MCC.



**Figure 4.16** The water absorption of composites with compatibilizer and uncompatibilizer

#### 4.3.1.2 Morphology

The fiber–matrix interface of the composite specimens was investigated by SEM to understand the failure mechanisms and also study possible interaction between different components. Overviews of the fractured surfaces of the uncompatibilized and compatibilized composites are given in **Figure 4.17, 4.18**, respectively. It is clear from the results in **Figure 4.17** that in uncompatibilized composites show uniform dispersion

of MCC in the PLA matrix. Another observation is that the MCC still remains as fibers aggregated into bundles and no separation had taken place during the extrusion process. Furthermore, in **Figure 4.18(b), (c), (d), and (e)**, a large number of holes in the PLA matrix are visible where MCC have been located before the fracture. It can also be seen that there was no wetting of fiber surfaces by PLA, possibly because the surface energy of fibers and polymeric matrix are significantly different that the cotton surface is hydrophilic, whereas the PLA surface is hydrophobic. [6]









### 4.3.2 Mechanical Properties

#### -Effect of CT-MCC content on mechanical properties

The effect of CT-MCC content on the tensile properties of neat PLA and CT-MCC/PLA composite films are shown in **Table 4.13** and **Figure 4.20** (a) tensile strength, (b) Young's modulus, and (c) elongation at break, respectively. The results showed that the addition of CT-MCC led to an increase in the Young's modulus but the tensile strength and the elongation at break were decreased.

The significant reduction of tensile strength and elongation at break with increasing CT-MCC content (**Figure 4.20(a), (c)**) is not surprising since other studies have also indicated. According to Mathew and co-worker [46], increasing of fiber or filler loading in composite materials decreased the tensile strength and elongation at break. This result is probably because of the poor adhesion between PLA and CT-MCC phase, as a result poor stress transfer at the MCC-PLA interface occurred. The presence of MCC in a PLA matrix gives rise to defects (voids) at the interfaces which are not only responsible of the decrease for the composite strength and elongation at break, as it has been shown by SEM analysis.

Additionally, the significant reduction in mechanical properties (tensile strength and elongation at break) at high MCC content might be due to the presence of many MCC ends in the composites which could cause crack initiation and, hence, potential material failure [6].

In contrast, MCC incorporation was associated with a significant increase of Young's modulus (**Figure 4.20**). The Young's moduli of PLA and cotton are 2.08 GPa and 5.5 – 12.6 GPa [14], respectively. The significantly high Young's modulus value of cotton fiber explains the increase in stiffness of the produced composites as the CT-MCC content increase.

The production of composites with >20wt% CT-MCC content was accompanied by appearance of increased MCC agglomeration into bundles. Thus, as can be seen, the best mechanical properties were obtained by 10%CT-MCC/PLA composite. Nevertheless, the mechanical properties of the films were still low indicating that the films were brittle when comparing to the commercial PLA films. Therefore, the properties of the PLA composite films should be improved by an incorporation of some additives, such as compatibilizer. [34,44]

**Table 4.13** Tensile properties of CT-MCC/PLA films

Materials	Tensile Strength (MPa)	Tensile Modulus (GPa)	Elongation at break (%)
Neat PLA	43.79±3.28	2.08±0.09	4.79±1.27
10%MCC/PLA	28.52±0.99	2.30±0.12	2.34±0.18
20%MCC/PLA	27.95±1.01	2.39±0.16	2.25±0.15
30%MCC/PLA	26.04±1.62	2.42±0.08	2.18±0.10
40%MCC/PLA	25.38±0.70	2.64±0.22	1.78±0.32
10%MCC/5%PLA-g- MA/PLA	33.44±0.97	1.96±0.11	3.09±0.22
20%MCC/5%PLA-g- MA/PLA	29.40±0.88	2.02±0.09	2.9±0.19
30%MCC/5%PLA-g- MA/PLA	29.32±1.78	2.09±0.12	2.77±0.18
40%MCC/5%PLA-g- MA/PLA	29.16±1.76	2.22±0.27	2.73±0.19

#### -Effect of compatibilizer on mechanical properties

Figure 4.20 and Table 4.13 also present the effect of compatibilizer on the tensile properties of CT-MCC/PLA composite films at various CT-MCC contents. The CT-MCC/PLA composite films with the addition of PLA-g-MA exhibited better tensile properties than those without PLA-g-MA. The most important factor for obtaining good fiber reinforcement in a composite is the strength of adhesion between PLA matrix and fiber [6]. Due to the difference in the polarity of hydrophilic cotton fibers and hydrophobic polymer matrix, a weak interfacial bonding between the two phases is obtained. The other one is the dispersion or uniformity of MCC.

Therefore, the mechanical properties of composites were improved by addition of compatibilizer as can be noticed from the study of Rozman [47]. In their work, the profile of impact strength before and after the addition of coupling agents showed that impact strength. This result confirms that the tendency of agglomeration or non-uniformity and poor adhesion can be decreased.

Similarly, in this work as clearly shown in Figure 4.20, the addition of the compatibilizers led to an improve in the tensile strength and elongation at break. The raising of elongation at break does affect the Young's modulus to decrease as seen in Figure 4.20. This behavior might be due to the interfacial adhesion improvement between two phases caused by PLA-g-MA.

The good performance of PLA-g-MA as a compatibilizer in composites could be attributed to the following two factors: (1) the ability of the MA to react with the hydroxyls of the cotton fibers, and (2) the great compatibility of the grafted copolymer PLA chain with the main PLA phase. [6]



### 4.3.3 Thermal properties

#### 4.3.3.1 Thermalgravimetric Analysis (TGA)

TGA was used to investigate the degradation temperature of MCC/PLA composites. The values of the onset of the degradation temperature are very important, because they could indicate the processing temperatures or initiating a process of decomposition.

##### -Effect of CT-MCC content on the degradation temperature

Figure 4.21 presents the effect of CT-MCC content on the thermal degradation behavior of the CT-MCC/PLA composites at various CT-MCC contents. Obviously, the CT-MCC/PLA composites degraded in single step of weight loss. Table 4.14 summarizes the onset of degradation temperature and residue at specific temperature for all the composites. The neat PLA exhibited the onset of degradation temperature at 342.89 °C, whereas the PLA film with 10, 20, 30, and 40%CT-MCC started to degrade at 327.33, 322.80, 325.16, and 324.85 °C, respectively. When increasing CT-MCC contents, the onset of degradation temperature decreased due to the lower thermal stability of CT-MCC, which had the onset of thermal degradation temperature at 285.48 °C. Therefore, the shift of thermograms towards lower temperature is due to effect of CT-MCC content.

The weight percentage of char at 400 °C for CT-MCC/PLA composites increased with the rise of cotton MCC content. This result means that thermal stability of the CT-MCC/PLA composite at 400 °C enhanced by CT-MCC reinforcements which acted as barrier for better heat insulation.



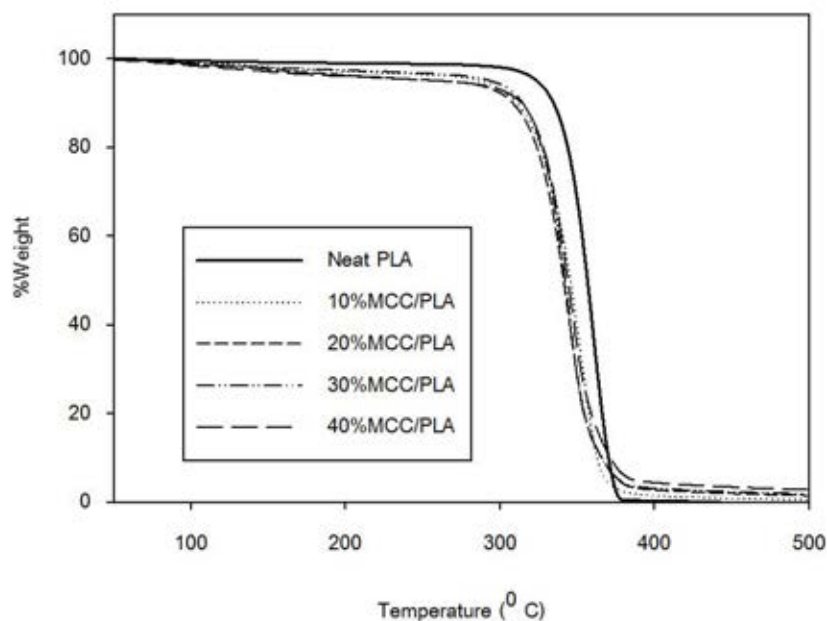


Figure 4.21 TGA curves of uncompatibilized MCC/PLA composites.

Table 4.14 The decomposition temperature at onset and char yield of uncompatibilized MCC/PLA composites.

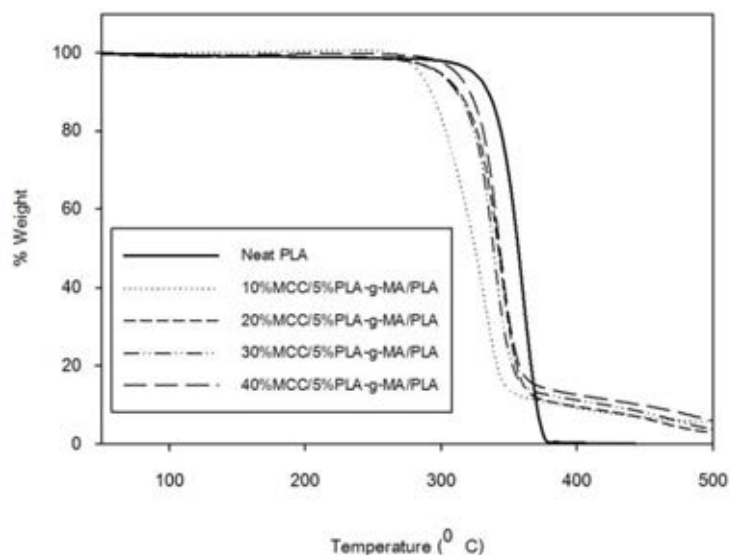
Materials	$T_{d \text{ onset}}$	% Char at 400°C
Neat PLA	342.89	0.26
10%MCC/PLA	327.33	1.43
20%MCC/PLA	322.80	2.72
30%MCC/PLA	325.16	3.06
40%MCC/PLA	324.85	4.35

#### - Effect of compatibilizer on the degradation temperature

The influence of PLA-g-MA is shown in Figure 4.22. The CT-MCC/PLA composite films with PLA-g-MA also show single stage of thermal decomposition. From Figure 4.22 and Table 4.15, as the amount of PLA-g-MA was kept constant, the thermograms of composites films were lower than neat PLA due to the CT-MCC decomposition.

However, in contrast to **Figure 4.21**, the addition of CT-MCC with the presence of PLA-g-MA in the composite films led to an increase in the thermal degradation temperature when the amount of CT-MCC increased. Nevertheless, comparing between the CT-MCC/PLA composite films with and without PLA-g-MA, it was found that the composite films containing PLA-g-MA at any CT-MCC contents (except 40% CT-MCC) had lower onset of decomposition temperature. This should be attributed to the lower onset of decomposition temperature of PLA-g-MA, as previously shown in **Figure 4.13**.

However, upon increasing the temperature upto 400 °C, as shown, thermal stability of the films increased with respect to the amount of PLA-g-MA. Furthermore, the weight percentage of char at 400 °C for CT-MCC/PLA composites with PLA-g-MA increased with the rise of CT-MCC content similar to **Figure 4.22**. **Table 4.3** summarizes the onset of degradation temperature and residue at specific temperature for all the composites with PLA-g-MA.



**Figure 4.22** TGA curves of compatibilized MCC/PLA composites.

**Table 4.15** The decomposition temperature at onset and char yield of compatibilized MCC/PLA composites.

Materials	$T_{d \text{ onset}}$	% Char at 400°C
Neat PLA	342.89	0.26
10%MCC/5%PLA-g-MA/PLA	298.22	9.30
20%MCC/5%PLA-g-MA/PLA	312.46	10.21
30%MCC/5%PLA-g-MA/PLA	322.74	11.24
40%MCC/5%PLA-g-MA/PLA	328.10	12.62

#### 4.3.3.2 Differential Scanning Calorimetry (DSC)

DSC was employed to observe thermal transitions and to get some information on the miscibility between CT-MCC and PLA. As described in the experimental section, three scans for each sample were performed. Second heating cycles provide more information on the reversible transitions by erasing any prior thermal histories associated with the sample.

##### -Effect of CT-MCC content on the thermal transition

Figure 4.23 presents DSC curves of CT-MCC/PLA composites. The DSC thermograms of PLA showed that upon heating, the polymer went through a glass transition at a temperature of about 63.33 °C followed by a single melting peak ( $T_m$ ) at about 149 °C. When increasing the amount of MCC at 10%, the DSC thermogram of 10%CT-MCC/PLA is very different from that of PLA. Double melting peaks at 145 and 150 °C were also observed. Depending on the processing conditions and DSC heating program, the melting peak at lower temperature sometimes appeared as a shoulder on the DSC thermogram. This indicates the co-existence of an  $\alpha$ -form and  $\alpha'$ -form crystals in the PLA. A higher melting temperature induces the formation of the  $\alpha$ -form whereas a



Figure 4.23 DSC thermograms of uncompatibilized CT-MCC/PLA composites

#### -Effect of compatibilizer on the thermal transition

From Figure 4.24, at the same CT-MCC content, the T<sub>g</sub> and T<sub>c</sub> of compatibilized CT-MCC/PLA composite films were lower than those of the uncompatibilized CT-MCC/PLA composite. This result may be because of the faster crystallization. Moreover, the marked drop of T<sub>c</sub> with the increasing CT-MCC content is suggestive of the nucleation activity of fillers.

However, percentage crystallinity of the compatibilized composites was increased at every CT-MCC content when compared to the uncompatibilized composites. This is resulted from the PLA-g-MA which can improve miscibility compatibility between CT-MCC and PLA matrix by increased potential hydrogen bonding. The increased interaction of the fiber with the matrix PLA could further help the fiber surface to act as nucleation sites for the crystallisation of PLA.

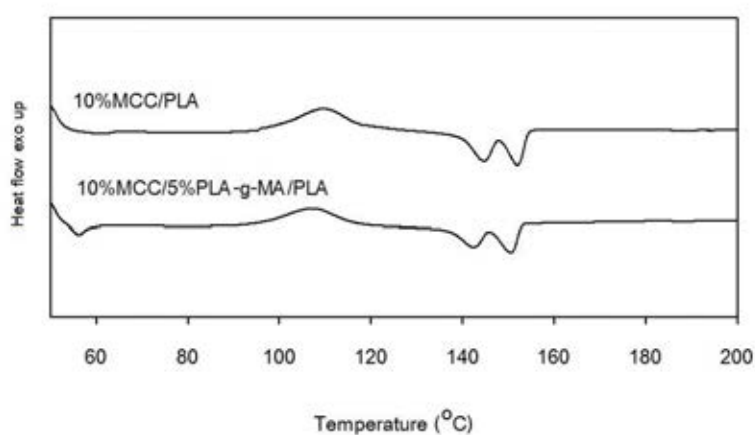


Figure 4.24 DSC thermograms of 10%CT-MCC/PLA and 10%CT-MCC/5%PLA-g-MA/PLA composite films.

**Table 4.16** Second-order transition temperature of MCC/PLA composites.

Materials	Tg(°C)	Tcc(°C)	Tm1(°C)	Tm2(°C)	$\Delta H_m$ (J/g)	$\Delta H_{cc}$ (J/g)	$\chi_c$ (%)
Neat PLA	62.30	115.47	147.64		6.82	5.17	1.77
10%MCC/PLA	61.72	112.74	145.89	150.47	22.43	20.69	2.08
20%MCC/PLA	61.46	108.80	141.14	147.79	20.32	18.69	2.19
30%MCC/PLA	60.49	112.90	143.01	149.52	21.73	18.22	5.39
40%MCC/PLA	60.43	110.47	142.50	148.81	22.77	18.82	7.08
10%CT-MCC/5%PLA-g- MA/PLA	59.76	107.88	141.57	148.68	20.24	17.04	3.82
20%CT-MCC/5%PLA-g- MA/PLA	60.79	107.67	140.72	145.97	17.25	12.20	6.73
30%CT-MCC/5%PLA-g- MA/PLA	60.52	112.45	144.03	148.38	18.85	13.71	7.90
40%CT-MCC/5%PLA-g- MA/PLA	60.74	108.07	140.54	148.45	17.73	11.44	11.27

#### 4.4 Biodegradability of PLA composite films

Biodegradability of PLA composite films was performed by enzymatic degradation and activated sludge degradation. The biodegradability of PLA composite films was followed periodically by determining the change in %weight loss, physical appearance of the film surface, and molecular weight.

Moisture susceptibility is the primary driving force towards PLA degradation and involves four steps, namely, (1) water absorption, (2) ester cleavage forming oligomers,

(3) solubilization of oligomer fractions, and (4) diffusion of soluble oligomers by bacteria.[46] Thus, The first step is important for PLA degradation.

#### 4.4.1 Enzymatic Degradation

##### 4.4.1.1 Lipase

Lipase is an enzyme that catalyzes the hydrolysis of a fatty acid of ester, as a result, it is expected that lipase can induce PLA degradation by appearing holes, %weight loss, shorter molecular chain, etc. Biodegradability evaluation was performed on the percentage of weight loss at every days for 7 days. The appearance of biocomposite films is presented in **Table 4.17 and 4.18**. Before degradation, as seen, the neat PLA films is transparent and very smooth, while the biocomposite films are brownish in color upon increasing the CT-MCC content and the surface was quite smooth. After the enzymatic degradation, the neat PLA film is still transparent and smooth. Similarly, the surface of biocomposite films is hardly changed in their color but became slightly rough.

**Figure 4.25** shows %weight loss of the uncompatibilized biocomposite films at various amounts of CT-MCC with the exposure time in lipase. It was shown that the percentage of weight loss increased as the exposure time and CT-MCC content increased. After 7 days, the 40%CT-MCC/PLA composite suffered a greater than 3% weight loss. In contrast, the neat PLA film can be degraded lower than the biocomposite films. These data clearly indicate that the biodegradability of the biocomposite films was enhanced by an incorporation of the higher CT-MCC content since increasing amount of CT-MCC giving rise to an increase in the surface area to react with water and an increase in the rate of degradation.

Meanwhile, compatibilized biocomposite films showed lower %weight loss than uncompatibilized biocomposite films (**Figure 4.26**). However, both 10%MCC/PLA and

10%MCC/5%PLA-g-MA/PLA composite films can be degraded at approximately the same amount of 1.5% after 7 days under lipase solution.

To confirm the above results, SEM micrographs of biocomposite films before and after lipase enzymatic degradation at 4 days are showed in **Table 4.19**. Before degradation, the results show that when the CT-MCC content increased in the biocomposite films, more CT-MCC was viewed on the surface. After 4 days of exposure, the neat PLA film showed no sign of biodegradation. On the other hand, the biocomposite films containing 30% and 40% CT-MCC were obviously degraded as observed by the holes and damaged surface on the films because they can be attacked by enzyme. Comparing with the uncompatibilized composite films, the compatibilized composite films show no obvious difference from the uncompatibilized composite films probably because lipase enzyme mainly attack the ester bonds in the PLA rather than CT-MCC.



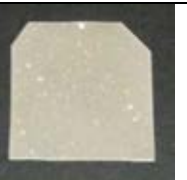


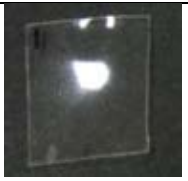


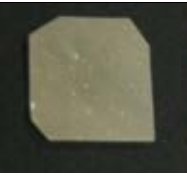

In addition, the molecular weight changes from GPC analysis are showed in **Figure 4.27**. The molecular weight ( $M_n$ ) of the uncompatibilized biocomposite films at various amounts of CT-MCC with the exposure time in lipase shows that the  $M_n$  decreased as time and CT-MCC content increased. These data clearly indicates that the biodegradability of the biocomposite films was enhanced by an incorporation of the higher CT-MCC content since in uncompatibilized composite films; there is a gap between CT-MCC and the PLA matrix. This gap can easily allow the enzyme and water attacking through the PLA matrix. Nevertheless, it can be observed that the molecular weight of PLA can be reduced approximately 70% under lipase enzyme degradation.

Meanwhile, the effect of PLA-g-MA and exposure time on the molecular weight of composite films is showed in **Figure 4.28**. The results show that the molecular weight of the uncompatibilized biocomposite films were decreased more than the compatibilized biocomposite films because the anhydride groups of the PLA-g-MA reacted with the hydroxyl groups on the fiber, increasing interfacial adhesion and



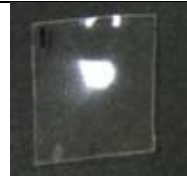







reducing the gaps between the interfaces; as a result the hydrolytic process induced by water absorption decreased.

**Table 4.17** Photographs of PLA and PLA biocomposites showing dependence on degradation time in lipase enzymatic degradation at 4 days

	Neat PLA	10%MCC/ PLA	20%MCC/ PLA	30%MCC/ PLA	40%MCC/ PLA
Before degrada- tion					
After 4 days					

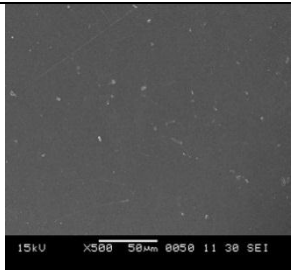
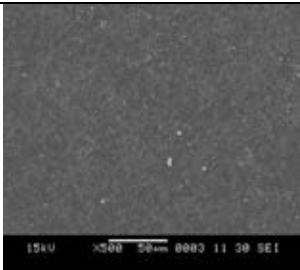
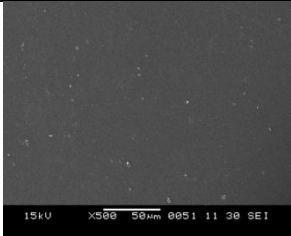
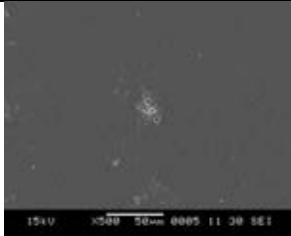
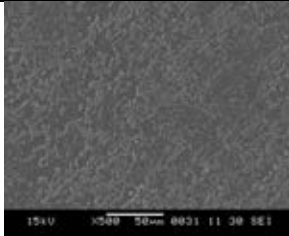
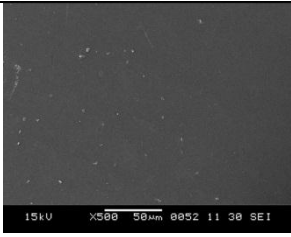
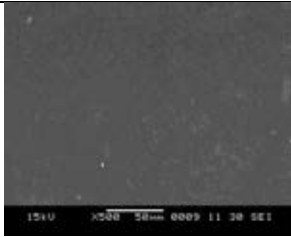
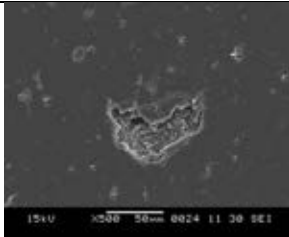
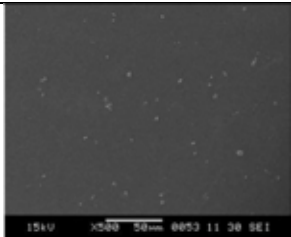
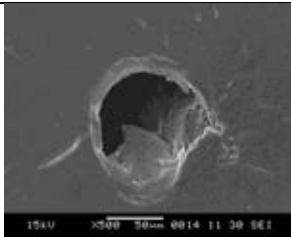
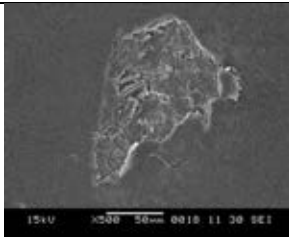
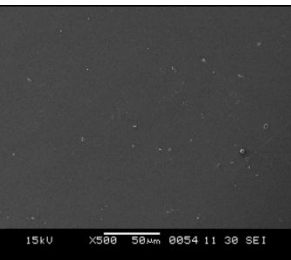
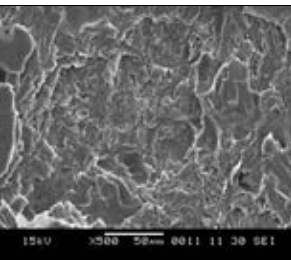
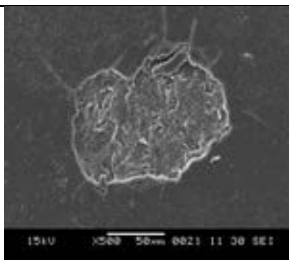
**Table 4.18** Photographs of PLA and 40%MCC/PLA biocomposites showing dependence on degradation time in lipase enzymatic degradation

	Before	2 days	4 days	6 days
Neat PLA				
40%MCC/PLA				





**Table 4.19** SEM micrographs of uncompatibilized and compatibilized biocomposite films before and after biodegradation testing under lipase enzymatic degradation for 4 days.

	Before	After	
		uncompatibilized	compatibilized
Neat PLA			
10% MCC /PLA			
20% MCC /PLA			
30% MCC /PLA			
40% MCC /PLA			

#### 4.4.1.2 Cellulase

Cellulase is an enzyme catalyzing the hydrolysis of cellulose, as a result, PLA biocomposite films containing MCC are expected to be degraded by this enzyme as evidenced by holes, weight loss, shorter molecular chain, etc. of the films. Biodegradability evaluation was performed at every day for 7 days.

From visual observation as shown in **Table 4.20, and 4.21**, after biodegradation, significant changes can be noticed such as roughening of surface, formation of holes or cracks, and changes in color. This result can be confirmed by SEM micrographs.

The micrographs for the uncompatibilized and compatibilized composite films took before and after enzymatic degradation are presented in **Table 4.22**. The undegraded films are characterized by a surface disperse with the CT-MCC. After exposure in cellulase enzyme for 4 days, the surface of biocomposite films exhibits voids since CT-MCC was consumed by enzyme. These micrographs are somewhat different from those presented in **Table 4.19** due to the different targets to be degraded by each enzyme.



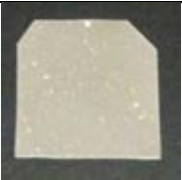







**Figure 4.29** shows %weight loss of the uncompatibilized biocomposite films at various amounts of CT-MCC with the exposure time in cellulase. Similar trends were also found when these films were tested under lipase enzymatic degradation that %weight loss increased upon increasing exposure time and CT-MCC content. These data clearly indicate that the biodegradability of the biocomposite films was increased by an incorporation of the greater amount of CT-MCC due to higher number of hydroxyl groups on the cellulose surface, which can be attacked by cellulase. Furthermore, the CT-MCC may agglomerate on the surface due to poor dispersion which may accelerate the water absorption. After 7 days, the 40%CT-MCC/PLA composite suffered a greater than 4% weight loss, whereas the %weight loss of the neat PLA film slightly increased

approximately upto 1% after 7 days of exposure due to the specific work of cellulase enzyme.









In addition, the effect of PLA-g-MA and exposure time on % weight loss of the biocomposite films is shown in **Figure 4.30**. Obviously, the 10%MCC/5%PLA-g-MA/PLA compatibilized biocomposite films had lower degradation rate than the uncompatibilized biocomposite films due to the hydrogen bonding between the anhydride group of maleic anhydride and hydroxyl groups of cellulose, so the transfer of water molecules and enzyme was interrupted by PLA-g-MA.

**Figure 4.31** presents the changes in molecular weight ( $M_n$ ) of the uncompatibilized biocomposite films at various amounts of CT-MCC as a function of the exposure time under cellulase. It is showed that the molecular weight of PLA decreased by 60% with respect to its initial value, while the molecular weight of biocomposite films was significantly lower than that of the neat PLA upon increasing exposure time since the higher amount of CT-MCC giving rise to an increase in the surface area and greater amount of hydroxyl groups resulted in an increase in the biodegradation rate by cellulase. As shown, the molecular weight of biocomposite films was decreased upto 90%. Meanwhile, **Figure 4.32** shows the effect of PLA-g-MA and exposure time on the molecular weight of composite films. The results show that the molecular weight of uncompatibilized biocomposite films was lower than that of the compatibilized biocomposite films, indicating higher degradation rate of the biocomposite films without PLA-g-MA. These results are in good agreement with the water absorption and SEM micrographs as already explained.

**Table 4.20** Photographs of PLA and PLA biocomposites showing dependence on degradation time in cellulase enzymatic degradation at 4 days

	Neat PLA	10%MCC/ PLA	20%MCC/ PLA	30%MCC/ PLA	40%MCC/ PLA
Before degrada- tion					
After 4 days					

**Table 4.21** Photographs of PLA and 40%MCC/PLA biocomposites showing dependence on degradation time in cellulase enzymatic degradation

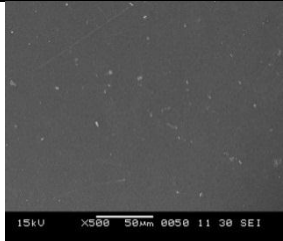
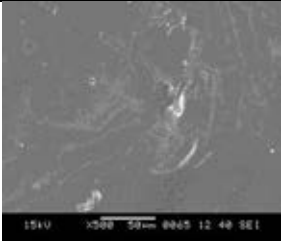
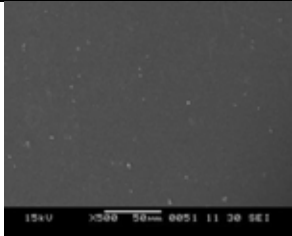
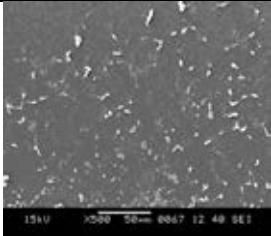
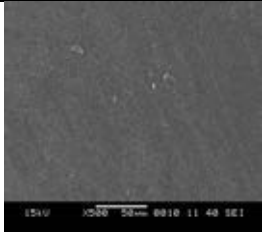
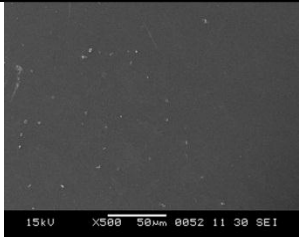

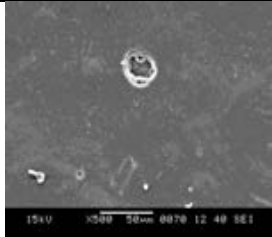
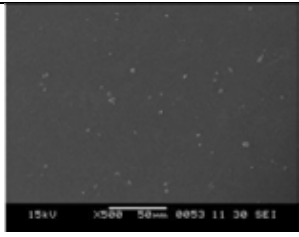
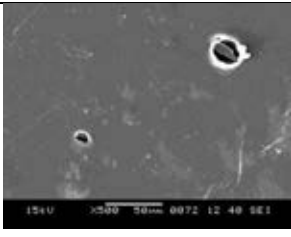

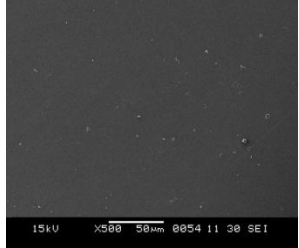
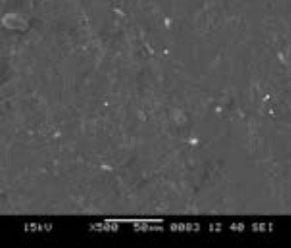
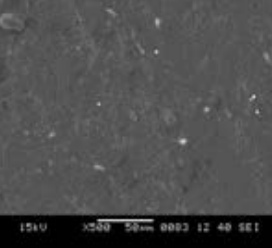
	Before degradation	2 days	4 days	6 days
Neat PLA				
40%MCC/PLA				







**Table 4.22** SEM micrographs of uncompatibilized and compatibilized biocomposite films before and after biodegradation testing under cellulase enzymatic degradation for 4 days.

	Before	After	
		uncompatibilized	compatibilized
Neat PLA			
10% MCC /PLA			
20% MCC /PLA			
30% MCC /PLA			
40% MCC /PLA			

Comparatively, from %weight loss and molecular weight, it can be seen that the neat PLA can be degraded under lipase better than cellulase solution because lipase hydrolyzes ester linkage on PLA as evidenced from % weight loss and molecular weight of PLA. For instance, in the 7 days of testing period, there is 1.5% weight loss of PLA under lipase solution, but only 1% weight loss of PLA in cellulase solution. Moreover, the molecular weight of PLA under lipase solution at 6 days was decreased around 70%, whereas there is only 60% dropped of PLA molecular weight in cellulase solution.

In contrast, the biocomposite films can be degraded under cellulase greater than lipase due to the higher MCC content. For example, in period of 7 days, 40%CT-MCC/PLA composite films under cellulase solution (4%) has shown higher % weight loss than MCC/PLA composite in lipase solution (3%). In addition, the decrease in molecular weight of CT-MCC/PLA composite films was greater than 80% in cellulase solution, in period of 6 days testing.

The effect of PLA-g-MA on both conditions degradation was evidenced from %weight loss and molecular weight. In case of lipase, there is no difference between uncompatibilized and compatibilized biocomposite films because lipase mainly attacks the ester bond of PLA as shown in **Figure 4.25**. While, in cellulase solution, there are differences in %weight loss between uncompatibilized and compatibilized composite films since the MCC was covered by PLA-g-MA. Hence, it is too difficult to attack MCC as shown in **Figure 4.30**.

Furthermore, the result of molecular weight shows similar trend to in both enzyme solutions because the decrease in molecular weight is mainly focused on the chain scission of PLA. At first, PLA composites films under lipase and cellulase solution were still in the first state of degradation or hydrolysis stage. After 2 days of testing

period, PLA composite weight began to decrease significantly according to the degradation mechanism of each enzyme.

#### 4.4.2 Activated Sludge Degradation

After being subjected to the water which was treated by activated sludge system, samples were removed for testing every 1 week. Biodegradation rate was also evaluated by measuring weight loss and molecular weight of the films. Moreover, SEM was used to observe the changes in physical appearance of the film surface.

Before degradation, when the CT-MCC content increased in the composite films, more granules were viewed on the surface, as seen in **Table 4.23**. After biodegradation, the biocomposites films became more opaque and brittle as shown in **Table 4.23 and 4.24**. The surface of the biocomposite films was rough because it was damaged by microorganisms. The degradation or %weight loss of biocomposite films is resulted from the consumption of microorganisms. Microorganisms such as fungi and bacteria can degrade biocomposite films by producing enzymes to digest the carbon molecules of PLA and cellulose backbone.

**Figure 4.33** shows %weight loss of the uncompatibilized biocomposite films at various amounts of CT-MCC with the exposure time under activated sludge system. It is showed that the percentage of weight loss increased when the exposure time and CT-MCC content increased, although changes in %weight loss can slightly be observed within 4 weeks. However, %weight loss increased significantly when the exposure time was extended to 8 weeks. Approximately 40% weight loss can be obtained for the PLA biocomposite films containing 30-40% CT-MCC content. Nevertheless, it can be noticed that the neat PLA film can be slightly degraded under this condition even after 8 weeks of exposure time. The result is very similar to the PLA biocomposite films reported in several researches. [2, 51, 52] The low biodegradability of the PLA films may be

attributed to their hydrophobicity and the resistance in water uptake and diffusion through the neat PLA compared to the biocomposite films.

The effect of compatibilizer and exposure time on the %weight loss of the biocomposite films containing 10%MCC is shown in **Figure 4.34**. As seen, at the first 4 weeks, the percentage of weight loss is still low, there is no difference between the uncompatibilized and compatibilized films. This results can be attributed to the hydrolysis reaction which is occurred at the first period (4 weeks). After 4 weeks, weight loss of both biocomposite films was dramatically increased. This is because the molecular weight of the films is low enough that can be attacked by microorganisms.











Comparing between the compatibilized and uncompatibilized biocomposite films, the uncompatibilized biocomposites film had higher degradation rate than the compatibilized biocomposite film because the uncompatibilized biocomposites film had a gap between MCC and PLA matrix which is contributed to an increase in the porosity of the biocomposites film and then can be easily attacked by microorganisms than the compatibilized biocomposite films.

To confirm the result of %weight loss, SEM micrographs of neat PLA and its biocomposite films before and after degraded in the activated sludge system were compared in **Table 4.25**. After 6 weeks of exposure, PLA films showed a little sign of biodegradation. In contrast, the PLA biocomposite films were obviously degraded as evidenced by the number of holes in the PLA biocomposite films. Upon increasing the exposure time, the surface of film exhibited many voids due to the bulk property of PLA biocomposite films which was quite brittle. Once the PLA biocomposite films were exposed into activated sludge system, physical force from circulating water can cause mechanism damage such as the cracking of the film into small pieces. Regarding the effect of PLA-g-MA as showed in **Table 4.25**, the uncompatibilized biocomposite films present numerous and larger holes than the compatibilized biocomposite films.





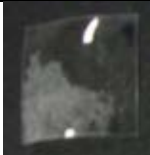

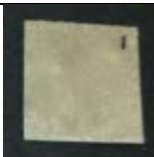

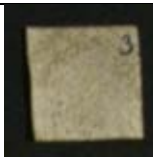

Futhermore, the changes in molecular weight were also observed by GPC as showed in **Figure 4.35**. The changes in molecular weight ( $M_n$ ) at various amounts of CT-MCC as a function of exposure time for the uncompatibilized biocomposite films in activated sludge degradation show that the  $M_n$  was significantly decreased as the exposure time and CT-MCC content increased. The decrease in molecular weight of biocomposite films was found to be two times greater than the neat PLA films. For instance, at 6 weeks, the  $M_n$  of neat PLA films was decreased upto 40%, whereas those of the biocomposite films were decreased upto 60%. The results indicated that the increase of biodegradation rate with increasing CT-MCC content was due to the fact that CT-MCC is highly hydrophilic and it can absorb water into the composite so the hydrolysis reaction and subsequent degradation mechanism of biocomposite films can be occurred easier than the neat PLA.

Meanwhile, the addition of compatibilizer in the composites led to a slight decrease of the biodegradation rate as a result of the hydrophilicity reduction due to the modification of interfacial adhesion. So, it has an effect on  $M_n$  as showed in **Figure 4.36**. The result shows that the molecular weight of the uncompatibilized biocomposite films was decreased more than the compatibilized biocomposite films, suggesting a strong connection between CT-MCC and PLA matrix due to the PLA-g-MA which can close the gaps between the interfaces.

**Table 4.23** Photographs of PLA and PLA biocomposites showing dependence on degradation time in activated sludge system at 8 weeks

	Neat PLA	10%MCC/ PLA	20%MCC/ PLA	30%MCC/ PLA	40%MCC/ PLA
Before degradation					
After 8 weeks					

**Table 4.24** Photographs of PLA and 40%MCC/PLA biocomposites showing dependence on degradation time in activated sludge system

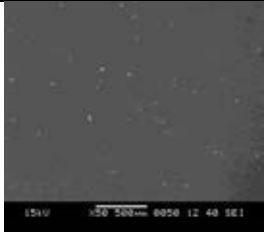
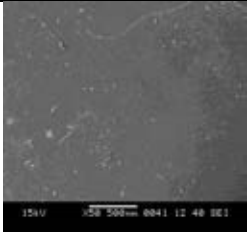
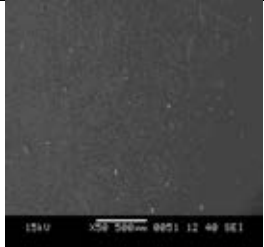
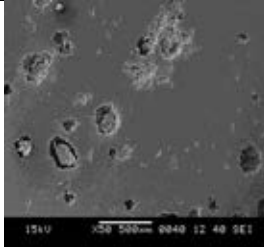
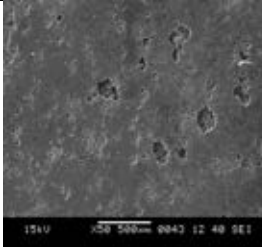
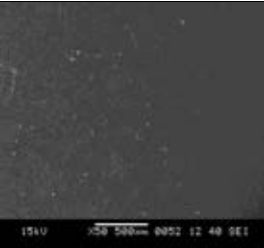
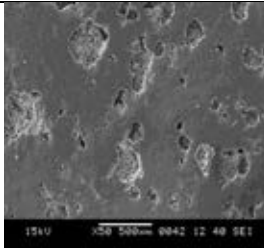
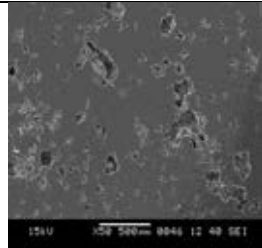
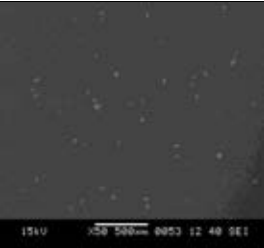
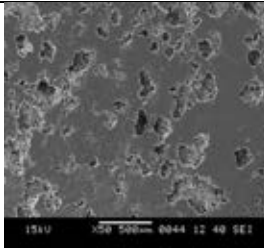
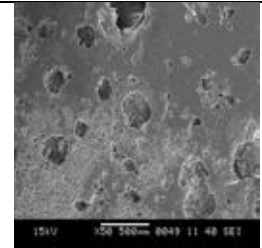
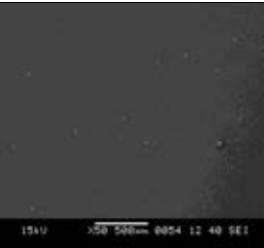
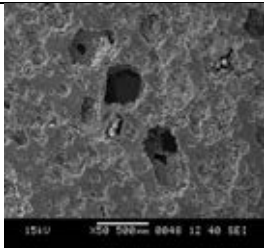
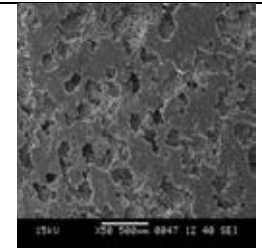
	Before degradation	2 weeks	4 weeks	6 weeks	8 weeks
Neat PLA					
40%MCC/PLA					







**Table 4.25** SEM micrographs of uncompatibilized and compatibilized biocomposite films before and after biodegradation testing under activated sludge system at 6 weeks.

	Before	After	
		uncompatibilized	compatibilized
Neat PLA			
10%MCC /PLA			
20%MCC /PLA			
30%MCC /PLA			
40%MCC /PLA			

## CHAPTER 5

### CONCLUSIONS

#### 5.1 Conclusions

In this research, the preparation of PLA biocomposite films reinforced with various amounts of cotton microcrystalline cellulose (CT-MCC) was studied. The synthesis of polylactic acid grafted maleic anhydride (PLA-g-MA) for improving interfacial adhesion between CT-MCC and PLA was also focused, with the goal of enhancing mechanical properties and biodegradability of the PLA biocomposite films. The results are summarized as follows.

#### **Part 1: Characterization of microcrystalline cellulose prepared from acid hydrolysis of cotton fabric**

- The physical appearance of CT-MCC prepared from hydrolysis of cotton fabric was exhibited shape as white fine powder as same as calcium carbonate powder. The mean particle size of the CT-MCC was small approximately 26.109  $\mu\text{m}$ . From SEM micrographs, CT-MCC presented as short fiber shape with smooth surface having aspect ratio of approximately 5-20  $\mu\text{m}$ .

#### **Part 2: Investigation of the optimum condition for preparation and characterization of PLA-g-MA**

- The optimum conditions for carrying out synthesis of PLA-g-MA was that PLA was dissolve PLA in THF and using BPO as an initiator under nitrogen atmosphere at 85 °C. Maleic anhydride (MA) had to be added into the reactor 30 minutes later and stirred at 80 rpm until 3 h. The grafted product was washed with acetone to remove the unreacted MA, and subsequently precipitating with excessive diethyl ether. The resulting solid was filtered and dried in a vacuum oven at 60 °C for 24 h.

- PLA-g-MA was successfully confirmed by FT-IR analysis. PLA-g-MA exhibited evidence of polymerization by showing the double characteristic adsorption bands of acid anhydride appeared at  $1744\text{ cm}^{-1}$  and  $1769\text{ cm}^{-1}$ . The % real grafting of PLA-g-MA calculated by titration technique is  $2.65\pm 0.09\%$ .

- From the  $^1\text{H-NMR}$  technique, the spectrum of PLA-g-MA showed new peak at 2.1 ppm which was a characteristic of the proton of  $\text{CH}_3$  atom connected with carbon atom and the peak between 4.2 and 4.5 ppm, corresponding to the proton of  $\text{CH}_2$  atom joined to the carbonyl of acid anhydride bond.

- The thermal stability ( $T_d$ ), glass transition temperature ( $T_g$ ), and melting temperature ( $T_m$ ) were  $300\text{ }^\circ\text{C}$ ,  $40.6\text{ }^\circ\text{C}$ , and  $141\text{ }^\circ\text{C}$ , which were lower than these of the pure PLA.

### Part 3: Characterization and testing of PLA biocomposite films

- For physical properties, CT-MCC/PLA composites had higher water absorption than neat PLA especially when increasing CT-MCC content because of the hydrophilic nature of natural fiber. In contrast, the addition of compatibilizer reduced the water absorption of the composites when compared with the uncompatibilized ones due to the formation of covalent bonds between the functional groups of maleic anhydride and the hydroxyl groups at the surfaces of CT-MCC.

- From SEM analysis, the production of composites with CT-MCC content greater than 20 wt% was accompanied by appearance of increased MCC agglomeration into bundles. As can be seen, the best mechanical properties were obtained from the 10%CT-MCC/PLA composite. On the contrary, composites containing compatibilizer showed better fiber dispersion, a more effective fiber wetting by the matrix, and an improved adhesion between the two phases.

- The thermal stability ( $T_d$ ) of biocomposite films was decreased when increasing CT- MCC contents. While, the glass transition ( $T_g$ ) and the melting temperature ( $T_m$ ) of biocomposite films did not change significantly.

- For mechanical properties of biocomposite films, the addition of CT-MCC led to an increase in the Young's modulus but the tensile strength and the elongation at break were decreased. While, the CT-MCC/PLA composite films with the addition of PLA-g-MA had better tensile strength and elongation at break than the uncompatibilized films. This is attributed to the reduction of the difference in the polarity of hydrophilic cotton fibers and hydrophobic polymer matrix by PLA-g-MA.

#### **Part 4: Biodegradability of PLA biocomposite films**

- For enzymatic degradation, after exposure in lipase and cellulase, The PLA biocomposite films started to be degraded slowly after exposure in both enzyme for 4 days. As evidenced by SEM analysis, the surface of film exhibited voids left from the degradation of the CT-MCC. In addition, %weight loss and molecular weight of biocomposite films were decreased.

- For activated sludge system, the PLA biocomposite films began to show slow sign of biodegradation after exposure in activated sludge system for 4 weeks. After that, the biodegradation of both biocomposite films was dramatically increased. To confirm the result by the %weight loss, SEM micrographs, and molecular weight, %weight loss and molecular weight of biocomposite films were reduced, while the surface of film exhibit many voids from the degradation of the films.

- Comparing between the compatibilized and uncompatibilized biocomposite film, the uncompatibilized biocomposites film had higher degradation rate than the compatibilized biocomposite film under both condition because uncompatibilized

biocomposites film had a gap between MCC and PLA matrix which is an increase in porosity of the biocomposites film and can be attacked by microorganism or enzyme.

## REFERENCES

- [1] Yu, L., Dean, K., and Lib, L. Polymer blends and composites from renewable resources. Progress in Polymer Science 31 (2006): 576–602.
- [2] Wu, C-S. Renewable resource-based composites of recycled natural fibers and maleated polylactide bioplastic: Characterization and biodegradability. Polymer Degradation and Stability 94 (2009): 1076–1084.
- [3] Lenglet, S., Li, S., and Vert, M. Lipase-catalysed degradation of copolymers prepared from 3-caprolactone and DL-lactide. Polymer Degradation and Stability 94 (2009): 688–692.
- [4] Belbacem, M.N., and Gandini, A. Monomers, Polymers, and Composites from Renewable Resources First Edition. India : Elsevier, 2008.
- [5] Huda, M.S., Drzal, L.T., Mohanty, A.K., and Misra, M. Effect of fiber surface-treatments on the properties of laminated biocomposites from poly(lactic acid) (PLA) and kenaf fibers. Composites Science and Technology 68 (2008): 424-432.
- [6] Tserki, V., Matzinos, P., and Panayiotou, C. Effect of compatibilization on the Performance of biodegradable Composites using Cotton Fiber Waste as Filler. Journal of Applied Polymer Science 88 (2003): 1825-1835.
- [7] Autar, K. K. Mechanics of Composite Materials, 2<sup>nd</sup> Edition. New York : Taylor & Francis Group, 2006.
- [8] Roylance, D. Introduction to Composite Materials (online). Available from: <http://ocw.mit.edu/courses/materials-science-andengineering/modules/composites.pdf>, (2010, March 24)
- [9] Hollaway, L. Handbook of polymer composites for engineers. Cambridge, UK : Woodhead. 1985.
- [10] Mel, M., and Schwart Z. Composites Materials: Volume I, New Jersey, USA : Prentice Hall PTR. 1996.

- [11] Kopeliovich, D. Interfacial bonding (online). Available from:  
[http://www.substech.com/dokuwiki/doku.php?id=structure\\_of\\_composites](http://www.substech.com/dokuwiki/doku.php?id=structure_of_composites),  
(2010, September 2)
- [12] Aminabhavi, T.M., Balundgi, R.H., Cassidy, P.E. Review on biodegradable plastics. Polymer Plastics Technology and Engineering 29 (1990): 235-262.
- [13] Ashwin Kumar, A., Karthick, K., and Arumugam, K.P. Properties of Biodegradable Polymers and Degradation for Sustainable Development. International Journal of Chemical Engineering and Applications 2(2011).
- [14] Mohanty, A.K., Misra, M., and Drzal, L.T. Natural Fibers, Biopolymers, and Biocomposites. New York: Taylor & Francis Group, 2006.
- [15] Rasal, R.M., Janorkar, A.V., and Hirt, D.E. Poly (lactic acid) modifications. Progress in Polymer Science 35(2010): 338-356.
- [16] Henton, D.E. Poly(lactic acid) technology (online). Available from:  
[http://www.jimluntllc.com/pdfs/poly\(lactic\\_acid\)\\_technology.pdf](http://www.jimluntllc.com/pdfs/poly(lactic_acid)_technology.pdf), (2010, September 2)
- [17] Blackburn, R.S. Biodegradable and sustainable fibres. UK : Woodhead Publishing. 2005.
- [18] Jacobsen, S., Fritz, H.G., Degee, P., Dutois, P., and Jerome, R. New developments on the ring opening polymerization of polylactide. Industrial Crops and Products 11(2000) : 265–275.
- [19] Lim, L.T., Auras, R., and Rubino, M. Processing technologies for poly (lactic acid). Progress in Polymer Science 33(2008) : 820–852.
- [20] Kassig, H.A. Cellulose structure. accessibility, and reactivity. Amsterdam: Gordon & Breach. 1993.
- [21] Salmon, S., Hudson, S.M. Crystal morphology biosynthesis and physical assemble of cellulose. chitin, and chitosan. JMS Rev Macromol Chew Phvs. 1997.



- [22] Richardson, R., and Gorton, L. Characterisation of the substituent distribution in starch and cellulose derivative. Analytica Chimica Acta. 2003.
- [23] Hon DN-S. Chemical modification of cellulose. Chemical modification of lignocellulosic materials. New York. Basel, Hong Kong: Marcel Dekker. 1996.
- [24] Nelson, M. L., and Tripp, V. W. Determination of the leveling-off degree of polymerization of cotton and rayon. Journal of Polymer Science 10(1953) : 577-586.
- [25] Avella, M., Bogoeva-Gaceva, G., Buzarovska, A., Errico, M.E., Gentile, G., and Grozdanov, A. Poly(lactic acid)-based biocomposites reinforced with kenaf fibers. Journal of Applied Polymer Science 108(2008) : 3542-3551.
- [26] García, M., Garmendia, I., and García, J. Influence of natural fiber type in eco-composites. Journal of Applied Polymer Science 107(2008) : 2994-3004.
- [27] Bax, B., and Mussig, J. Impact and tensile properties of PLA/Cordenka and PLA/flax composites. Composites Science and Technology 68(2008) : 1601-1607.
- [28] Bodros, E., Pillin, I., Montrelay, N., and Baley, C. Could biopolymers reinforced by randomly scattered flax fibres be used in structural applications. Composites Science and Technology 67(2007) : 462-470.
- [29] Hu, R., and Lim, J.-K. Fabrication and mechanical properties of completely biodegradable hemp reinforced PLA composites. Journal of composite materials 42(2007) : 1655-1669.
- [30] Tokoro, R., Vu, D.M., Okubo, K., Tanaka, T., Fujii, T., and Fujiura, T. How to improve mechanical properties of polylactic acid with bamboo fibers. Journal of composite materials 43(2008) : 775-787.
- [31] Huda, M.S., Drzal, L.T., Mohanty, A.K., and Misra, M. Wood-fiber-reinforced poly(lactic acid) composites: Evaluation of the physicomechanical and

- morphological properties Journal of Applied Polymer Science 102(2006) : 4856-4869.
- [32] Plackett, D., Andersen, T. L., Pedersen, W. B., and Nielsen, L. Biodegradable composites based on L-poly lactide and jute fibres. Composites Science and Technology 63(2003) : 1287–1296.
- [33] Buzarovska, A., Bogoeva-Gaceva, G., Grozdanov, A., Avella, M., Gentile, G., and Errico, M.E. Potential use of rice straw as a filler in eco-composite materials. Australian Journal of Crop Science 1(2008) : 37-42.
- [34] John, M. J., and Anandjiwala, R. D. Recent developments in chemical modification and characterization of natural fiber-reinforced composites. Polymer Composites 29(2008) :187–207.
- [35] Nyambo C., Mohanty, A.K., and Misra, M. Effect of Maleated Compatibilizer on Performance of PLA/Wheat Straw-Based Green Composites. Macromolecular Materials and Engineering 296(2011) : 710–718
- [36] Moura, I., Machado, A.V., Duarte, F.M., and Nogueira, R. Biodegradability Assessment of Aliphatic Polyesters-Based Blends Using Standard Methods. Journal of Applied Polymer Science 119(2011) : 3338–3346.
- [37] Wu, C.-S. Preparation, Characterization, and Biodegradability of Renewable Resource-Based Composites from Recycled Polylactide Bioplastic and Sisal Fibers. Journal of Applied Polymer Science (2011).
- [38] Sae-On, J. Influence of degree of substitution on physical properties and biodegradability of modified cellulose films from pineapple leaf, corn husk, and waste cotton fabrics under microwave energy. Master's Thesis, Department of Materials Science, Faculty of Science, Chulalongkorn University, 2009.
- [39] Sakhawy, M.E., Hassan, M.L. Physical and mechanical properties of microcrystalline cellulose prepared from agricultural residues. Carbohydrate Polymers 67(2007) : 1-10.

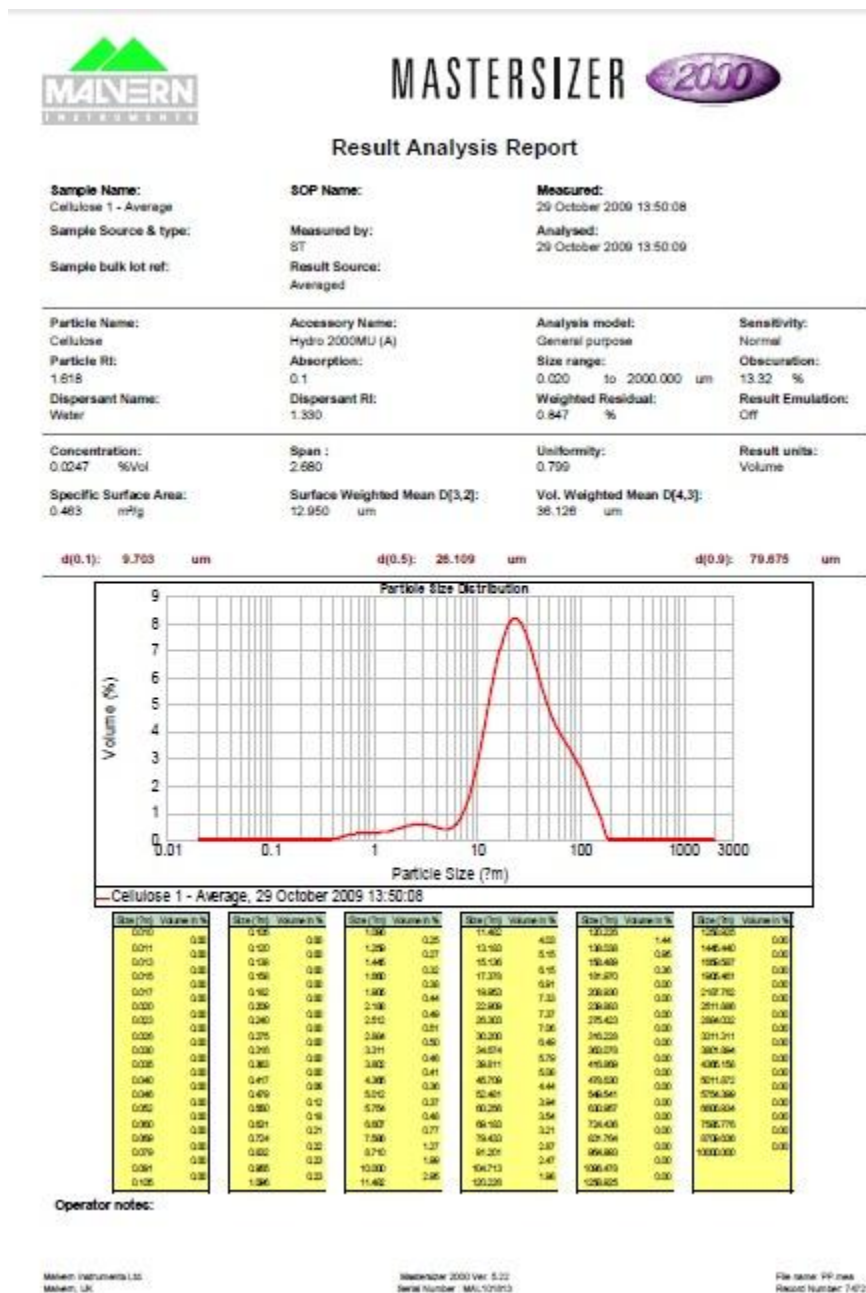
- [40] Abeer, M. A., and others. Characterization of microcrystalline cellulose prepared from lignocellulosic materials. Part I. Acid catalyzed hydrolysis. Bioresource Technology 101(2010) : 4446-4455.
- [41] Odian, G. Principles of Polymerization. 4<sup>th</sup> Edition. New York: A John Wiley & Sons publication, 2004.
- [42] Wikimedia commons. Tetrahydrofan (Online). Available from:  
<http://en.wikipedia.org/wiki/Tetrahydrofuran> (2011, June 31).
- [43] Cao, C., and others. Two-step modification of poly(D,L-lactic acid) by ethylenediamine-maleic anhydride. Biomedical Materials 3(2008).
- [44] Wu, C.-S. Performance and Biodegradability of a Maleated Polyester Bioplastic/recycled Sugarcane Bagasse System. Journal of Applied Polymer Science 121(2011) : 427-435.
- [45] Oksman, K., Skrifvars, M., Selin, J.F. Natural fibres as reinforcement in polylactic acid (PLA) composites. Composites Science and Technology. 63 (2003): 1317–1324.
- [46] Mathew, A.P., Oksman, K., Sain, M. Mechanical properties of Biodegradable Composites from Poly Lactic Acid (PLA) and Microcrystalline Cellulose (MCC). Journal of Applied Polymer Science 97(2005) : 2014-2025.
- [47] Rozman, H.D., Lai, C.Y., Ismil, H. Mohd, Z.A. The effect of coupling agents on the mechanical and physical properties of oil palm empty fruit bunch–polypropylene composites Polymer International 49(2000) : 1273-1278
- [48] Tsai, C.-C., and others. Crystallinity and dimensional stability of biaxial oriented poly(lactic acid) films. Polymer Degradation and Stability 95(2010) : 1292-1298.

- [49] Yasuniwa, M., Tsubakihara, S., Sugimoto, Y., Nakafuku, C. Thermal analysis of the double-melting behavior of poly(L-lactic acid). Journal of Polymer Science Part B: Polymer Physics 42(2004) : 25–32.
- [50] Pracella, M., Chionna, D., Anguillesi, I., Kulinski, Z., Piorkowska, E. Functionalization, compatibilization and properties of polypropylene composites with Hemp fibres. Composites Science and Technology 66(2006) : 2218-2230.
- [51] Hui, P., Jun, L., Jinzhi, L., Ning, Z., Xufeng, N., Zhiquan S., Controlled enzymatic degradation of poly(3-caprolactone)-based copolymers in the presence of porcine pancreatic lipase. Polymer Degradation and Stability. 95 (2010): 643-650.
- [52] Gabriela, S., Nadaeajah, V., Morphological Changes of Annealed Poly- $\epsilon$ -caprolactone by Enzymatic Degradation with Lipase. Journal of Polymer Science: Part B: Polymer Physics. 48, (2010): 202–211.
- [53] Jausovec, D. and others, The antimicrobial reagent role on the degradation of model cellulose film. Journal of Colloid and Interface Science 327(2008) : 75-83.

## APPENDICES

# Appendix A

## A1. Particle size analysis of CT-MCC



## Appendix B

## B1. Water absorption of biocomposite films

Formula : Neat PLA

No. sample	Dry weight	Wet weight	% WAC
1	0.2301	0.2307	0.26
2	0.2229	0.2231	0.09
3	0.2388	0.239	0.08
4	0.2199	0.2204	0.23
5	0.2388	0.2392	0.17
	Average 0.17		
	S.D. 0.08		

Formula : 10%MCC/PLA

No. sample	Dry weight	Wet weight	% WAC
1	0.1815	0.1822	0.39
2	0.1822	0.1824	0.11
3	0.171	0.1712	0.12
4	0.1691	0.1691	0
5	0.1406	0.141	0.28
	Average 0.18		
	S.D. 0.15		

Formula :20%MCC/PLA

No. sample	Dry weight	Wet weight	% WAC
1	0.1958	0.1969	0.56
2	0.182	0.1822	0.11
3	0.1988	0.1989	0.05
4	0.1863	0.187	0.38
5	0.1943	0.1945	0.10
	Average 0.24		
	S.D. 0.22		

Formula :30%MCC/PLA

No. sample	Dry weight	Wet weight	% WAC
1	0.1681	0.1688	0.42
2	0.1793	0.1805	0.67
3	0.1834	0.1846	0.65
4	0.1715	0.1724	0.52
5	0.1765	0.1767	0.11
Average 0.48			
S.D. 0.23			

Formula :40%MCC/PLA

No. sample	Dry weight	Wet weight	% WAC
1	0.2106	0.2123	0.81
2	0.2136	0.2159	1.08
3	0.2068	0.2091	1.11
4	0.2032	0.2051	0.94
5	0.1857	0.1874	0.92
Average 0.97			
S.D. 0.12			

Formula : 10%MCC/5%PLA-g-MA/PLA

No. sample	Dry weight	Wet weight	% WAC
1	0.2178	0.2184	0.28
2	0.2127	0.2128	0.05
3	0.2141	0.2145	0.19
4	0.178	0.1785	0.28
5	0.1934	0.1935	0.05
Average 0.17			
S.D. 0.11			



Formula :20%MCC/5%PLA-g-MA/PLA

No. sample	Dry weight	Wet weight	% WAC
1	0.1513	0.1517	0.26
2	0.1396	0.1397	0.07
3	0.1358	0.1361	0.22
4	0.1357	0.136	0.22
5	0.1385	0.1389	0.29
Average 0.21			
S.D. 0.08			

Formula :30%MCC/5%PLA-g-MA/PLA

No. sample	Dry weight	Wet weight	% WAC
1	0.1455	0.146	0.34
2	0.1579	0.1585	0.38
3	0.139	0.1398	0.58
4	0.1602	0.1611	0.56
5	0.158	0.1583	0.19
Average 0.41			
S.D. 0.16			

Formula : 40%MCC/5%PLA-g-MA/PLA

No. sample	Dry weight	Wet weight	% WAC
1	0.1851	0.1868	0.92
2	0.2032	0.2045	0.64
3	0.2255	0.227	0.67
4	0.2267	0.2284	0.75
5	0.2228	0.2243	0.67
Average 0.73			
S.D. 0.11			

## B2. Tensile Properties of biocomposite films

Formula : Neat PLA

No. Sample	Tensile strength (MPa)	Young's Modulus (GPa)	Elongation at break (%)
1	41.84	2.07	4.49
2	44.53	2.09	3.73
3	49.03	2.00	6.75
4	40.53	2.23	3.69
5	43.01	2.04	5.28
Average	43.79	2.08	4.79
S.D.	3.28	0.09	1.27

Formula : 10%MCC/PLA

No. Sample	Tensile strength (MPa)	Young's Modulus (GPa)	Elongation at break (%)
1	28.09	2.15	2.56
2	27.55	2.44	2.16
3	30.11	2.41	2.36
4	28.79	2.28	2.45
5	28.07	2.23	2.18
Average	28.52	2.30	2.34
S.D.	0.99	0.12	0.18

Formula :20%MCC/PLA

No. Sample	Tensile strength (MPa)	Young's Modulus (GPa)	Elongation at break (%)
1	29.39	2.38	2.28
2	27.62	2.65	2.03
3	28.35	2.30	2.42
4	27.74	2.25	2.35
5	26.66	2.36	2.20
Average	27.95	2.39	2.25
S.D.	1.01	0.16	0.15

Formula :30%MCC/PLA

No. Sample	Tensile strength (MPa)	Young's Modulus (GPa)	Elongation at break (%)
1	27.77	2.52	2.19
2	27.64	2.46	2.06
3	24.18	2.44	2.09
4	25.79	2.35	2.24
5	24.85	2.33	2.31
Average	26.04	2.42	2.18
S.D.	1.62	0.08	0.10

Formula :40%MCC/PLA

No. Sample	Tensile strength (MPa)	Young's Modulus (GPa)	Elongation at break (%)
1	26.49	3.01	1.85
2	25.45	2.58	1.99
3	24.96	2.47	1.90
4	25.34	2.51	1.92
5	24.66	2.64	1.22
Average	25.38	2.64	1.78
S.D.	0.70	0.22	0.32

Formula :10%MCC/5%PLA-g-MA/PLA

No. Sample	Tensile strength (MPa)	Young's Modulus (GPa)	Elongation at break (%)
1	34.47	1.81	3.48
2	32.69	1.90	2.95
3	33.04	1.99	2.98
4	34.48	2.09	2.99
5	32.50	2.01	3.05
Average	33.44	1.96	3.09
S.D.	0.97	0.11	0.22

Formula :20%MCC/5%PLA-g-MA/PLA

No. Sample	Tensile strength(MPa)	Young's Modulus (GPa)	Elongation at break (%)
1	28.01	1.89	2.72
2	29.58	2.02	3.03
3	30.46	2.12	3.19
4	29.47	2.09	3.14
5	29.49	1.97	2.89
Average	29.40	2.02	2.99
S.D.	0.88	0.09	0.19

Formula :30%MCC/5%PLA-g-MA/PLA

No. Sample	Tensile strength (MPa)	Young's Modulus (GPa)	Elongation at break (%)
1	26.83	2.18	2.89
2	29.00	1.90	2.49
3	31.80	2.14	2.95
4	29.76	2.18	2.78
5	29.19	2.02	2.75
Average	29.32	2.09	2.77
S.D.	1.78	0.12	0.18

Formula :40%MCC/5%PLA-g-MA/PLA

No. Sample	Tensile strength (MPa)	Young's Modulus (GPa)	Elongation at break (%)
1	26.54	2.05	2.42
2	28.47	2.08	2.95
3	30.77	2.31	2.75
4	29.32	2.64	2.79
5	30.71	2.00	2.76
Average	29.16	2.22	2.73
S.D.	1.76	0.27	0.19

### B3. Enzymatic degradation: Lipase

Formula : Neat PLA

Time (days)	Sample No.	Wi	Wf	%Weight loss	Average	SD
1	1	0.1320	0.1319	0.08	0.11	0.05
	2	0.1369	0.1367	0.15		
2	1	0.1326	0.1326	0.00	0.30	0.43
	2	0.1326	0.1318	0.60		
3	1	0.1231	0.1223	0.65	0.32	0.46
	2	0.1422	0.1422	0.00		
4	1	0.1338	0.1332	0.45	0.58	0.19
	2	0.1258	0.1249	0.72		
5	1	0.1312	0.1310	0.15	0.71	0.79
	2	0.1335	0.1318	1.27		
6	1	0.1319	0.1303	1.21	0.79	0.60
	2	0.1392	0.1387	0.36		
7	1	0.1429	0.1418	0.77	1.51	1.05
	2	0.1201	0.1174	2.25		

Formula :10%MCC/PLA

Time (days)	Sample No.	Wi	Wf	%Weight loss	Average	SD
1	1	0.1113	0.1109	0.36	0.31	0.07
	2	0.1128	0.1125	0.27		
2	1	0.1320	0.1304	1.21	0.88	0.47
	2	0.1272	0.1265	0.55		
3	1	0.1108	0.1096	1.08	1.04	0.06
	2	0.0896	0.0887	1.00		
4	1	0.1331	0.1313	1.35	1.17	0.26
	2	0.1115	0.1104	0.99		
5	1	0.1188	0.1169	1.60	1.34	0.37
	2	0.1213	0.1200	1.07		
6	1	0.1058	0.1041	1.61	1.51	0.14
	2	0.1273	0.1255	1.41		
7	1	0.1014	0.0990	2.37	1.51	1.21
	2	0.1074	0.1067	0.65		

Formula :20%MCC/PLA

Time (days)	Sample No.	Wi	Wf	%Weight loss	Average	SD
1	1	0.1165	0.1161	0.34	0.57	0.32
	2	0.1137	0.1128	0.79		
2	1	0.0992	0.0986	0.60	0.92	0.45
	2	0.0964	0.0952	1.24		
3	1	0.1050	0.1034	1.52	0.96	0.80
	2	0.1259	0.1254	0.40		
4	1	0.1331	0.1318	0.98	0.98	0.01
	2	0.1115	0.1104	0.99		
5	1	0.1403	0.1377	1.85	1.94	0.12
	2	0.1383	0.1355	2.02		
6	1	0.1138	0.1115	2.02	2.11	0.13
	2	0.1133	0.1108	2.21		
7	1	0.1155	0.1122	2.86	2.57	0.41
	2	0.1406	0.1374	2.28		

Formula :30%MCC/PLA

Time (days)	Sample No.	Wi	Wf	%Weight loss	Average	SD
1	1	0.1102	0.1100	0.18	0.67	0.69
	2	0.1381	0.1365	1.16		
2	1	0.1147	0.1123	2.09	1.40	0.98
	2	0.1135	0.1127	0.70		
3	1	0.1093	0.1075	1.65	1.72	0.11
	2	0.1168	0.1147	1.80		
4	1	0.1164	0.1158	0.52	1.82	1.84
	2	0.1122	0.1087	3.12		
5	1	0.1134	0.1105	2.56	1.93	0.89
	2	0.1154	0.1139	1.30		
6	1	0.1240	0.1209	2.50	2.17	0.46
	2	0.1193	0.1171	1.84		
7	1	0.1181	0.1157	2.03	2.37	0.47
	2	0.1112	0.1082	2.70		

Formula :40%MCC/PLA

Time (days)	Sample No.	Wi	Wf	%Weight loss	Average	SD
1	1	0.1305	0.1283	1.69	1.16	0.74
	2	0.1106	0.1099	0.63		
2	1	0.1031	0.1019	1.16	1.99	1.17
	2	0.1173	0.1140	2.81		
3	1	0.1383	0.1354	2.10	2.18	0.11
	2	0.1241	0.1213	2.26		
4	1	0.1295	0.1260	2.70	2.23	0.66
	2	0.1077	0.1058	1.76		
5	1	0.1221	0.1179	3.44	2.82	0.87
	2	0.1224	0.1197	2.21		
6	1	0.1054	0.1013	3.89	2.95	1.32
	2	0.1239	0.1214	2.02		
7	1	0.1301	0.1256	3.46	2.99	0.66
	2	0.1150	0.1121	2.52		

Formula :10%MCC/5%PLA-g-MA/PLA

Time (days)	Sample No.	Wi	Wf	%Weight loss	Average	SD
1	1	0.1253	0.1238	1.20	1.00	0.28
	2	0.1121	0.1112	0.80		
2	1	0.0927	0.0916	1.19	1.08	0.15
	2	0.0820	0.0812	0.98		
3	1	0.1215	0.1200	1.23	1.14	0.14
	2	0.1251	0.1238	1.04		
4	1	0.0889	0.0873	1.80	1.23	0.80
	2	0.1203	0.1195	0.67		
5	1	0.1217	0.1201	1.31	1.40	0.12
	2	0.1208	0.1190	1.49		
6	1	0.1071	0.1049	2.05	1.49	0.80
	2	0.1190	0.1179	0.92		
7	1	0.1175	0.1159	1.36	1.59	0.33
	2	0.1261	0.1238	1.82		

Formula :20%MCC/5%PLA-g-MA/PLA

Time (days)	Sample No.	Wi	Wf	%Weight loss	Average	SD
1	1	0.1269	0.1260	0.71	1.14	0.60
	2	0.1280	0.1260	1.56		
2	1	0.1040	0.1038	0.19	1.27	1.52
	2	0.0981	0.0958	2.34		
3	1	0.1194	0.1177	1.42	1.33	0.13
	2	0.1209	0.1194	1.24		
4	1	0.1192	0.1183	0.76	1.52	1.08
	2	0.1359	0.1328	2.28		
5	1	0.1081	0.1060	1.94	1.64	0.43
	2	0.1280	0.1263	1.33		
6	1	0.1375	0.1339	2.62	1.97	0.92
	2	0.1060	0.1046	1.32		
7	1	0.1106	0.1082	2.17	2.26	0.13
	2	0.1362	0.1330	2.35		

Formula :30%MCC/5%PLA-g-MA/PLA

Time (days)	Sample No.	Wi	Wf	%Weight loss	Average	SD
1	1	0.1347	0.1340	0.52	0.93	0.58
	2	0.1192	0.1176	1.34		
2	1	0.1331	0.1310	1.58	1.46	0.17
	2	0.1348	0.1330	1.34		
3	1	0.1222	0.1204	1.47	1.47	0.01
	2	0.1371	0.1351	1.46		
4	1	0.1150	0.1121	2.52	1.73	1.12
	2	0.1275	0.1263	0.94		
5	1	0.1156	0.1130	2.25	1.82	0.60
	2	0.1214	0.1197	1.40		
6	1	0.1214	0.1193	1.73	1.87	0.20
	2	0.1393	0.1365	2.01		
7	1	0.1335	0.1323	0.90	2.40	2.12
	2	0.1105	0.1062	3.89		



Formula :40%MCC/5%PLA-g-MA/PLA

Time (days)	Sample No.	Wi	Wf	%Weight loss	Average	SD
1	1	0.1464	0.1456	0.55	0.87	0.45
	2	0.1350	0.1334	1.19		
2	1	0.1383	0.1361	1.59	1.17	0.59
	2	0.1331	0.1321	0.75		
3	1	0.1407	0.1380	1.92	1.18	1.05
	2	0.1157	0.1152	0.43		
4	1	0.1401	0.1374	1.93	1.25	0.95
	2	0.1378	0.1370	0.58		
5	1	0.1473	0.1455	1.22	1.32	0.13
	2	0.1276	0.1258	1.41		
6	1	0.1328	0.1309	1.43	1.43	0.00
	2	0.1403	0.1383	1.43		
7	1	0.1325	0.1305	1.51	1.46	0.08
	2	0.1355	0.1336	1.40		

#### B4. Enzymatic degradation: Cellulase

Formula : Neat PLA

Time (days)	Sample No.	Wi	Wf	%Weight loss	Average	SD
1	1	0.1455	0.1452	0.21	0.25	0.07
	2	0.1326	0.1322	0.30		
2	1	0.1277	0.1272	0.39	0.38	0.02
	2	0.1369	0.1364	0.37		
3	1	0.1389	0.1381	0.58	0.39	0.26
	2	0.1422	0.1419	0.21		
4	1	0.1398	0.1394	0.29	0.42	0.19
	2	0.1258	0.1251	0.56		
5	1	0.1324	0.1314	0.76	0.61	0.21
	2	0.1318	0.1312	0.46		
6	1	0.1168	0.1155	1.11	1.03	0.12
	2	0.1387	0.1374	0.94		
7	1	0.1429	0.1418	0.77	1.09	0.46
	2	0.1201	0.1184	1.42		

Formula : 10%MCC/PLA

Time (days)	Sample No.	Wi	Wf	%Weight loss	Average	SD
1	1	0.1113	0.1109	0.36	0.31	0.07
	2	0.1128	0.1125	0.27		
2	1	0.1034	0.1025	0.87	0.55	0.45
	2	0.1265	0.1262	0.24		
3	1	0.1167	0.1161	0.51	0.57	0.08
	2	0.1273	0.1265	0.63		
4	1	0.1236	0.1228	0.65	0.68	0.05
	2	0.1115	0.1107	0.72		
5	1	0.1278	0.1269	0.70	0.74	0.05
	2	0.0896	0.0889	0.78		
6	1	0.1216	0.1206	0.82	0.79	0.05
	2	0.1200	0.1191	0.75		
7	1	0.1361	0.1348	0.96	0.94	0.02
	2	0.1074	0.1064	0.93		

Formula :20%MCC/PLA

Time (days)	Sample No.	Wi	Wf	%Weight loss	Average	SD
1	1	0.0945	0.0937	0.85	0.73	0.16
	2	0.1128	0.1121	0.62		
2	1	0.0965	0.0953	1.24	0.83	0.58
	2	0.0952	0.0948	0.42		
3	1	0.1085	0.1065	1.84	1.44	0.57
	2	0.1254	0.1241	1.04		
4	1	0.1208	0.1189	1.57	1.47	0.15
	2	0.1104	0.1089	1.36		
5	1	0.1147	0.1135	1.05	1.63	0.83
	2	0.1355	0.1325	2.21		
6	1	0.1132	0.1109	2.03	1.96	0.10
	2	0.1108	0.1087	1.90		
7	1	0.1011	0.0989	2.18	2.23	0.07
	2	0.1406	0.1374	2.28		

Formula :30%MCC/PLA

Time (days)	Sample No.	Wi	Wf	%Weight loss	Average	SD
1	1	0.1018	0.1003	1.47	1.50	0.03
	2	0.1381	0.1360	1.52		
2	1	0.1127	0.1114	1.15	1.19	0.06
	2	0.1135	0.1121	1.23		
3	1	0.1003	0.0977	2.59	2.44	0.22
	2	0.1139	0.1113	2.28		
4	1	0.1075	0.1045	2.79	2.51	0.40
	2	0.1168	0.1142	2.23		
5	1	0.1049	0.1027	2.10	2.61	0.72
	2	0.1122	0.1087	3.12		
6	1	0.1049	0.1026	2.19	2.86	0.94
	2	0.1193	0.1151	3.52		
7	1	0.1076	0.1023	4.93	3.95	1.38
	2	0.1112	0.1079	2.97		

Formula :40%MCC/PLA

Time (days)	Sample No.	Wi	Wf	%Weight loss	Average	SD
1	1	0.1621	0.1593	1.73	1.77	0.06
	2	0.1106	0.1086	1.81		
2	1	0.1626	0.1580	2.83	2.47	0.51
	2	0.1140	0.1116	2.11		
3	1	0.1676	0.1634	2.51	2.54	0.05
	2	0.1241	0.1209	2.58		
4	1	0.1674	0.1634	2.39	2.73	0.48
	2	0.1239	0.1201	3.07		
5	1	0.1665	0.1626	2.34	2.75	0.58
	2	0.1077	0.1043	3.16		
6	1	0.1660	0.1620	2.41	2.76	0.49
	2	0.1224	0.1186	3.10		
7	1	0.1646	0.1594	3.16	2.84	0.45
	2	0.1150	0.1121	2.52		

Formula :10%MCC/5%PLA-g-MA/PLA

Time (days)	Sample No.	Wi	Wf	%Weight loss	Average	SD
1	1	0.1218	0.1217	0.08	0.22	0.19
	2	0.1121	0.1117	0.36		
2	1	0.1280	0.1276	0.31	0.28	0.05
	2	0.0820	0.0818	0.24		
3	1	0.1139	0.1131	0.70	0.60	0.14
	2	0.1203	0.1197	0.50		
4	1	0.1255	0.1247	0.64	0.62	0.03
	2	0.1179	0.1172	0.59		
5	1	0.1273	0.1268	0.39	0.64	0.35
	2	0.1238	0.1227	0.89		
6	1	0.1245	0.1234	0.88	0.72	0.23
	2	0.1261	0.1254	0.56		
7	1	0.1255	0.1247	0.64	0.74	0.15
	2	0.1179	0.1169	0.85		

Formula :20%MCC/5%PLA-g-MA/PLA

Time (days)	Sample No.	Wi	Wf	%Weight loss	Average	SD
1	1	0.1277	0.1274	0.23	0.20	0.06
	2	0.1280	0.1278	0.16		
2	1	0.1316	0.1314	0.15	0.27	0.17
	2	0.1280	0.1275	0.39		
3	1	0.1128	0.1124	0.35	0.43	0.11
	2	0.0981	0.0976	0.51		
4	1	0.1291	0.1277	1.08	1.04	0.06
	2	0.1209	0.1197	0.99		
5	1	0.1297	0.1286	0.85	1.20	0.49
	2	0.1359	0.1338	1.55		
6	1	0.1205	0.1189	1.33	1.32	0.00
	2	0.1060	0.1046	1.32		
7	1	0.1250	0.1226	1.92	2.13	0.30
	2	0.1362	0.1330	2.35		

Formula :30%MCC/5%PLA-g-MA/PLA

Time (days)	Sample No.	Wi	Wf	%Weight loss	Average	SD
1	1	0.1436	0.1424	0.84	0.63	0.29
	2	0.1176	0.1171	0.43		
2	1	0.1470	0.1449	1.43	0.90	0.74
	2	0.1330	0.1325	0.38		
3	1	0.1275	0.1260	1.18	1.06	0.16
	2	0.1371	0.1358	0.95		
4	1	0.1349	0.1327	1.63	1.48	0.21
	2	0.1275	0.1258	1.33		
5	1	0.1458	0.1439	1.30	1.35	0.07
	2	0.1214	0.1197	1.40		
6	1	0.1443	0.1418	1.73	1.76	0.04
	2	0.1393	0.1368	1.79		
7	1	0.1391	0.1367	1.73	2.81	1.53
	2	0.1105	0.1062	3.89		

Formula :40%MCC/5%PLA-g-MA/PLA

Time (days)	Sample No.	Wi	Wf	%Weight loss	Average	SD
1	1	0.1298	0.1282	1.23	1.10	0.18
	2	0.1331	0.1318	0.98		
2	1	0.1185	0.1168	1.43	1.19	0.34
	2	0.1152	0.1141	0.95		
3	1	0.1442	0.1426	1.11	1.26	0.21
	2	0.1276	0.1258	1.41		
4	1	0.1205	0.1190	1.24	1.29	0.06
	2	0.1350	0.1332	1.33		
5	1	0.1383	0.1363	1.45	1.34	0.15
	2	0.1378	0.1361	1.23		
6	1	0.1254	0.1231	1.83	2.17	0.48
	2	0.1355	0.1321	2.51		
7	1	0.1397	0.1360	2.65	2.30	0.49
	2	0.1383	0.1356	1.95		

## B5. Activated Sludge Degradation

Formula : Neat PLA

Time (week)	Sample No.	Wi	Wf	%Weight loss	Average	SD
1	1	0.1233	0.1220	1.05	0.44	0.47
	2	0.1276	0.1275	0.08		
	3	0.1156	0.1156	0.00		
	4	0.1229	0.1226	0.24		
	5	0.1222	0.1212	0.82		
2	1	0.1109	0.1101	0.72	0.46	0.41
	2	0.1221	0.1218	0.25		
	3	0.1228	0.1215	1.06		
	4	0.1443	0.1440	0.21		
	5	0.1226	0.1225	0.08		
3	1	0.0992	0.0989	0.30	0.55	0.37
	2	0.1245	0.1234	0.88		
	3	0.1280	0.1267	1.02		
	4	0.1166	0.1163	0.26		
	5	0.1340	0.1336	0.30		
4	1	0.1247	0.1237	0.80	1.04	1.11
	2	0.1248	0.1213	2.80		
	3	0.1107	0.1092	1.36		
	4	0.1166	0.1165	0.09		
	5	0.1185	0.1183	0.17		
5	1	0.1041	0.1023	1.73	1.17	0.39
	2	0.1204	0.1190	1.16		
	3	0.1201	0.1185	1.33		
	4	0.1209	0.1200	0.74		
	5	0.1146	0.1136	0.87		
6	1	0.1142	0.1125	1.49	1.22	0.80
	2	0.1188	0.1176	1.01		
	3	0.1261	0.1253	0.63		
	4	0.1204	0.1198	0.50		
	5	0.1130	0.1102	2.48		
7	1	0.1265	0.1243	1.74	1.41	0.58
	2	0.1273	0.1258	1.18		
	3	0.1124	0.1114	0.89		
	4	0.1279	0.1250	2.27		
	5	0.1205	0.1193	1.00		
8	1	0.1325	0.1298	2.04	2.84	1.18
	2	0.1090	0.1047	3.94		
	3	0.1191	0.1140	4.28		
	4	0.1216	0.1190	2.14		
	5	0.1227	0.1205	1.79		

Formula :10%MCC/PLA

Time (week)	Sample No.	Wi	Wf	%Weight loss	Average	SD
1	1	0.1139	0.1115	2.11	1.52	0.70
	2	0.1028	0.1010	1.75		
	3	0.1192	0.1175	1.43		
	4	0.1114	0.1110	0.36		
	5	0.1183	0.1160	1.94		
2	1	0.1260	0.1228	2.54	2.01	0.58
	2	0.1179	0.1156	1.95		
	3	0.1266	0.1243	1.82		
	4	0.1287	0.1254	2.56		
	5	0.1193	0.1179	1.17		
3	1	0.1210	0.1170	3.31	2.46	1.22
	2	0.1296	0.1266	2.31		
	3	0.1272	0.1259	1.02		
	4	0.1096	0.1078	1.64		
	5	0.1213	0.1164	4.04		
4	1	0.1071	0.1043	2.61	3.87	0.82
	2	0.1201	0.1147	4.50		
	3	0.1151	0.1097	4.69		
	4	0.1271	0.1222	3.86		
	5	0.1186	0.1142	3.71		
5	1	0.1259	0.1211	3.81	4.89	0.92
	2	0.1031	0.0988	4.21		
	3	0.1263	0.1199	5.07		
	4	0.1124	0.1066	5.16		
	5	0.1182	0.1109	6.18		
6	1	0.1131	0.1006	11.05	9.95	2.59
	2	0.0924	0.0870	5.84		
	3	0.1261	0.1105	12.37		
	4	0.1002	0.0911	9.08		
	5	0.1159	0.1027	11.39		
7	1	0.1269	0.1123	11.51	10.28	2.98
	2	0.1254	0.1136	9.41		
	3	0.1245	0.1061	14.78		
	4	0.1187	0.1103	7.08		
	5	0.1287	0.1176	8.62		
8	1	0.1279	0.1080	15.56	23.72	10.67
	2	0.1263	0.1090	13.70		
	3	0.1030	0.0611	40.68		
	4	0.1248	0.0945	24.28		
	5	0.1276	0.0965	24.37		



Formula :20%MCC/PLA

Time (week)	Sample No.	Wi	Wf	%Weight loss	Average	SD
1	1	0.1273	0.1255	1.41	1.61	0.21
	2	0.1200	0.1183	1.42		
	3	0.1331	0.1309	1.65		
	4	0.1465	0.1437	1.91		
	5	0.1490	0.1465	1.68		
2	1	0.1397	0.1352	3.22	2.38	0.72
	2	0.1392	0.1374	1.29		
	3	0.1603	0.1558	2.81		
	4	0.1595	0.1558	2.32		
	5	0.1701	0.1663	2.23		
3	1	0.1490	0.1456	2.28	2.60	0.37
	2	0.1407	0.1375	2.27		
	3	0.1373	0.1339	2.48		
	4	0.1499	0.1452	3.14		
	5	0.1452	0.1411	2.82		
4	1	0.1384	0.1307	5.56	6.15	1.48
	2	0.1270	0.1162	8.50		
	3	0.1348	0.1286	4.60		
	4	0.1338	0.1264	5.53		
	5	0.1255	0.1173	6.53		
5	1	0.1609	0.1471	8.58	8.83	0.76
	2	0.1577	0.1423	9.77		
	3	0.1484	0.1362	8.22		
	4	0.1444	0.1307	9.49		
	5	0.1311	0.1205	8.09		
6	1	0.1617	0.1305	19.29	17.32	2.37
	2	0.1619	0.1381	14.70		
	3	0.1623	0.1344	17.19		
	4	0.1512	0.1208	20.11		
	5	0.1559	0.1320	15.33		
7	1	0.1326	0.1056	20.36	19.12	3.59
	2	0.1422	0.1191	16.24		
	3	0.1452	0.1233	15.08		
	4	0.1327	0.1007	24.11		
	5	0.1494	0.1198	19.81		
8	1	0.1581	0.1151	27.20	29.81	2.57
	2	0.1212	0.0804	33.66		
	3	0.1510	0.1043	30.93		
	4	0.1542	0.1110	28.02		
	5	0.1541	0.1090	29.27		

Formula :30%MCC/PLA

Time (week)	Sample No.	Wi	Wf	%Weight loss	Average	SD
1	1	0.1457	0.1430	1.85	1.67	0.12
	2	0.1394	0.1372	1.58		
	3	0.1625	0.1597	1.72		
	4	0.1580	0.1554	1.65		
	5	0.1618	0.1593	1.55		
2	1	0.1428	0.1393	2.45	2.50	0.14
	2	0.1432	0.1396	2.51		
	3	0.1383	0.1345	2.75		
	4	0.1490	0.1454	2.42		
	5	0.1299	0.1268	2.39		
3	1	0.1304	0.1243	4.68	3.94	1.31
	2	0.1276	0.1201	5.88		
	3	0.1538	0.1490	3.12		
	4	0.1645	0.1600	2.74		
	5	0.1528	0.1478	3.27		
4	1	0.1388	0.1269	8.57	8.28	1.54
	2	0.1583	0.1486	6.13		
	3	0.1604	0.1480	7.73		
	4	0.1293	0.1159	10.36		
	5	0.1311	0.1198	8.62		
5	1	0.1367	0.1278	6.51	11.23	3.81
	2	0.1417	0.1242	12.35		
	3	0.1485	0.1355	8.75		
	4	0.1207	0.1008	16.49		
	5	0.1270	0.1117	12.05		
6	1	0.1615	0.1364	15.54	16.41	1.75
	2	0.1645	0.1407	14.47		
	3	0.1797	0.1465	18.48		
	4	0.1773	0.1453	18.05		
	5	0.1786	0.1509	15.51		
7	1	0.1348	0.1014	24.78	24.84	5.08
	2	0.1337	0.0906	32.24		
	3	0.1308	0.1043	20.26		
	4	0.1218	0.0974	20.03		
	5	0.1223	0.0894	26.90		
8	1	0.1476	0.0997	32.45	38.82	19.29
	2	0.1369	0.0908	33.67		
	3	0.1398	0.0394	71.82		
	4	0.1364	0.1078	20.97		
	5	0.1345	0.0872	35.17		

Formula :40%MCC/PLA

Time (week)	Sample No.	Wi	Wf	%Weight loss	Average	SD
1	1	0.1726	0.1675	2.95	1.96	1.43
	2	0.1449	0.1396	3.66		
	3	0.1254	0.1250	0.32		
	4	0.1548	0.1515	2.13		
	5	0.1249	0.1240	0.72		
2	1	0.1443	0.1386	3.95	4.13	1.73
	2	0.1528	0.1484	2.88		
	3	0.1509	0.1445	4.24		
	4	0.1535	0.1495	2.61		
	5	0.1895	0.1763	6.97		
3	1	0.1441	0.1370	4.93	5.21	0.75
	2	0.1715	0.1639	4.43		
	3	0.1732	0.1640	5.31		
	4	0.1815	0.1725	4.96		
	5	0.1863	0.1743	6.44		
4	1	0.1698	0.1516	10.72	11.76	1.69
	2	0.1633	0.1444	11.57		
	3	0.1828	0.1634	10.61		
	4	0.1707	0.1456	14.70		
	5	0.1582	0.1405	11.19		
5	1	0.1661	0.1442	13.18	14.59	3.57
	2	0.1699	0.1404	17.36		
	3	0.1797	0.1562	13.08		
	4	0.1955	0.1582	19.08		
	5	0.1766	0.1585	10.25		
6	1	0.1411	0.1138	19.35	18.06	1.36
	2	0.1619	0.1336	17.48		
	3	0.1461	0.1200	17.86		
	4	0.1324	0.1067	19.41		
	5	0.1618	0.1356	16.19		
7	1	0.1192	0.0839	29.61	27.45	4.07
	2	0.1388	0.1042	24.93		
	3	0.1468	0.1152	21.53		
	4	0.1477	0.1032	30.13		
	5	0.1408	0.0971	31.04		
8	1	0.1888	0.1210	35.91	37.03	9.68
	2	0.1465	0.1081	26.21		
	3	0.1515	0.1030	32.01		
	4	0.1675	0.0802	52.12		
	5	0.1807	0.1104	38.90		

Formula :10%MCC/5%PLA-g-MA/PLA

Time (week)	Sample No.	Wi	Wf	%Weight loss	Average	SD
1	1	0.1382	0.1363	1.37	1.48	0.18
	2	0.1239	0.1221	1.45		
	3	0.1334	0.1314	1.50		
	4	0.1090	0.1076	1.28		
	5	0.1189	0.1168	1.77		
2	1	0.1123	0.1122	0.09	1.77	1.50
	2	0.1012	0.0995	1.68		
	3	0.1082	0.1056	2.40		
	4	0.1229	0.1220	0.73		
	5	0.1169	0.1123	3.93		
3	1	0.1079	0.1050	2.69	2.42	0.57
	2	0.1107	0.1088	1.72		
	3	0.1139	0.1102	3.25		
	4	0.0982	0.0960	2.24		
	5	0.1166	0.1140	2.23		
4	1	0.1139	0.1083	4.92	3.81	0.77
	2	0.1091	0.1057	3.12		
	3	0.1246	0.1205	3.29		
	4	0.0860	0.0823	4.30		
	5	0.1233	0.1191	3.41		
5	1	0.1196	0.1152	3.68	4.20	2.05
	2	0.1328	0.1275	3.99		
	3	0.1079	0.1052	2.50		
	4	0.0971	0.0896	7.72		
	5	0.1329	0.1288	3.09		
6	1	0.1040	0.0958	7.88	6.59	1.46
	2	0.1078	0.1016	5.75		
	3	0.1222	0.1143	6.46		
	4	0.1199	0.1101	8.17		
	5	0.1044	0.0995	4.69		
7	1	0.1147	0.1051	8.37	8.40	1.32
	2	0.1277	0.1190	6.81		
	3	0.1299	0.1198	7.78		
	4	0.1102	0.1007	8.62		
	5	0.1105	0.0990	10.41		
8	1	0.1211	0.1037	14.37	17.81	2.49
	2	0.1243	0.1045	15.93		
	3	0.1222	0.0981	19.72		
	4	0.1130	0.0911	19.38		
	5	0.1135	0.0912	19.65		

Formula :20%MCC/5%PLA-g-MA/PLA

Time (week)	Sample No.	Wi	Wf	%Weight loss	Average	SD
1	1	0.1340	0.1285	4.10	1.52	1.53
	2	0.1314	0.1300	1.07		
	3	0.1347	0.1335	0.89		
	4	0.1258	0.1240	1.43		
	5	0.1093	0.1092	0.09		
2	1	0.1316	0.1291	1.90	2.00	0.29
	2	0.1163	0.1136	2.32		
	3	0.1409	0.1385	1.70		
	4	0.1313	0.1283	2.28		
	5	0.1415	0.1390	1.77		
3	1	0.1210	0.1184	2.15	2.45	0.67
	2	0.1502	0.1469	2.20		
	3	0.1149	0.1108	3.57		
	4	0.1318	0.1285	2.50		
	5	0.1480	0.1453	1.82		
4	1	0.1169	0.1121	4.11	4.09	0.91
	2	0.1422	0.1379	3.02		
	3	0.1120	0.1058	5.54		
	4	0.1357	0.1303	3.98		
	5	0.1164	0.1120	3.78		
5	1	0.1294	0.1206	6.80	7.05	1.18
	2	0.1339	0.1222	8.74		
	3	0.1227	0.1152	6.11		
	4	0.1375	0.1269	7.71		
	5	0.1391	0.1309	5.90		
6	1	0.1127	0.1012	10.20	11.38	1.56
	2	0.1218	0.1083	11.08		
	3	0.1415	0.1267	10.46		
	4	0.1385	0.1190	14.08		
	5	0.1346	0.1197	11.07		
7	1	0.1546	0.1338	13.45	11.53	1.32
	2	0.1277	0.1133	11.28		
	3	0.1246	0.1098	11.88		
	4	0.1288	0.1143	11.26		
	5	0.1216	0.1097	9.79		
8	1	0.1467	0.1221	16.77	23.21	5.44
	2	0.1388	0.1090	21.47		
	3	0.1435	0.1141	20.49		
	4	0.1371	0.1004	26.77		
	5	0.0900	0.0625	30.56		

Formula :30%MCC/5%PLA-g-MA/PLA

Time (week)	Sample No.	Wi	Wf	%Weight loss	Average	SD
1	1	0.1173	0.1157	1.36	1.65	0.47
	2	0.1370	0.1340	2.19		
	3	0.1330	0.1302	2.11		
	4	0.1312	0.1297	1.14		
	5	0.1155	0.1138	1.47		
2	1	0.1155	0.1129	2.25	2.45	1.00
	2	0.1339	0.1311	2.09		
	3	0.1417	0.1402	1.06		
	4	0.1315	0.1271	3.35		
	5	0.1283	0.1238	3.51		
3	1	0.1282	0.1253	2.26	2.93	0.70
	2	0.1327	0.1281	3.47		
	3	0.1355	0.1327	2.07		
	4	0.1282	0.1237	3.51		
	5	0.1347	0.1302	3.34		
4	1	0.1319	0.1257	4.70	5.83	1.30
	2	0.1483	0.1420	4.25		
	3	0.1383	0.1286	7.01		
	4	0.1265	0.1176	7.04		
	5	0.1172	0.1100	6.14		
5	1	0.1143	0.1020	10.76	10.21	5.33
	2	0.1457	0.1440	1.17		
	3	0.1313	0.1134	13.63		
	4	0.1333	0.1138	14.63		
	5	0.1430	0.1275	10.84		
6	1	0.1439	0.1247	13.34	15.60	2.03
	2	0.1359	0.1130	16.85		
	3	0.1268	0.1089	14.12		
	4	0.1441	0.1220	15.34		
	5	0.1405	0.1147	18.36		
7	1	0.1219	0.0745	38.88	22.21	9.59
	2	0.1513	0.1263	16.52		
	3	0.1362	0.1140	16.30		
	4	0.1385	0.1082	21.88		
	5	0.1516	0.1251	17.48		
8	1	0.1402	0.1014	27.67	30.93	5.53
	2	0.1376	0.0945	31.32		
	3	0.1251	0.0761	39.17		
	4	0.1464	0.0995	32.04		
	5	0.1396	0.1055	24.43		

Formula :40%MCC/5%PLA-g-MA/PLA

Time (week)	Sample No.	Wi	Wf	%Weight loss	Average	SD
1	1	0.1455	0.1417	2.61	1.74	0.71
	2	0.1807	0.1787	1.11		
	3	0.1514	0.1494	1.32		
	4	0.1838	0.1794	2.39		
	5	0.1508	0.1489	1.26		
2	1	0.1238	0.1203	2.83	2.88	0.09
	2	0.1432	0.1391	2.86		
	3	0.1380	0.1340	2.90		
	4	0.1357	0.1316	3.02		
	5	0.1372	0.1334	2.77		
3	1	0.1534	0.1493	2.67	3.49	0.75
	2	0.1361	0.1312	3.60		
	3	0.1125	0.1077	4.27		
	4	0.1454	0.1414	2.75		
	5	0.1423	0.1364	4.15		
4	1	0.1192	0.1113	6.63	7.44	1.96
	2	0.1234	0.1164	5.67		
	3	0.1293	0.1195	7.58		
	4	0.1341	0.1197	10.74		
	5	0.1506	0.1407	6.57		
5	1	0.1521	0.1335	12.23	12.02	1.17
	2	0.1380	0.1197	13.26		
	3	0.1455	0.1288	11.48		
	4	0.1381	0.1204	12.82		
	5	0.1475	0.1323	10.31		
6	1	0.1505	0.1276	15.22	17.79	1.63
	2	0.1301	0.1078	17.14		
	3	0.1450	0.1174	19.03		
	4	0.1250	0.1015	18.80		
	5	0.1423	0.1156	18.76		
7	1	0.1703	0.1309	23.14	23.74	3.30
	2	0.1525	0.1115	26.89		
	3	0.1673	0.1364	18.47		
	4	0.1595	0.1210	24.14		
	5	0.1638	0.1211	26.07		
8	1	0.1330	0.0942	29.17	31.98	3.77
	2	0.1146	0.0810	29.32		
	3	0.1474	0.0927	37.11		
	4	0.1525	0.1077	29.38		
	5	0.1096	0.0713	34.95		

## Biography

Miss Dhananya Masamran was born in Bangkok, Thailand on May 1<sup>st</sup>, 1987. She received her Bachelor's Degree of Science in Materials Science from Faculty of science, Chulalongkorn University in 2009. After that, she continued a further study in a Master Degree in the field of Applied Polymer Science and Textile Technology at the Department of Materials Science, Faculty of science, Chulalongkorn University in 2009, and ultimately completed the Degree of Master of Science in Applied Polymer Science and Textile Technology in October 2011.

### Publication:

### International Presentation:

- D. Masamran, and D. Aht-Ong, 2011. "Biodegradability of Microcrystalline Cellulose/Polylactic acid Composite Film under Waste Water Treatment System Condition and Effective microorganism in controlled compost", Fifth International Symposium on the Separation and Characterization of Natural and Synthetic Macromolecules (SCM-5), Amsterdam, Netherlands, January 26 -28, 2011
- D. Aht-Ong, V. Suchaiya, T. Tayomma, and D. Masamran, 2010. "Green Composite Film of Polylactic Acid and Microcrystalline Cellulose", InnoBioPlast 2010, Bangkok, Thailand, September 9-11, 2010

### Local Presentation:

- D. Masamran, and D. Aht-Ong, 2011. "Morphological, Thermal and Mechanical Properties of Microcrystalline Cellulose/PLA Composites", The 2<sup>nd</sup> Research Symposium on Petroleum, Petrochemicals, and Advanced Materials and The 17<sup>th</sup> PPC Symposium on Petroleum, Petrochemicals, and Polymers, Bangkok, Thailand, April 26, 2011



- D. Aht-Ong, V. Suchaiya, T. Tayomma, and D. Masamran, 2011. "Green Composite Film of Polylactic Acid and Microcrystalline Cellulose", Bioplastics Research Forum, Bangkok, Thailand, July 25, 2011